Cape Peninsula
University of Technology

BIOENGINEERING OF GOLD NANOPARTICLES USING SELECTED SOUTH AFRICAN EXTRACTS

By

Wakwanyembo Eloge Lwamba (213071177)

Thesis submitted in fulfilment of the requirements for the degree

Master of Applied Science: Chemistry

in the Faculty of Applied Science

at the Cape Peninsula University of Technology

Supervisor: Prof AHMED MOHAMMED
Co-supervisor: Dr SUBELIA BOTHA

Bellville campus

Submitted in September 2021

Declaration of authenticity

I, **Eloge WAKWANYEMBO LWAMBA**, declare that the contents of this thesis represent my unaided work and that the thesis has not previously been submitted for academic examination towards any qualification. Furthermore, it represents my own opinions and not necessarily those of the Cape Peninsula University of Technology.

Signed **Date 13th September 2021**

Abstract

The use of pharmaceutical products has played a big role in maintaining or improving the health of humans, and these benefits have driven pharmaceutical industries to be the most lucrative investments for many years including 2020. Lives have been saved, extended, and preserved through the use of medication since it was introduced. Although the use of medication has been known to provide relief to human health, the record of drug resistance, as well as the discovery of pharmaceutical drugs in municipal effluents was proof that pharmaceutical drugs need monitoring due to their impact on the ecosystem. A possible response to this concern lies in the exploration of potential sources of biologically active compounds from green nanotechnology. Noble metal nanoparticles, such as gold nanoparticles, have been identified as a potential alternative. The formation of gold nanoparticles was therefore achieved using *Olea exasperata* leave extract and isolated compounds as reducing agents. Three phytochemicals were isolated from *Olea exasperata* namely hydroxytyrosol, hydroxytyrosol glucoside, and oleuropein. Nuclear Magnetic Resonance and Infrared spectroscopy were used to confirm the structure of the isolated compounds. The formation of gold nanoparticles was confirmed using Ultraviolet-Visible (UV-VIS) spectroscopy by examining the surface plasmon resonance absorption between 530 and 560 nm. The synthesis of gold nanoparticles using oleuropein and hydroxytyrosol glucoside proved that all the selected reducing agents successfully reduced the gold ions to produce gold nanoparticles. The formed nanoparticles were fully characterised and showed a better Gaussian distribution than the nanoparticles obtained from the total extract. The stability of the gold nanoparticle solution was proven by a negative value of Zeta potential. X-Ray Diffraction (XRD) and Selected Area Electron Diffraction (SAED) analysis confirmed the crystallinity of the particles. The micrographs from High-Resolution Transmission Electron Microscopy (HRTEM) revealed the distinct shapes of the formed gold nanoparticles. The biological studies showed that both gold nanoparticles prepared by oleuropein and *Olea exasperata* extract have an affinity towards cancerous cells in comparison to normal cells.

In summary, this work validated the necessity to form gold nanoparticles from pure reducing agents against the use of total fraction or fraction containing mixtures of compounds toward biomedical application.

Keywords: toxic waste, green chemistry, nanoparticles, biomedical application

Acknowledgements

My appreciation goes to my supervisor, **Professor AHMED MOHAMMED** for his practical experience and wealth of information. His heart to gather all students around a table and have fun while doing science is a key trait of his kind character. It is a blessing to benefit from his discipline and intolerance to complacency.

My heartfelt appreciation to my co-supervisor **Dr SUBELIA BOTHA** who has been a candle on this path from the early beginning. Her sense of humour, peace and encouragement in downtime has been a milestone in the making of this work, may she finds here the expression of my gratefulness.

A special thanks to **Dr ENAS ISMAIL** for her kind support in the laboratory, to **Dr ABDULRAHMAN ELBAGORY** for a great moment of insight, to **Dr RAJAN** for his kindness, to **Dr OMAR BADEGGI** for his kind heart, to **Dr NINON ETSATSELA** for his sympathy and openness. to **JUSTIN MOSER** for a great time in the laboratory, to **BARA'A JAD** a wonderful teammate and friend, to **Mr AKEEM, BONGIWE, Mr DAVID KOK, KHADI, ALIWA** your interaction brought light to this work.

Special thanks to Mr **NDUMISO MSCHICILELI** at the Food technology department (Agrifood technologist agency) and Professor **JANINE MANERWICK** at the oxidative stress unit (Health and wellness department) for providing with the facility for freeze-drying plant extracts at the Cape Peninsula University of Technology.

A special thanks to my wife **NATACHA KAKAMA LWAMBA** and my daughter **FAVEUR GRACE LWAMBA** who has accepted to be part of my life during my master's degree journey. My wife is one of the pillars upon which my life stands next to **YAHWE**. I fondly appreciate their friendship, kindness, patience, and encouragement.

My appreciation goes to my line manager at the Cape Peninsula University of Technology and First-Year Experience coordinator, **Dr Le Roux** for always being supportive. Fondly appreciate all lecturers and laboratory staff **Sisi Zandile** and **Gillian Fennessy** who greatly contributed to our studies.

Many thanks to the General Board of Global Ministries for funding my first two years of this program. I am very grateful for their generosity towards me.

Declaration of plagiarism

The financial assistance of the National Research Foundation towards this research is highly appreciated. Opinions expressed in this thesis and the conclusions arrived at, are those of the author, and are not necessarily to be attributed to the National Research Foundation.

Dedication

I am dedicating this work to the God of heaven and hearth who stood by my side in my youth and set me up on this course of life. I am very grateful for the gift of loving parents, my four sisters, and friends. To my parents, for always praying for me and keeping me in their hearts. And to my sisters for always being a bunch of lovely friends. What would childhood fun be without you! I love you all so dearly! To my late nephew Professor Masangu Shabangi that I dearly consider as a brother, I am expressing my appreciation for your kindness and support in the early beginning of my studies. To my first mentor in business and friend Robert Lubasa for providing love and care in my early days in business.

Glossary

µL:	Microliter
1D-NMR:	One-dimensional nuclear magnetic resonance
^{1}H-NMR:	Proton nuclear magnetic resonance
2D-NMR:	Two-dimensional nuclear magnetic resonance
ARC:	Agriculture Research Council
B16:	Mouse melanoma
C1**:**	Compound 1
C2:	Compound 2
C3:	Compound 3
CFK:	Cape Floral Kingdom
CPUT:	Cape Peninsula University of Technology
d:	Doublet
DCM:	Dichloromethane
dd :	Doublet of doublet
ddd :	Doublet of doublet of doublet
DLS:	Dynamic Light Scattering
DMSO:	Dimethyl sulfoxide
E:	*O. exasperata*-AuNPs
EDS:	Energy Dispersive Spectroscopy
EDX:	Energy Dispersive X-ray spectroscopy,
EELS:	Electron Energy Loss Spectroscopy
EK	KMST-6 treated with *O. exasperata*-AuNPs
EtOH:	Ethanol
EU:	European Union
FBS:	Fetal Bovine Serum
FDA:	Food and Drugs Administration
FTIR:	Fourier Transform-Infrared spectroscopy
g:	Gram
GNPs:	Gold nanoparticles
H :	HT-29 cells
HAADF:	High Angle Angular Dark Field.
HaCat:	Human keratinocytes
HPLC:	High Pressure Liquid Chromatography
HRTEM:	High-Resolution Transmission Electron Microscopy
HT-29:	Colon cancer cells
ICP-OES:	Inductively Coupled Plasma- Optical Emission Spectroscopy
KMST-6:	Human normal fibroblast
L:	Liter
LSPR:	Localised Surface Plasmon Resonance
m :	Multiplet
MCF-7:	Human breast adenocarcinoma, pleural View
Mel-1:	Human embryo
MeOH:	Methanol
mg:	Milligram
mL:	Mililiter
NMR:	Nuclear Magnetic Resonance

OL GNPs:	Oleuropein gold nanoparticles
PLE:	Pressurised Liquid Extraction
R&D:	Research and Development
s:	Singlet
SAED:	Selected Area Electron Diffraction
SPR:	Surface plasmon resonance
t :	Triplet
UNEP:	The United Nations Environmental Program
UV-Vis:	Ultraviolet-Visible spectroscopy
UWC:	University of the Western Cape

Table of contents

Declaration of authenticity i

Abstract ii

Acknowledgements iii

Declaration of plagiarism iv

Dedication v

Glossary vi

Table of contents viii

List of figures xiii

List of tables xvi

1. CHAPTER ONE 1

INTRODUCTION 1

1.1 Introduction and background to the study 1

1.2 Aim 3

1.3 Problem statement 3

1.4 Hypothesis 4

1.5 Objectives 4

1.6 Thesis layout 5

2. CHAPTER TWO 6

LITERATURE REVIEW 6

2.1 Introduction 6

2.2 Plant selection and selection criteria 6

2.2.1 Understanding plants and their curative properties 7

2.2.1.1 *Olea exasperata* 9

2.2.2 Phytochemicals in plants 9

2.2.3 Biological activities of plants 10

2.3 Isolation and purification of phytochemicals 11

2.3.1 Extraction technique 12

2.3.1.1 Type of extraction techniques: 13

a) Maceration 13
b) Percolation 13
c) Reflux extraction 14
d) Soxhlet extraction 14
e) Pressurised Liquid Extraction (PLE) 14
f) Supercritical fluid extraction 14
g) Microwave-assisted extraction and Ultrasound-assisted extraction 15
h) Decoction 15
2.3.1.2 Types of chromatography 15
a) Adsorption technique 17
b) Affinity chromatography 17
c) Ion exchange chromatography 18
d) Size exclusion chromatography 18
e) Partition chromatography 18
f) Ion exclusion chromatography 18
g) Planar chromatography and column chromatography 19
h) High-Pressure Liquid Chromatography 19
2.4 Identification of isolated phytochemicals 19
2.4.1 Infrared analysis 20
2.4.2 Nuclear magnetic resonance 20
2.4.3 Mass spectrometry 21
2.5 Nanochemistry 21
2.5.1 Nanoparticles 22
2.5.1.1 Synthesis of nanoparticles 22
a) Top-down method 23
b) Bottom-up method 23
2.5.1.2 Stabilisation of nanoparticles 24
a) Electrostatic, steric and electrosteric stabilisation 25
b) Stabilising agents and surfactants 25
2.5.1.3 Green nanochemistry 27

2.5.1.4 Reducing ability of phytochemicals 27
2.5.1.5 Characterisation of nanoparticles 29
a) Ultraviolet-Visible spectroscopy 29
b) X-Ray Diffraction 31
c) Average size and Zeta potential 32
d) High-Resolution Transmission Electron Microscopy 32
e) Fourier Transform Infrared (FTIR) analysis 33
2.6 Application of nanoparticles as Nanomedicine 34
2.6.1 Biological studies 35
2.6.1.1 Luminometric assay 37
2.6.1.2 Dye exclusion: 37
2.6.1.3 Colourimetric assays: 38
2.6.1.4 Fluorometric assays 38
3. CHAPTER THREE 40
METHODOLOGY 40
3.1 Introduction 40
3.2 Collection and identification 40
3.3 Materials used 40
3.4 Extraction and isolation of phytochemicals from *O. exasperata* leaf extract 41
3.4.1 Lyophilisation of total extract 45
3.5 Characterisation of Isolated compounds 46
3.5.1 Isolated phytochemicals 46
a) Isolation of compound 1(C1) 46
b) Isolation of compound 2 (C2) 47
c) Isolation of compound 3 (C3) 48
3.6 Nanoparticle synthesis 49
3.6.1 Preliminary formation of gold nanoparticles from *Olea exasperata* total extract 49
3.6.2 Determination of optimal concentration through serial dilution of lyophilised *Olea exasperata* 49
3.6.3 Nanoparticle synthesis using pure compounds 50

3.7 Characterisation of gold nanoparticles 50
3.7.1 Ultraviolet-Visible 50
3.7.2 X-ray diffraction 51
3.7.3 Size and Zeta potential distribution 51
3.7.4 High-Resolution Transmission Electron Microscopy 52
3.7.5 IR spectroscopy 53
3.8 Biological studies 53
4. CHAPTER FOUR 55
RESULTS AND DISCUSSION 55
4.1 Introduction 55
4.2 Isolation and chemical characterisation of *Olea exasperata* phytochemicals 55
4.2.1 Chemical characterisation of compound 1 (C1) 55
4.2.2 Chemical characterisation of Compound 2 (C2) 58
4.2.3 Chemical characterisation of compound 3 (C3) 63
4.3 Synthesis of gold nanoparticles 65
4.3.1 Nanoparticle synthesis using *Olea exasperata* total extract 65
4.3.1.1 Reducing ability of Olea exasperata extract 66
a) Optical properties 66
b) Crystallinity 67
c) Size and zeta potential measurement 68
d) Morphological examination and particle size measurement 70
e) Energy dispersive x-ray analysis 71
f) Infrared analysis of *Olea exasperata* extract gold nanoparticles 72
4.3.2 Nanoparticle synthesis using pure compounds 73
4.3.2.1 Reducing ability of hydroxytyrosol glucoside 73
a) Optical properties 74
b) Crystallinity 75
c) Size and zeta potential measurement 76
a) Morphological examination and particle size measurement 76
e) Energy dispersive X-ray analysis 78
a) Infrared analysis of hydroxytyrosol glucoside gold nanoparticles 80

4.3.2.2 Reducing ability of oleuropein 81
a) Optical properties 81
b) Crystallinity 82
c) Size and Zeta potential 83
d) Morphological examination and particle size measurement 84
e) Energy dispersive x-ray spectroscopy 85
f) Infrared analysis of Oleuropein gold nanoparticles 86
5. CHAPTER FIVE 88
BIOLOGICAL STUDIES 88
5.1 Introduction 88
5.2 Stability test 88
5.3 MTT Cytotoxicity assay and safety of gold nanoparticles 89
5.4 Gold nanoparticles uptake 89
6. CHAPTER SIX 91
GENERAL CONCLUSIONS AND RECOMMENDATIONS 91
Reference 93

List of figures

Figure 2.1 Surface plasmon resonance shift as a function of colour of CdSe nanoparticles in solution . The various bands observed were a result of the different shapes and sizes of CdSe nanoparticles. 30
Figure 3.1 Preliminary chromatographic column fraction's TLC fractions under UV (254nm, 366nm, and heated plate with vanillin) 43
Figure 3.2 TLC of combined fraction in Figure 3 1 leading to sub-fractions I to XVIII at 254 nm (A), 366 nm (B), and (C) vanillin charred plate 44
Figure 3.3 Pure phytochemicals isolation pathway and yields 45
Figure 3.4 TLC featuring a pure C1 in a vanillin charred plate 47
Figure 3.5 TLC of Compound 2 at 254nm (A) vanillin charred plate (B) and 366nm (C) 48
Figure 3.6 Thin layer chromatography structure of compound 3 49
Figure 4.1 Chemical structure of Compound 1 55
Figure 4.2 Infrared spectrum of Compound 1 confirmed the presence of the functional groups observed in the inserted structure 56
Figure 4.3 ^{1}H-NMR (400 MHz, DMSO) spectrum of Compound 1 56
Figure 4.4 ^{13}C-NMR (400 MHz, DMSO) spectrum of Compound 1 57
Figure 4.5 DEPT135-NMR (400 MHz, DMSO) spectrum of Compound 1 57
Figure 4.6 Chemical structure of Oleuropein 58
Figure 4.7 Infrared spectrum of Compound 2 confirmed the presence of all the functional groups of the inserted structure 59
Figure 4.8 H-NMR (400 MHz, DMSO) spectrum of C2 60
Figure 4.9 13C-NMR (400 MHz, DMSO) spectrum of C2 60
Figure 4.10 DEPT135-NMR (400 MHz, DMSO) spectrum of C2 61
Figure 4.11 Chemical structure of compound 3 (C3) 63
Figure 4.12 1H-NMR (400 MHz, DMSO) spectrum of compound 3 63
Figure 4.13 ^{13}C-NMR (400 MHz, DMSO) spectrum of compound 3 64
Figure 4.14 DEPT-135-NMR (400 MHz, DMSO) spectrum of C3 64
Figure 4.15 The UV absorption band of gold nanoparticles from serially diluted *Olea exasperata* (A) showed they were concentration-dependent (B) and the absorption at 4mg/mL reflected a good peak symmetry (C) suggesting the existence of spherical gold nanoparticles 66
Figure 4.16 XRD pattern of Olea exasperata extract gold nanoparticles 68
Figure 4.17 The size distribution graph of gold nanoparticles prepared from Olea exasperata showing a size distribution below 100nm with a mean value around 73.9nm its corresponding zeta potential distribution graphed had a value was -21.6 mV 69

Figure 4.18 TEM micrograph of *O. exasperata* GNPs (A) and its magnified image showing defined shapes (B) with corresponding histogram pattern (C) showing spherical and crystalline rings (D), with sizes within 20-40 nm bracket. 70
Figure 4.19 Energy-dispersive X-ray spectrum of Olea exasperata gold nanoparticles 71
Figure 4.20 Infrared spectra of Olea exasperata leave extract (A) and gold nanoparticles (B) showed an increase in transmitted intensity as the gold nanoparticle formed 72
Figure 4.21 UV-Vis spectrum of gold nanoparticles from hydroxytyrosol glucoside showing a symmetrical absorption peak at 548nm..... 74
Figure 4.22 XRD pattern of gold nanoparticles formed using hydroxytyrosol glucoside..... 75
Figure 4.23 Size (A) and zeta potential (B) of gold nanoparticle from hydroxytyrosol glucoside 76
Figure 4.24 TEM micrograph of hydroxytyrosol glucoside gold nanoparticles showed spherical crystalline particles on micrograph A. The micrograph B was an insert of some selected area in A. The histogram in C and SAED in D were corresponding to the micrograph in A. The histogram of the same gold nanoparticles revealed particles with sizes 40 and 50nm were abundant..... 78
Figure 4.25 EDS spectrum of hydroxytyrosol glucoside gold nanoparticles showing the presence of gold nanoparticles 79
Figure 4.26 Infrared spectra of hydroxytyrosol glucoside compound (A) and its gold nanoparticles (B)..... 80
Figure 4.27 UV absorption spectrum of Oleuropein gold nanoparticles 81
Figure 4.28 XRD pattern of gold nanoparticles synthesised using oleuropein 82
Figure 4.29 Oleuropein gold nanoparticle size distribution by intensity graph (A) and Zeta potential measurement (B)..... 83
Figure 4.30 TEM micrograph of oleuropein gold nanoparticles (A) and its magnified image (B), presenting broad size distribution of particles. The histogram (B) and SAED pattern (C) corresponding to the micrograph showed particles were crystalline. The TEM image in D was an insert of A showing abundant spherical particles below 10nm..... 84
Figure 4.31 EDS spectrum of oleuropein gold nanoparticles provided evidence of the presence of gold..... 85
Figure 4.32 Oleuropein compound infrared (A) and oleuropein gold nanoparticle infrared (B) showing the shifted intensity to the right and increased intensity. The absence of some peaks that are involved in gold nanoparticle formation after forming the gold nanoparticle..... 86
Figure 5.1 Stability tests of *Olea exasperata* extract gold nanoparticles (A) and PEG stabilised oleuropein based gold nanoparticles (B) showing their stability over a 24hr period..... 88
Figure 5.2 Error bars of cells KMST-6 treated with *O. exasperata* GNPs (EK), HT-29 cells treated with *Olea exasperata* GNPs (EH), KMST-6 cells treated with OL GNPs (CK), HT-29

cells treated with OL GNPs (CH), KMST-6 cells with no GNPs (K-), HT-29 cells with no GNPs (H-) 90

List of tables

Table 2.1 Summary of Chromatographic techniques 16
Table 3.1 Chromatographic extraction of *O. exasperata* total extract (Main fraction) 41
Table 3.2 Fraction collected from the column of C1 46
Table 3.3 Chromatographic column of fractions collected from the column of compound 2 . 47
Table 3.4 Pure fraction collected from the column of compound 2 48
Table 4.1 ^{1}H and ^{13}C NMR spectroscopic data assignments (400 MHz) for C1 (δ in ppm, m, J in Hz) in DMSO 58
Table 4.2 ^{1}H and ^{13}C NMR spectroscopic data assignments (400 MHz) for compound 2 (δ in ppm, m, J in Hz) in DMSO 62
Table 4.3 ^{1}H and ^{13}C NMR spectroscopic data assignments (400 MHz) for compound 4 (δ in ppm, m, J in Hz) in DMSO 65
Table 4.4 Summary of the screening of lyophilised Olea exasperata 69

1. CHAPTER ONE

INTRODUCTION

1.1 Introduction and background to the study

The pharmaceutical industries are reported to be part of the fastest-growing industries in the world. A study of its global trend through the past years has revealed that these industries have made a trillion-dollar in turnover in the year 2014 alone and growth in this sector was expected to break this record soon after 2019. These industries are extremely significant for the production, development, and marketing of medication globally. American companies are great contributors to this number, but those from China have a much higher growth rate in pharmaceuticals according to recent updates (Teramae et al., 2020).

When the human impact on the environment was minimal in the absence of machinery, nature was self-regulating so that a certain harmony existed on earth. Emerging concepts such as climate change, emerging contaminants, environmental pollution, cyclones, and environmental degradation were not spoken of. It was only recently that global temperatures, rain, and other climatic factors are breaking their records. While these can be regarded now only as symptoms of environmental degradation, the signs are suggesting a very rough future. Today's global degradation crisis was reached very quickly with rapid industrialisation through the increase of greenhouse gasses so that the process is almost irreversible due to accelerated pollution, production, and environmental degradation. The earliest industrial revolution was recorded in Britain in the 18th century when agriculture was first mechanised. Today, it has spread all around the globe in various areas including petrochemical, pharmaceutical, mining, etc. (Merck, 1950).

The development in pharmaceutical industries evolved progressively as the industrialisation of Europe was born. In the nineteenth century, Merck, one of today's well-established pharmaceutical industries, was born (Walsh, 2010). It started with natural products and moved from herbal medicine to the industrialisation of the idea through the implementation of chemicals for mass production. Since then, the growth of these enterprises kept on breaking new records. Many other pharmaceutical companies were born later and grew stronger by building strong research and development (R&D) units in joint ventures. This desire to absorb new developments in the field at a high pace gave rise to corporations joining efforts to further

their growth. This exponential growth led to the belief that pharmaceutical industries were given a prescription for success (Merck, 1950).

The uptake of medication in humans is also its intrusion into the ecosystem. Human waste is part of the ecosystem and thus pharmaceutical waste is following the same route. After the use of any products, humans discard them in the environment in certain proportions. The growth in the use of any product equates to the growth in its impact on the ecosystem, be it directly or indirectly. In other words, the environment has been a beneficiary of the wrong impact of medication and many other chemical products. While the growth in spending on medicines has increased with time, there has also been an increase in the number of environmental events recorded that is appealing to curative responses on the environment (Teramae et al., 2020).

Many organisations and bodies have been brought up to protect the environment from pollution. As early as 1972, the United Nations had established a body that linked, for the first time, environmental protection to human rights. The United Nations Environmental Programme (UNEP) was introduced and has since advocated and provided a space for more bodies to join their effort in protecting the environment. Under that same amendment, pharmaceutical industries were subjected to strict regulations as a result of the act provided by the UNEP, which considered it a violation of human rights to dump or let toxic products from industries enter water or the environment (Weiss, 2011).

Some studies published on the FDA website report the adverse effects of drugs on fish, animals, and flora. It was only until 2003, that the Food and Drug Administration (FDA) agency introduced the regulation to protect the environment by preventing drugs with an ill effect on the environment. In addition, the European Union (EU) placed a similar requirement on the medicines before they are released (Boxall, 2004). In agriculture, the concept is achieved using no persistent chemicals in pest control while in the food industry, fats and antioxidant containing products are avoided (Weiss, 2011).

Using green products has proven to improve livelihood through proper diet and proper medication. Returning to a more natural way of consuming has great benefits in health, the environment, and many other sectors. The use of natural plants in medication has minimum adverse effects on consumers and therefore shows great benefits for the future design of drugs (Tripoli et al., 2005). New technological advancements in nanotechnology created green pathways in biochemistry, which allowed the synthesis of drugs with green properties that improved bioavailability and biological activity. A good example was a study that involved the

use of a mixture of tea with selenium salt to improve the antioxidant properties of rooibos tea through the formation of its nanoparticles (Supriadi et al., 2017). This new approach had no side effects both on the patients nor the environment where the medication was extracted and manufactured. This formulation to nanoparticles would be the main focus of this work using alternative precursors (Supriadi et al., 2017).

1.2 Aim

The aim was to evaluate a green route of forming gold nanoparticles using the water extract of a known biologically active plant, *Olea exasperata,* and its isolated phytochemicals, and test the resulting nanoparticles thereof for use in biomedical applications.

1.3 Problem statement

Pharmaceutical companies are known to use toxic chemicals that require strict regulations. The choice of the material used in pharmaceutical drugs has to do with the positive biological outcomes recorded when the product gets into biological systems. Therefore, the biological activities of these products require that they get highly regulated not only before manufacturing but also when they leave the shelves to the consumers (Küster & Adler, 2014)

Production of pharmaceutical products goes along with the use of a huge amount of chemicals. Due to the poor atom economy in drug manufacturing, a small portion of the precursors, the intermediates, and the final products in the synthesis often end up in the effluent after manufacturing. Evidence of these species has been found in the environment including soil, surface, and underground water despite efforts to recycle them. Chemicals that have recently been recorded in nature include anorexic, antibiotics, antiretroviral drugs, antibacterial, analgesic, etc. The presence of chemicals in the soil is predicted to make microorganisms very resistant to current drugs, causing exposed patients to require stronger doses of medication. (Boxall, 2004).

One concern attached to the use of pharmaceutical products is highly related to the lack of biodegradability of most pharmaceutical products. These products are not fully absorbed in the human body. Therefore, the remnant of the drug is soon found in the environment where their presence has the above-mentioned adverse effects. There are different types of contaminants. Some are persistent, some deactivate reasonably soon enough with time, and some turn into other less toxic substances. A study conducted in Germany revealed that about 156 different pharmaceutical products have been found in surface water at a concentration below $10 \mu g/l$

(Boxall, 2004). A recent global study also reveals that over 600 different pharmaceutical products have been found in surface water. Exposure to a low concentration of these wastes could cause substantial physiological changes in some species while in others, the change is yet to be investigated (Küster & Adler, 2014). Therefore, this work will be an attempt to suggest a green alternative to the challenges found in current drugs by evaluating green nanoparticles as a potential alternative. In light of this, gold nanoparticles have been identified as a good candidate due to their limited ill effects.

1.4 Hypothesis

The persistence of pharmaceutical products in the environment would be addressed by providing alternative products made of new materials. The chemical substances used in conventional medication often require strict dosage due to advert effects that would result from mishandling the products. They also present an environmental concern as they enter nature. Therefore, it is proposed that the use of green chemistry and nanotechnology produce nanoparticles with outstanding features, which will have the ideal properties of future pharmaceutical drugs upon biomedical evaluation.

The use of medicinal plants in nanoparticle drugs would have the higher end goal of getting a bioactive compound involved in the reduction of the metal as well as an improvement of their biological activities and absorptivity. The selected plants would be used as a possible lead molecule in the implementation and the study of more natural products. It was expected from this work that the synthesis of metal nanoparticles from natural products yields safe compounds with improved properties.

1.5 Objectives

The evaluation of the reducing ability of the plant and its isolated compounds to form bio-stable gold nanoparticles as potential candidates for biomedical applications. The introduction of gold nanoparticles as an alternative to other drugs would therefore require an assessment of the formation parameters. Since this is only approached through the effective study of formed nanoparticles from pure compounds, an attempt to effectively characterise the nanoparticles will be made to guarantee a proper understanding of the formation process. In addition, it would require that a product with verifiable medicinal properties be found.

The work covered will be tailored around the following steps:

- Isolation of pure compounds from the total extract,
- Characterisation of the isolated compounds,
- Synthesis of gold nanoparticles from the total extract of the *Olea exasperata* leaves,
- Synthesis of nanoparticles from the isolated compounds,
- Characterisation of nanoparticles from pure compounds,
- Evaluation of the biological activity of nanoparticles formed with compounds from plants versus the total extract thereof

1.6 Thesis layout

Chapter one is an introduction to the study. Chapter two gives an overview of the literature. while all experimental details are given in chapter three. Chapter four contains the result and discussion. Chapter five covers the biological studies and chapter six concludes the study.

2. CHAPTER TWO

LITERATURE REVIEW

2.1 Introduction

This chapter discusses general considerations around plants, It highlights their healing properties and various uses. It presents the potential of the Cape Floral Region in the Western Cape, South Africa as a reservoir of unique plant species and the benefits it brings to the region in the development in the development of new drugs.

2.2 Plant selection and selection criteria

The knowledge of medicinal plants has grown to be a rare commodity. The use of medicinal plants as a cure has been reported in early civilisations. That knowledge preserved through ages can form a solid ground where one can stand to claim the relevance of that type of treatment today. As this science evolved with time, it resulted in the creation of well-organized pharmacopoeia of pharmaceuticals. The need to make health products available to a global market led this practice to be industrialised and turned into pharmaceutical companies where synthetic processes prevailed. While plants are important, not all plants are medicinal. any discoveries of biological activities in plants were random and the groundwork had been done in traditional ethnic groups and held the record in selecting specific plants that can cure certain diseases (Toma & Crişan, 2018).

Shen Nung; the emperor of China used and reported up to 365 drugs 2500 years ago. In his days, Camphor, jimson weed, and cinnamon bark were already known. The Ebers papyrus in Egypt reported up to 700 plants and 800 drugs. Some religious books like the Bible and Talmud prescribed the use of plant-like incense, myrtle, as a form of medication. The use of plants has grown ever since and the search for medicinal plants has been a long, endless process. The use of plants has also been documented and Dioscorides was the most prominent writer on medicinal plant literature. He studied and classified plants according to their place of occurrence, medical effect, and formulation. He was a pharmacologist who was honoured as the father of pharmacognosy. He reported in *De materia Medica* some 944 drug formulations (Petrovska, 2012).

2.2.1 Understanding plants and their curative properties

The selection of medicinal plants requires knowledge of the factors that underlie the classification of the plant as medicinal. The number of medicinal plants known today is very important both to industries and to the interest of perpetuating plant species. In the year 2006, the World Health Organisation had recorded 20000 medicinal plants in 91 countries globally. Many more medicinal plants are yet to be identified from traditional users in many ethnic groups around the globe. More and more researches are being covered requiring the help of traditional healers in the identification of plants that have been known active. Most discoveries of medicinal plants have led to their use in modern medicine as a cure (Sasidharan et al., 2007). A common pattern was observed among many medicinal plants. They have been known for standing rough climate conditions or dryness for years. In some cases, they have survived many fires or natural roughness. These events often make plants build up resistance to external strain so that they could be expected to have some substances in them that would help them resist any added stress such as dryness, change in climate, etc. The substance found in plants varies with seasons throughout the year in some species, depending on the need in the plant. In some seasons, the presence of certain substances is more prominent than in others. Alarcón-Flores et al (2015) reported the presence of abundant phenolic compounds in tomatoes during the winter season than he did in any other season. He also observed the abundance of more phenolic compounds in fresh tomatoes than he did in matured ones. After a year spent monitoring the variation of phenolic compounds in these fruits, he found that the presence of phytochemicals in plants can vary with various external strains. Thus, the sample of plants selected should contain the compounds in good quantity for representative predictions to be made (Alarcón-Flores et al., 2015).

are governing the classification of plants and they are based on similarities that rule the world of plants. A family to which a plant belongs can be used as a guideline to determine the possible type of metabolites available in them. *Achillea* L. (Asteraceae) for instance is a plant whose species is found in a family with similarities in biological activities, scent, and geographic occurrence. There are many types of plants showing the same pattern, but they occur according to a specific order such as type of leaves, height, shape, and texture. This concept has made it easy to classify and establish a plant taxonomy (Ali et al., 2017).

There are metabolites reported in all types of plants, but characterising plants as either herb, trees, and shrubs makes it convenient for distinction. The screening of these categories reveals that the distribution of phytochemicals in plants is such that herbal plants contain more antioxidants than shrubs and the latter contain more than trees. Herbaceous plants are also

known as “non-apparent” while trees and shrubs are apparent. While it might require instinct to identify a plant, science is mandatory in the compilation of information that tells which plant is better (Da Silva et al., 2018).

While taxonomy is not the only base in plant selection, many other factors can be considered. One is the available knowledge of different ethnic groups and the understanding of their biodiversity. The latter suggests that a plant hosting many spiders that hunt in its branches can be suspected to be attractive to many other animals coming either for food, shelter, pollination, or even relief. Therefore, careful observation of some plants can lead to a discovery of plenty of facts.

Many medicinal plants have been known for their recorded potential in various studies throughout the years. The identification of compounds in various taxonomy of plants is so important that it allows one to build up important libraries of known biologically active phytochemicals with their potential biological responses. The identification of compounds would either go through traditional users of nature or the exploration of biological activities of unidentified plants.

The use of medicinal plants in research, foods, or even nutrition is subject to ethical criteria defining sustainability. Cultivation, propagation, and processing of medicinal plants are the backbone requirements needed for the sustainable use of medicinal plants. They are prescribed by the Agriculture Research Council (ARC) of South Africa to make sure plants are used in a way that prevents their extension with time. The same agency stipulates that the explorative study of plant extracts in research is also one step to sustainably use plants as they point out to which plant requires more care in terms of cultivation, propagation, and future use (Rasethe et al., 2019).

South Africa is considered one of the most bio-diversified countries on earth. It is home to many animals and plants in their diversities. South African Flora is the centre of a lot of interest for its biodiversity. A comparative study has shown that South African flora accounts for 10% of the world's plant species within its borders; that is 22000 plant species found within South Africa. The most attractive place in this region is called the “Cape Floral Kingdom” (CFK). This is the world’s most diverse spot in terms of plant diversity and it is as small as 90000 km^2. This region, mostly Mediterranean, has unique vegetation, the Fynbos. There are other areas around the globe with the same pattern such as in Australia and the northern hemisphere, but the CFK is the smallest of them all. This region has provided a wealth of information that sustains many industries and yet, this has not stopped. The CFK exists as a large reservoir

that is continually understudy up to today. In the same way, the present research is exploring a species obtained from this region (Sridhar & Ramakrishna, 2015). *Olea exasperata was* identified for this study.

2.2.1.1 *Olea exasperata*

Olea exasperata, a species of the *Olea* genus found in the Mediterranean regions and the Western Cape, South Africa, was used for this study. It's also found in the tropical regions of Europe and Africa. This species is ubiquitous in the Mediterranean region where it is widely known for its oil-producing ability and its therapeutics use. *Olea exasperata* belongs to the family of Oleaceae, among which 19 can withstand hot weather. It is commonly known as a coastal olive or dune olive. It's an evergreen shrub, which can grow into a tree, reaching a 1 to 7 m height on sandy dunes and high hill regions. The plant extracts are reported to contain many phenolic compounds with great anti-oxidant properties (Tripoli et al., 2005).

The isolation of phytochemicals from *Olea e uropea* leaves has been achieved in the past years. The interest in *Olea* has been reported to be great. The plant has been reported to exhibit widespread medicinal benefits from its leaf extracts to its bark and roots and is considered to be a piece of medical wonder that has proven itself before many ailments including diabetes, hypertension, fresh wounds, urinary disease, rheumatism, sore throat, colds, and many more (Zhang et al., 2018). The plant is reported to contain phenolic glucoside (hydroxytyrosol glucoside, oleanolic acid glucoside, hydroxytyrosol diglucoside, secoiroids (oleuropein, verbascoside, oleuropein aglycone, etc.). Oleuropein has been ascribed to a wide range of biological activities which include anti-viral, anti-microbial, anti-fungal activities (Tsukamoto et al., 1984). Although the isolation of phytochemicals has been great at providing impressive biological activities, the yield of these isolations has remained relatively low. Since *Olea exasperata* displayed so much biological activity, it had more to offer.

2.2.2 Phytochemicals in plants

As mentioned by (Alarcón-Flores et al., 2015), phytochemicals are species found in most parts of plants, including leaves, roots, barks. Phytochemicals are primary or secondary metabolites. Secondary metabolites differ from the primary metabolites in function. Secondary metabolites are known to be great contributors to pharmaceutical properties since they are engaged with the defence of plants and the adaptation thereof to new conditions of their environment (Ramakrishna & Ravishankar, 2011). The use of the total extract from the leaves of the plants does not allow the evaluation of the singular effect of multiple phytochemicals, thus the need

to isolate phytochemicals so that they are used for meaningful studies and predictions (Boyer & Liu, 2004).

The use of plant leaves as a source of potentially active compounds has been motivated by the potential presence of phytochemicals in all plant leaves. It is also motivated by the fact that plants can be used without endangering their species. They are a sustainable source of lead molecules in synthetic chemistry and other chemical applications since they can be cultivated and multiplied at a reasonable rate.

Phytochemicals are classified based on many aspects which can include functional groups, skeleton structures, and many more. The most commonly known phytochemicals in extractive sciences are flavonoids, phenolics, isoflavones, lignans, phenolic acids, terpenes, saponins, carotenoids, monoterpenes, etc. Most of these molecules contain hydroxide groups or a series of benzene rings. In some cases, they have sugars in their structure. When a study was conducted on a batch of various fruits to study which one displayed a better antioxidant property, cranberry was found to be most active and beneficial, followed by red apples or red grape, strawberry, peach, lemon, etc. This study indicated that different plants have different levels of biological activities (Boyer & Liu, 2004).

The presence of phytochemicals is subject to natural dynamics. The change in phytochemicals in different cells causes leaves to turn green, yellow, brown, or other colours. Those changes considered to bring a strain on plants are often the main reason why plants undergo the variation in phytochemical concentration. The presence of phytochemicals or their absence also affects the texture of the leaves and that of the plant itself. A change in season also induces a change in strain on the plant causing it to produce compounds that are protecting the plant from the applied strain.

2.2.3 Biological activities of plants

The general use of natural products from the plant kingdom as an alternative cure has focused on total extracts. The use of these extracts in biological studies has helped provide relevant conclusions on the biological activity of specific plant extracts. It has also helped stir the interest into identifying the specific compounds responsible for remote biological activity. This is the essence of focusing on the isolation of natural products from these compounds.

Many compounds have been identified and screened for their biological activities and the outcome has been promising with respect to the potential hidden in natural products. The use

of plants or the secondary metabolites therein as potential drugs could introduce some limitations in the therapeutic process involving plants. Aqueous plant extract treatment is made up of a bulk of extracts showing poor absorptivity of the active compounds or low bioavailability, which therefore necessitates high dosage. There have been successful attempts in the treatment involving plant extracts, but the result has often been an additive effect of more than one compound so that the curator is unidentified. This has made this kind of treatment very scientifically unreliable in terms of implementation into a systematic process. (Sentkowska & Pyrzyńska, 2019)

The use of aqueous plant extracts as medication has been proven to work in traditional medicines. However, the implementation of these materials as a recognised treatment has required evidence that these products are reproducible in response and that it can respond to the suitability test any drug should pass. Although the aqueous extract from certain plants has been known for its medicinal benefits, medical and traditional practitioners were reported to lack a pharmacotherapeutic approach, which supplies scientific proof that this drug can be administered in a sustained manner without requiring additional dosage. (Ansari et al., 2012). Pharmacotherapeutic information could be obtained through the isolation of the phytochemicals before using them in the synthesis of the derivatives for any biological evaluation.

2.3 Isolation and purification of phytochemicals

One highlight of most phytochemical research is their existence in pure form during research. Obtaining them in pure form requires an extraction, isolation, and identification of the pure compounds from the total extract. The extraction and isolation of compounds from plants is a common practice in phytochemical studies. The best illustration of this practice is making a cup of tea from a teabag using boiled water. The tea extracts are forced out of the bag when hot water is brought in contact with the teabag, making most compounds soluble and diffuse in water.

Each isolation of phytochemicals has to be followed by the evaluation of the biological activities from plant extracts. During the process of isolation of phytochemicals, a minimum knowledge of the possible functional groups present on the molecule is needed to make predictions of the type of solvent required in the process. The isolated compounds are subject to characterisation for their identification (Sasidharan et al., 2007).

The isolation of certain chemical compounds in plants helps reach very interesting conclusions that can lead to more studies on the subject. Pure substances obtained from a plant could be used to explore the antioxidant activity of the extracts, the formation of derivatives, and much more information. In some cases, they can be used to make special nutrients or other substances leading to further studies. This type of work would add value to the plant being studied by providing additional information about the possible use of the obtained material. The major concern with isolated compounds is mainly the poor bioavailability of the compounds (Boyer & Liu, 2004).

The isolation and purification of phytochemicals from various *Olea* species have been completed in the past as a result of the importance this plant carries in the Mediterranean region and around the world. Phytochemicals such as quinic acid, hydroxytyrosol glucoside, secloganoside, rutin, oleanolic acid glucoside, verbascoside, oleuropein aglycone, hydroxyoleuropein, luteolin 7-oglucoside, oleuropein glucoside isomers 1,2 and 3; 2-methoxy oleuropein, were successfully isolated (Yulizar et al., 2017). The plant studied in this work was *Olea exasperata*. Isolation of phytochemicals in *Olea exasperata* was performed to evaluate what compounds are found in them.

The isolation of phytochemicals is achieved using several isolation techniques including traditional column chromatography, Thin Layer Chromatography, and modern techniques involving the use of computers or probes such as size exclusion chromatography, microwave-induced chromatography, size exclusion chromatography, high-pressure liquid chromatography, and ion-exchange chromatography, gas chromatography, dye-ligands chromatography, hydrophobic interaction chromatography, pseudo-affinity chromatography, partition chromatography, and affinity chromatography. While there are old and new separation techniques, they have an identical mode of separation which only varies in the approach taken to isolate compounds from extracts. The mobile phase is always a liquid or a gas (liquid chromatography and gas chromatography) in most separation techniques, but the stationary phase can be a solid material or liquid material adsorbed on some solid material (Yulizar et al., 2017). The choice of a separation technique is key in achieving the isolation. The method used has to guarantee the sample wholeness so that it is not destroyed before collection.

2.3.1 Extraction technique

before any isolation work, a well-selected technique of extraction has to be considered to guarantee the success of the isolation. The aim of the extraction is of simplifying the complexity of the sample by removing any part of the sample that would form a separate phase or an

impurity in the sample as it is taken further for separation. It has been found that hydro and steam distillation, ultrasound-assisted extraction, pressurised liquid extraction, enzyme-assisted extraction, maceration, decoction (reflux extraction), percolation, soxhlet extraction, supercritical fluid extraction, pulsed electric field extraction, and microwave-assisted extraction have been known as extraction techniques (Rai, 2015).

The most used of these techniques is solvent extraction and it is reported to occur according to the following steps: Solvent penetration in the sample, dissolution of solute into the solvent, diffusion of solvent out of the sample, and collection of the diffused solvent. The principle occurs according to the law of similarity and inter-miscibility which states “Like dissolves like”. Polar solvents tend to better dissolve polar compounds and non-polar ones, while non-polar solvents only dissolve non-polar compounds alone. It thus stands to reason that when separating compounds, it is best to slowly increase the polarity so that the less polar compounds are eluted and collected followed by the most polar ones (Khairnar et al., 2012). Organic molecules are handled in an organic solvent according to the principle “like dissolves like” applied in all extraction work. A non-polar solvent like hexane would extract very non-polar compounds while a very polar solvent will extract both non-polar and polar compounds. The following techniques were reviewed for a better understanding of extraction.

2.3.1.1 Type of extraction techniques:

a) Maceration

Maceration is the simplest extraction technique conducted at room temperature. However, it has the shortcoming of providing a poor yield of extraction. The technique is simple but can be time-consuming as it requires that the compounds be allowed to maximise its contact time with the solvent for efficient isolation to take place at room temperature. The polarity of the solvent could be polar, non-polar, or aqueous dependent on the sample. Maceration uses a substantial amount of solvent, thus, the cost, selectivity, and safety of the solvent should be taken into account before using this technique (Khairnar et al., 2012).

b) Percolation

This is an improved maceration technique in which the solvent is being replaced to avoid its saturation, thus driving the yield higher than the maceration technique. The working conditions are similar, but the use of solvent is substantial although the yield is higher than it is in maceration (Eustis et al., 2006).

c) Reflux extraction

Reflux extraction is known for its high yield over maceration and percolation. The technique requires reasonable time and less solvent. The technique requires heating the sample, thus less energy-efficient and requiring only samples that are heat resistant. The technique is not suitable for thermolabile natural products (Eustis et al., 2006).

d) Soxhlet extraction

The soxhlet technique is an advanced technique of both percolation and reflux extraction. It is an extraction technique that only requires organic solvent and offers both high yield and time-effective extraction. A much higher yield than maceration and reflux extraction can be obtained using this technique. It has the advantage of being automated with a constant supply of fresh solvent, producing a high yield resulting from excessive consumption of solvent to avoid its saturation. Heat tolerant samples are suitable for this technique, which includes natural products, which have an average tolerance for heat (Eustis et al., 2006).

e) Pressurised Liquid Extraction (PLE)

When pressure is introduced to a system using heat for extraction, the rate of extraction is increased. The pressure applied on the surface of the solvent causes the boiling point to shift above the known value. This upward shift in temperature causes the temperature to continue surging causing the rate of infusibility and dissolution. This technique is ideal for a solution whose sample has a poor rate of penetration. It is known for producing repeatable results (Mocanu et al., 2009).

f) Supercritical fluid extraction

The supercritical fluid extraction technique derives its name from the liquid it uses to achieve its mandate. This extraction technique makes use of a solvent that undergoes drastic changes near critical point so that near this point, the small changes in pressure and temperature alter their solvating properties to the point that the solubility of both liquid and gas is increased. The overall effect of this change is a good extraction of all natural products. Carbon dioxide has been widely used as a supercritical solvent for its various physical properties including selectivity, inertness, cost-effectiveness, the low critical temperature of thirty-one degrees

Celsius, and extraction of labile compounds. The technique uses less time for a high yield at room temperature and atmospheric pressure. (Mocanu et al., 2009).

g) Microwave-assisted extraction and Ultrasound-assisted extraction

The ultrasound-assisted extraction or sonication is where ultrasound is used to create cavities to speed up diffusion and dissolution of the solute as well as the heat transfer. This improves the overall extraction efficiency of the system when compared to a normal maceration.
Microwave-assisted extraction however speeds up extraction by making polar organic compounds and water heat up when they come in contact with the microwave radiation. This causes the heat in the vessel to get transferred from one point to another inducing an increase in extraction.

These two techniques are very similar in working conditions, are cost-effective, and suitable for high yield, and have short extraction times (Eustis et al., 2006).

h) Decoction

A decoction is an extraction technique suitable for compounds that can easily dissolve in water. The technique requires the use of samples with no likelihood of damage in water. Volatile compounds are not suitable for this technique. The technique is not time-effective. In addition, it is not energy efficient. It often requires the use of heat at atmospheric pressure. The technique has a low throughput and is thus suitable mostly for polar samples (Makarov et al., 2014).

2.3.1.2 Types of chromatography

As far as separation is concerned, the number of isolation techniques has increased with the development of computers. The type of analyte being isolated commends the type of technique used. Most chromatographic techniques involve the use of a stationary phase and a mobile one. The separation of compounds is a result of the relative motion of compounds or interaction between the stationary phase, the mobile phase, and an analyte. Certain techniques are more suitable for very polar samples and some for less polar compounds. This is dependent on the type of stationary phase used. When the stationary phase is polar, a polar analyte will spend more time on its surface leaving the non-polar one moving relatively faster with the flow of solvent. The same applies to the less polar stationary phase with a less polar analyte. The type of solvent used highly depends on the type of compounds sought after. Good extraction is

often preceded by a process in which the surface area of the extracts is increased by crushing the initial material to a fine powder and then distributed according to various solvent extracts (Sasidharan et al., 2007)

Table 2.1 Summary of Chromatographic techniques

Chromatography	Mobile phase	- Liquid chromatography - Supercritical fluid chromatography - Gas chromatography
	Technique	- Planar chromatography: Paper chromatography, Thin Layer Chromatography, - Column chromatography: Gas chromatography, High-Pressure Liquid Chromatography, Supercritical Fluid Chromatography
	Development mode	- Elution - Displacement - Frontal
	Separation mechanism	- Adsorption chromatography - Affinity chromatography - Ion exchange chromatography - Complexation chromatography - Size exclusion chromatography - Partition chromatography - Micellar chromatography - Ion exclusion chromatography - Countercurrent chromatography

The classification in Table **2**.**1** showed that based on the type of mobile phase used, chromatography can be grouped as follows: liquid chromatography, supercritical fluid chromatography, and gas chromatography. These three techniques respond to the need for different types of solvents. The supercritical fluid technique mobile phase is often used under a pressure of 150 MPa at 50 degrees Celsius with a solid or liquid stationary phase. It is very efficient but requires some use of energy. The technique has a source of heat to heat both the column and the sample. The use of gas chromatography requires samples that are volatile or

which can be converted into volatile materials. The stationary phase is coated in a capillary pipe where the separation is observed. The liquid chromatography technique is used mostly for liquid samples ranging from organic to inorganic (Eustis et al., 2006).

As far as the chromatographic technique is considered, there are only two types of chromatography, namely planer, and column. Both achieve separation but the column has a closed space and the planer is on an open plate. The column has a much higher yield and loading capacity. Thin Layer Chromatography (TLC) uses aluminium or glass as a plate on which a stationary phase is pre-coated before analysis. The solvent moves up the plate placed in a solvent chamber saturated with the mobile phase separating the sample in the process. This technique is often used as an accompanying technique to a column or as an isolation technique, it has been reported in the isolation of steroids, amino acids, and bile acids from urine. Some auxiliary substances have been isolated with Thin Layer Chromatography including preservatives, and pharmaceutical components. It is a cost-effective technique, easy to set up and run. Compounds purified with TLC are often viewed under UV at 366nm and 254nm wavelength. Some practice suggests the use of vanillin followed with charring (Eustis et al., 2006). The column however is loaded with the mobile phase going down under gravity or pump. The technique is used to isolate compounds of various polarities. Many separation techniques are known:

a) Adsorption technique

Adsorption technique is a liquid chromatography technique in which the different materials are retained by their ability to adsorb on the liquid stationary phase fixed on some inert support at different rates of migration. Similar compounds are adsorbing at the same rate allowing their elution. Most organic compounds are collected using adsorption chromatography. This technique has many variables depending on the type of support used as material and sample being analysed (Eustis et al., 2006).

b) Affinity chromatography

Affinity chromatography is working on the ability of the targeted analyte in a given matrix to form a complex. This technique has been used to isolate proteins, enzymes, antibodies, etc. Once a complex between the targeted analyte is formed with the expected analyte, allowing the spectator agent to elute, only the analyte is lastly collected by changing either the pH or the ionic strength through salts. In some cases, it has been referred to as complexation chromatography (Kalyani et al., 2016).

c) Ion exchange chromatography

Ion exchange chromatography isolates analytes from a matrix employing electrostatic forces. These forces retain the analyte of interest on the stationary phase by adjusting the pH, the buffer strength, or the salt concentration. Finally, the isolated compound is collected through adjustment of the retention parameters. Proteins and peptides have been isolated with these techniques (Kalyani et al., 2016).

d) Size exclusion chromatography

Size exclusion chromatography is a technique of separation which isolates compounds based on their sizes. The isolation is based on the ability of particles in the mobile phase to penetrate or diffuse into beads mounted on an inert stationary phase. The small particles tend to spend more time in the stationary phase because they spend more time in the porous beads before they diffuse. The technique thus separates based on size and thus links them to molecular mass. The technique has achieved the isolation of bio proteins and the aggregates thereof, biomolecules, peptides, and sugar alcohols (Eustis et al., 2006).

e) Partition chromatography

Partition chromatography is often the starting point of column chromatography. The separation is happening in a liquid medium forming the stationary phase. The compounds are separated to move into one of the phases based on their solubility. Generally, the polar and non-polar groups are separated so that polar compounds move in the polar solvent and the nonpolar compounds in the non-polar section. This separation never gives rise to pure compounds when the starting materials were made of multiple compound components. It is therefore ideal for a dual system (Zhang et al., 2018).

f) Ion exclusion chromatography

Ion exclusion chromatography is a technique of separation in which resin cations and anions are used to achieve separation of the sample containing either a partially ionised solution or a neutral one based on charge. This technique is opposite to ion-exchange chromatography. In fact, during separation, the positive ions in the sample are separated at the anion resin and the negative charges in the aqueous sample are separated at the cation resin on the stationary

phase. This technique has helped with the isolation of polyalbumin in blood, proteins, biomolecules, polynucleotides, etc. (Biao et al., 2018).

.

g) Planar chromatography and column chromatography

Planar chromatography and column chromatography are widely reported in the early isolation of phytochemicals from various plant extracts. Planar chromatography on aluminium coated with silica or any other stationary phase has been used to monitor the extent of separation being achieved in column chromatography. It provided evidence of separation or evidence for lack thereof. The use of this technique in conjunction with the chromatographic column techniques has been effective, easy to run, however, it is time-consuming (Kalyani et al., 2016).

h) High-Pressure Liquid Chromatography

High-pressure liquid chromatography (HPLC) is the automation of Liquid Chromatography. It is an analytical technique used for the quantification and identification of an analyte. High-Pressure Liquid Chromatography is effective in the determination of evidence of isolation of compounds from natural plant extracts when possessing a standard or when using a preparative mode followed with a collection. An HPLC profile allows establishing evidence that the isolated compound is indeed present. However, it has been reported that not any HPLC can provide the analysis of all the components from plant leaf extracts in a single run due to the complexity of these types of matrices; it was only considered for pure compounds. HPLC has been widely used in extensive isolation and it has provided an accurate exploration of plant extracts (Eustis et al., 2006).

The separation mechanism in Table **2**.**1** had many separation techniques which included some techniques in the previous classification. The parameters used to achieve separation determined the identity of the technique. While the basic mode of operation remains the same, the techniques in this category have little discrepancies in their applications.

2.4 Identification of isolated phytochemicals

The identification of isolated phytochemicals is a challenging endeavour that requires clear isolation of the pure compounds. Proper handling of the separation techniques is key in obtaining pure compounds. The identification of phytochemicals goes by the way of spectroscopy and understanding the nature of the sample. The latter commands that the sample stability in time be known and understood. Many techniques of identification have been

developed such as Ultraviolet-Visible absorption, Fourier Transform Infrared spectroscopy, mass spectroscopy, polarimetry, x-ray diffraction, crystallography, circular dichroism, nuclear magnetic spectroscopy, etc. These techniques and more have been reported to help with the validation of the structure of isolated chemicals. Although they are all very important, there are circumstances where they are not used at the same time. The identification of an unknown compound would require the use of all these techniques, but in the event, the isolated compound has already been known, the minimum use of the spectral technique is needed to find the structure. The use of Infrared and Nuclear magnetic resonance would then be enough to validate the proposed structure (Biao et al., 2018).

2.4.1 Infrared analysis

Infrared Spectroscopy is one of the techniques used to characterise pure isolated phytochemicals. The technique provides evidence of the presence of functional groups or absence thereof through their vibrations recorded with the interferometer of Fourier. The technique provides vibration frequencies relative to various functional groups. Infrared spectroscopy is a complementary technique; it does not provide the relative position of functional groups. It can be used with nuclear magnetic resonance for the full characterisation of phytochemicals. The technique is quick, non-destructive, and cost-effective. It is suitable for organic materials which can absorb radiation. Infrared can also be used to identify isomers due to the sensitivity of the techniques to account for small variations in the structure of the molecule (Freitas et al., 2018). The latest version of the FTIR-ATR, which has an attenuated total reflectance, has improved the sensitivity of the IR measurement by allowing the beam to cross the sample multiple times so that it has higher penetration and reliable results. It has been used to evaluate yeast and micro-organism such as bacteria. The spectrum ranging from 3700 to 500 cm^{-1} is a fingerprint of the molecule in which each peak represents an energy transition and the absorbed radiation. (Savarese et al., 2007).

2.4.2 Nuclear magnetic resonance

Nuclear Magnetic Resonance is a spectral technique developed after World War II to study the structures of organic molecules. In 1971, the technique was able to generate images for medical applications and chemical shifts were used in the structure elucidation of organic molecules. The technique provided chemical shifts that related the position of different atoms C and H in a molecule. The technique is very sensitive so that it requires a small amount of sample, in some cases 1-10 micrograms, to provide an NMR spectrum. It can relate a proton to its neighbouring hydrogen and help provide a network of carbon atoms and their inter-relationship. The peak observed is based upon the ability of the nuclei to generate a magnetic

field of their own which is different from the external one. The ability of this spin to produce a chemical shift or surge of peaks is based upon small variations in a given structure introduced in the NMR field. The technique has led to the analysis of organic and inorganic structures, and to generate high-resolution images in medical sciences (Rajakumar et al., 2016). The use of NMR in structure elucidation has been improved by the use of software and computer models for data processing and generation. These tools help improve confidence in the validation of isolated compounds with a high measure of trust. Unlike other characterisation techniques, NMR is reputed for being non-destructive of the sample. It has a wide range of fields of applications including organic and inorganic to determine ^{15}N, ^{19}F, ^{31}P (Savarese et al., 2007).

2.4.3 Mass spectrometry

Mass spectrometry is an analytical technique based on the determination of the elemental composition of a molecule. This technique is a combination of a chromatographic technique and a mass spectrometry technique. The chromatography section (liquid or gas) separates the sample into various components and the mass spectrometry breaks the separated molecules using an electron ionisation device, which provides the molecular mass reading starting from the molecular ion peak to the other components. The electron ionisation part of the mass spectrometry is standardised to be reproducible in the determination of the components. It is a good technique used to obtain the molecular mass of a newly found compound. It also has an incorporated library of pre-run files to which each scan is compared to provide the extent of similarity (Rajakumar et al., 2016).

The sample preparation in this technique has to ensure that a matrix, which can be turned into gas with the sample is used to guarantee the proper working of the instrument.

2.5 Nanochemistry

Nanotechnology has achieved not only the production of nanoparticles but also the design of materials necessary to create relatively small, cheap, cost-effective, safe, portable, and easy to handle objects. Nano-objects have been widely used recently in medical fields, energy storage, cosmetics, optical devices, sensor technology, catalysis, optical devices, and many other fields. The success in using nanoparticles in many fields has a lot to do with their inherent properties such as optical and biological activities, antibacterial response, etc. (Haroon Anwar, 2018).

In 5000 BC an ancient practice in Indian archives reported the use of metals as a source of active relief from many ailments. The practice was reported to make use of metals such as gold, silver, iron, copper, lead, tin, and some alloys for therapeutic purposes. The Indian classic, Sambita, reproduced this information by providing a procedure in which a fine powder of the metal was obtained by specific guidelines to yield a nano-powder. Some metals were used for internal and others for external applications. Others were applied after forming an alloy from metals to make a more potent drug by additive effect. Therefore, the use of metals was recorded to carry potential in the traditional treatment of ancient civilisation (Galib et al., 2011).

Gold has been known very early in China and Egypt for its decorative properties. It had been used early to build decorative objects like ruby glass, ceramics, and many art objects. The unique optical properties of soluble gold made it the main ingredient in the design of objects. This is still a fact today. The earliest memory of nanoparticles was seen in the Lycurgus cup. This is a dichroic cup known as early as the fourth century AD. The cup was made of two metals, silver, and gold, in the respective ratio of 4:1. The presence of these two metals gave very attractive optical properties to the glass so that when the light was shone from within the cup, it gave a reddish colour and in the absence of light, it was green. The tuning of colour or energy was observed but not grasped. At that time, it was reported that the use of gold metal was confined to its curative power. It was mostly administered as a colloid solution to address epilepsy, heart problems, and tumours as reported by Francisci antonii in 1618. A more recent analysis of the cup particles reveals that the size of the components was 70nm on average (Haroon Anwar, 2018).

2.5.1 Nanoparticles

Particles whose sizes are found in the range of a billionth of a meter in size are said to be in the nanoscale range. Nanoparticles are particles with sizes below 100 nm. Only these particles were studied here. A nanoparticle is larger than an atom and way smaller than an average molecule. Many substances have been used as precursors in nanoparticle synthesis, including metals, inorganic compounds, etc. Silver, gold, etc. are some of them (Eustis et al., 2006).

2.5.1.1 Synthesis of nanoparticles

Nanoparticle synthesis is the process through which nanoparticles are obtained. Two main synthesis techniques can be followed, namely the top-down and bottom-up techniques.

a) Top-down method

The **top-down** method of synthesis involves the breaking down of larger particles into smaller ones through physical processes like grinding, milling particles according to electric potential difference and the viscosity at the surface. The formed particles are then sprayed into the reaction vessel chamber. The technique offers encapsulation efficiency and eases to automate. However, milling requires the use of energy which would induce thermal stress on the formed materials. The product-formed ais ideal for drug delivery matrices (Casasanta & Garra, 2018).

The production of nanoparticles using a laser ablation technique is the most efficient technique known to produce high-quality nanoparticles when top-down techniques are concerned. The nanoparticle size and quality are highly dependent on the quality of the ambient gas and the laser optimization parameters. The laser technique vaporises a metal before depositing it slowly onto some prepared surface. The technique is not cost-effective as it requires high energy input. Many techniques involving the top-down process are known including the metal condensation technique used to make metal oxide nanoparticles by having oxygen for ambient gas like in the previous technique (Rafique et al., 2017).

b) Bottom-up method

The **bottom-up** method of synthesis is the technique in which nanoparticles are into a built-in solution from the interaction of smaller atomic particles. This can either be conducted in the gas or liquid phase (Rafique et al., 2017). In the gas phase, the step involves vaporisation of the precursors, their nucleation, and finally, their growth, while in liquid form, particles are allowed to undergo nucleation then growth, sometimes needing catalysts (Fong et al., 2012).

Nanoparticles are growing from a solution according to thermodynamic and kinetic laws of particle growth. The expected growth of particles is endless in most cases leading to precipitation. Therefore, control of the synthetic process is often a challenge in this kind of research (Rafique et al., 2017).

The bottom-up method in gas form is mostly used by researchers to synthesise nanoparticles being a cost-effective technique, easy to manage and automate in a chain of production. Some of the formed products, polymers and drugs, have been reported to be biodegradable. It has been used to design calcium phosphate microscopic spheres of calcium phosphate. The bottom-up method in liquid form involves nucleation and growth, which may require a catalyst,

then its removal. It is mostly used in biomedical applications and drug synthesis (Eustis et al., 2006).

The use of plants, or the total extract thereof, in nanotechnology synthesis is growing into common practice. Noble metals like iron, gold, cobalt, and others have been successfully synthesised using plant extracts. The use of the total extract benefits from the combined effect attached to the presence of more than one phytochemical present. The case of *Eclipta prostrata* leaf total extract showed that the formed gold nanoparticles were crystalline after confirming with X-ray diffraction and SAED. The formed particles met the criteria of previously formed gold nanoparticles including the Ultraviolet-visible spectroscopy, which occurred at 534nm. Transmission Electron Microscopy provided a micrograph of the formed nanoparticles confirmed the formation of spherical gold nanoparticles. The EDX analysis showed that the formed nanoparticles contained gold. (Rajakumar et al., 2016).

2.5.1.2 Stabilisation of nanoparticles

Stabilizing agents are substances capable of stopping the growth process of particles in solution by either capping them into a matrix, modifying the particle surface tension, or changing the structure of the particles (Kim et al., 2016). The **capping and stabilizing agent** work for both liquid and solid solutions. During growth, one particle carries the potential to grow in any direction to assume any possible shape. In addition to this, it can also grow by agglomeration with other particles. Any change of size in particles results in particles of different properties. In some emulsions, more than one compound is used to maintain the particle size and properties. Thus, the use of stabilising, capping, and surfactants has made a difference in the synthesis of nanoparticles (Kim et al., 2016).

The stabilisation of nanoparticles can also be achieved by mastering the interaction of particles. It is an important aspect in the synthesis of nanoparticle or any substance that grow from solution; In fact, the high surface energy of nanoparticles causes them to be unstable. Kraynov's work in atom surface interaction concluded that the energy reduces when adsorption occurs (Kraynov & Müller, 2011). When interaction among particles causes nanoparticles to attract each other, the nanoparticle will achieve their stability in solution only when they come in contact with one another. The same is true of repulsion. In a normal synthesis, the desired outcome is that nanoparticles remain apart from one another. After synthesis. There are three ways to achieve the stability of nanoparticles in aqueous solution. The first one is steric stabilisation, the second one is electrostatic stabilisation and the third one is electrosteric stabilisation (Zewde et al., 2016).

a) Electrostatic, steric and electrosteric stabilisation

The **electrostatic stabilisation** originates from repulsive electrostatic forces which overcome Vanderwalt attractive forces; in fact, when nanoparticles are placed in the presence of a double layer of electric charge, they are repelled since they share the sameness of charge with the electric double layer. The electron on the surface of the metal attracts a cation and stabilise electronically. The impact of this interaction is not very lasting. **Steric stabilisation** results from the repulsion between particles (molecules) adsorbed on the surface of a nanoparticle. When those repulsions overcome the Vanderwalt forces attracting particle to each other, they can be felt as inducing nanoparticle stability (Kraynov & Müller, 2011) strong steric forces is achieved by electron-deficient metal and an electron pair donating atom such as sulfur, aromatic ring, phosphorus. The strength of a steric stabilisation is function of the size or the shape of the adsorbed unit. Elongated substrates are good for approaching mechanisms and bulky one are especially good for lasting stability (Kraynov & Müller, 2011). Surfactants are good at steric stabilisation. Carboxylic acid and CTAB makes good examples of them. **Electrosteric stabilisation** is a type of stabilisation that results from the combination of both earlier categories. It emanates from nanoparticle's surface modification with a charged macromolecules which achieve both steric and electrostatic effects. It works better for high ionic strength solutions. It is a combination of the two techniques. Silver nanoparticles have been synthesised with polyethyleneimine effectively and showed better stability with this mode when compared with electrostatic stabilisation (Zewde et al., 2016). Next to stabilisation using this technique, there are stabilising agents that can help stabilise nanoparticles including colloids.

b) Stabilising agents and surfactants

There are many categories of stabilising agents used, however, only amphiphilic compounds and surfactants will be discussed briefly because they have a mechanism of action that summarises that of other stabilising agents. Some of the properties of these substances overlap but they are very distinct in action.

The amphiphilic compounds have a dual polarity and often find themselves at the interface of the solvent. When mixed to a solution with dual polarity, one hand of the compounds is on the polar side of the solution and the other is headed in the less polar side of the solvent (Salager, 2002). Some amphiphilic compounds can also act as surfactants when the extent of

polarity versus a polarity falls within the same range. When this equality is not evident, the amphiphilic remain in one phase.

Therefore, the main difference between surfactants and amphiphilic compounds is found in their mode of action. While surfactants operate by lowering the surface tension at the interface between a particle and its solution to stabilise particles, the amphiphilic have polar ends like sulfur, oxygen, phosphorus, nitrogen and sulfate, sulfonate, amines, and nonpolar ends like alkane chains which tend to move at the interface of two solvents (Salager, 2002).

Surfactants are substances stabilising particle growth by the steric effect. Many surfactants are known today including some anionic surfactants, non-ionic surfactants, cationic surfactants, and amphoteric surfactants. The use of surfactants varies so much that their ability to control size is restricted to a few by their surface tension lowering properties. Surfactants produce very stable particles, especially when capping agents are involved (Salager, 2002).

Anionic surfactants are negatively charged substrates that induce a negative charge when in an aqueous solution. It is a build-up of a carbon chain connected to an ionic end such as carboxylic acid. It can be used to repel particles with the same charge form; thus, its use as a dishwasher in the form of dodecyl sulfate (Dave & Joshi, 2017). **Cationic surfactants** are similar in composition to the anionic but they induce a positive charge in solution since they are made up of a positive end. They make good emulsifiers and are used as a disinfectant due to their germicidal properties. CTAB is a good example of cationic surfactants. They are also used as softeners in washing (Mustafa & Hussein, 2020). **Non-anionic surfactants** are not able to dissociate like is the case for ionic ones. They are mostly organic and are safe from water hardness thus their use as grease remover, drug delivery matrix, etc. The last category is the amphoteric one that displays both anionic and cationic properties, they are known as **amphoteric surfactants.** They are both cationic (ammonium) and anionic end (sulfate, carboxylic). Their use is wide and compatible with all the other classes. They have been used as detergents, shampoos, etc. (Fuller, 2018).

The ideal situation desired in this work is to obtain a compound with properties of a reducing, capping, and stabilizing agent embedded in a single compound. Many attempts have led scientists to use reducing agents like sodium borohydride, sodium dodecyl sulfate, sodium citrate, and polyvinyl pyrrolidone. These compounds were reported to act both as reducing and stabilizers. The interest of surfactants in nanotechnology comes in because they are used in nanoemulsions as emulsifiers (Dave & Joshi, 2017).

2.5.1.3 Green nanochemistry

The idea behind departing from toxic products to ones that are more friendly to consumers and the environment has been regarded as a green way of consuming a product. The concept is not limited to plants alone as many fields have already borrowed the concept including the motor industry, which is using the term “green” in association with better sources of energy such as EV engines over fuel-based engines. It equally applies to the use of solar energy over the use of fuel to produce electricity. In chemistry, when reactions or changes that are conducted lead to more environmentally friendly materials and products, this practice is considered “green” in its approach. The same can be said about the use of plant extracts instead of chemicals generally used in pharmaceutical industries. Apart from the preventive and disease inhibiting properties of some plants, they are also known for their ability to reduce metal ions to their metallic form. The observed reduction of silver nanoparticles in the presence of plant extracts suggested that there are compounds in plant extracts that are responsible for the reduction of the silver ion to its reduced form (Reda et al., 2019).

The use of plants in the synthesis of gold nanoparticles has been reported toxic in some studies. The toxicity has been reported to be related to the choice of taxonomy, the size of nanoparticles, the shape of the formed nanoparticles, and the delivered dosage (Taylor et al., 2014). While the toxicity has been recorded in certain taxon, it is not a generalised observation that disqualifies gold nanoparticles because they are widely used as a drug delivery matrix and in imaging with no record of negative side effects. (Tao, 2018). It was this use of plants in nanotechnology that led to the green approach or green nanochemistry involving water as a synthetic medium (Choi et al., 1993). Green chemistry in this context is thus a science at the interface between two fields, phytochemistry and nanotechnology and it provides the benefits of both to combine the two fields to make nano-sized products that carry great potential in nanomedicine (Pathway et al., 2014).

2.5.1.4 Reducing ability of phytochemicals

The term reduction refers to metal reduction from a higher oxidation state to its lower one for the extraction of metals. The use of reduction is going to be relating to the decrease in oxidation state observed in metal cations when reduced from a higher oxidation state to a lower one as they are brought in contact with plant extracts. While this process occurs electrochemically in metallurgy with very high cost, in this step, it is monitored at room temperature with the solution changing colour when a shift in oxidation state is fulfilled to lower oxidation state. Other

successful attempts include the use of species like fungi and bacteria in the synthesis (Swain, 2016).

The ability of plants to reduce metals is not new; a concept known as bio-reduction and phytomining affirms the genesis of these concepts. In phytomining, plants are used to extract precious metals from land that are not easy to mine by extracting them from the soil through a natural process. Much of the metals obtained had the size falling into the nanoparticle range (De Jong & Borm, 2008).

Metal reduction by plant extracts yields particles with relative stability. The observed stability is highly dependent on the type of reducing agent, capping agent, and type of metal used. The mode of reduction also contributes a great deal to the stability of the formed nanoparticles. The limitation observed in the reduction of metals using plant extracts has a lot to do with the stability of the final product. Therefore, a careful choice of these various parameters determines the type of stability observed for the yielded nanoparticles. Since this is a new field, only experimental data would determine which proportions are ideal for proper stabilisation.

The synthesis of gold nanoparticles with plant extracts proved that phytochemicals can be used both as a reducing agent and stabilizing agent toward the synthesis of gold nanoparticles (Freitas et al., 2018). However, the use of the total extract has had limiting effects on the very study that should bear witness to the ability of the plant extract to be used as a cure. In fact, a plant contains more than one phytochemical; using it raw in the reduction of metal ions provides no understanding in the study of the mechanism of reduction of metal ions, nor does it help in the identification of the species responsible for the reduction of the gold nanoparticles. The identification of the specific compound responsible for the reduction of gold ions would serve a greater purpose of predicting the reactivity of the reaction and the rate thereof for one compound. (Nadeem et al., 2017). Much work has been done on the isolation of pure compounds toward the synthesis of gold nanoparticles, while some works have covered certain sub-fractions such as antioxidant-rich methanol extracts and the flavonoids rich n-hexane extracts in the formation of some gold nanoparticles. Others have used pure compounds such as phenols, flavonoids, benzophenones, and anthocyanin from *Garcinia mangostana* (mangosteen) to form stable and biologically active gold nanoparticles (Apu et al., 2012).

2.5.1.5 Characterisation of nanoparticles

The characterisation of synthetized nanoparticles is a very important step in obtaining meaningful information about the formed particles. The discrepancies in the type of reducing agent, solvent, temperature, etc. would be resolved by monitoring the properties of the formed nanoparticles. In some cases, the shape, size, and properties are better understood through this step. The most commonly used instruments to characterise nanoparticles are Ultraviolet-Visible spectroscopy, High Resolution-Transmission Electron Microscopy, Fourier Transform-Infrared (FTIR) spectroscopy, X-Ray Diffraction, Energy Dispersive X-ray spectroscopy (EDX), size distribution by intensity, and zeta potential, (Rajakumar et al., 2016).

a) Ultraviolet-Visible spectroscopy

Particles below a hundred nanometers cause the atoms to get closer to one another so that electron interaction increases between the two atoms. The outcome of this arrangement is the confinement of electrons and an increase in surface area, which leads to an increase in the bandgap. (Dabbousi et al., 1997)

Nanoparticle synthesis produces particles of various sizes and shapes. The change in particle size and shape has been reported to have a great effect on the ability of nanoparticles to tune the energy band of the nanoparticles. Gold nanoparticles undergo a shift in optical properties the moment part of the gold associates with a reducing agent. There is an increase in the optical band so that nanoparticles are used as a diagnostic tool in tumour detection. In nanoparticles, gold has a bandgap that is way larger than the bulk gold so that the transition of electrons in the nanoparticle is more pronounced than what it is in a normal gold atom (Eustis et al., 2006).

Pure and homogeneous precursors in synthetic reactions would produce specific and predictable shapes, sizes, and colours of nanoparticles when the free energy involved in the synthesis and the dielectric is kept unchanged. Most nanoparticles tune the energy gap throughout the visible region. In fact, the formation of gold nanoparticles is confirmed when the solution colour turns from green or yellow to a red colour. This feature has helped scientists trace nanoparticle formation using UV visible spectroscopy. At the nanoscale, the surface plasmon resonance is characteristic of some specific size and shape of nanoparticles. This phenomenon is not reproducible for particles whose size goes beyond 100nm.

Elements with an unfilled d electron have their electrons moving around so that at the nanoscale, the size of the particles is smaller than the wavelength of light. Electrons on the surface of the particles interact with light to cause electron oscillations. The vibration frequency of the electron changes on the particle surface. This is the origin of the term surface plasmon resonance. The recorded frequency is changing with the size, shape and dielectric of the medium. Any modification to the solvent or the dielectric medium will affect the ability of the medium to accommodate the electron and thus the frequency of the electrons. These factors are the source for the existence of a surface plasmon resonance and its effects are depicted in Figure 2.1 (Eustis et al., 2006).

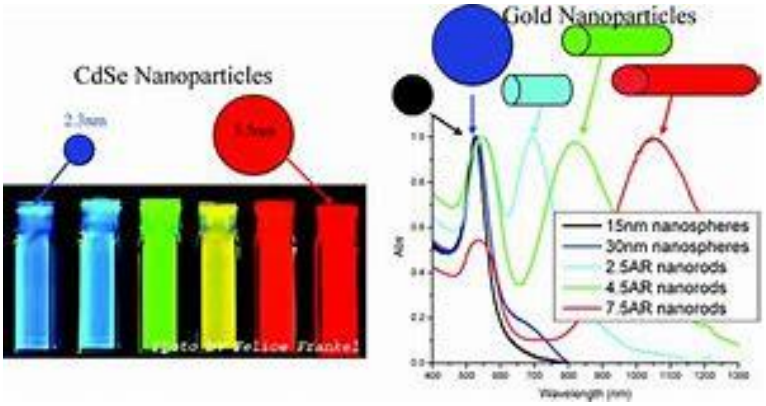

Figure 2.1 Surface plasmon resonance shift as a function of colour of CdSe nanoparticles in solution . The various bands observed were a result of the different shapes and sizes of CdSe nanoparticles.

As presented in Figure 2.1 by Dabboussi, (Dabbousi et al., 1997).The shape of the nanoparticle is dictating the range of absorption. At about 540nm, spherical nanoparticles are observed. At shorter frequencies or higher values of wavelength, the rod shape is prominent. Observing more than one absorption is proof two nanoparticles with different shapes coexists in the vessel (Eustis et al., 2006).

The direct consequence of an increase or decrease in the size of the nanoparticles is shown in the shift, red or blue, of the plasmon. Experimental data has revealed that larger particles undergo a redshift and smaller particles have a blue one. Many factors can affect the observed shift including the type of reducing agent and the metal ions being reduced. When the size of the particles exceeds a certain limit, the solution turns colourless. (Dabbousi et al., 1997).

The unique optical properties of nanoparticles help with the monitoring of absorption and scattering of light leading to the plasmon resonance curve of the nanoparticle. The absorbance curve collected would provide information about the state of agglomeration of particles, the refractive index of the medium, the approximate size, concentration, and the shape of the

particles. But in this work, only the evidence of nanoparticle formation was sought for by observation of the UV curve.

A vast number of materials are manufactured based on their optical properties to determine their purity, their energy conversion ability, etc., and this applies equally to nanoparticles because they have been reported to have well-defined energy bands relating to their size and extent of aggregation. (Dabbousi et al., 1997).

A reported synthesis of gold nanoparticles formed using *Leucosidea sericea* (Badeggi et al., 2020) had a variable surface plasmon resonance changing with the concentration of the reducing agent. It reached its highest absorbance of 540nm in UV light at a given concentration of *Leucosidea sericea* reducing agent. In addition, besides the absorbance changing, it was also observed that the solution at the optimal concentration was pink-red unlike the solution away from the optimal conditions (Bankar et al., 2010).

The synthesis of gold nanoparticles using *Polyscias Scutellaria* leaf extract as a reducing agent has provided nanoparticles with surface plasmon resonance ranging between 510 and 580nm. The formed nanoparticles were a red solution. It was reported that at a higher concentration of reducing agent, a better formation of gold nanoparticles was observed, thus a higher absorption of the light of the UV spectrum, and beyond a certain threshold, the particle undergoes sedimentation as a result of rapid agglomeration (Yulizar et al., 2017). Deraedt reported the use of solution with a poor concentration of gold nanoparticles in the presence of sodium borohydride as a reducing and capping agent to afford gold nanoparticles with 3 nm of size in solution. The formed gold nanoparticle absorbed light at 514nm for nearly a month without sedimentation (Deraedt et al., 2014).

b) X-Ray Diffraction

The use of X-Ray analysis on nanoparticles is a means to do structural analysis and provide crystallographic information. The measurement is also compared with the SAED data to verify the compliance and similarities (Rajakumar et al., 2016).

X-ray diffraction is a simple and quick technique used to determine the crystallinity and structure of the particles. In addition to this, the technique can be used with other techniques such as the Warren-Averbach method, which provides a correlation with the electron microscopy data. This method provides an alternative way to estimate the size of the formed nanoparticle. Three methods are commonly used to determine the sizes of gold nanoparticles

namely Scheerer, Williamson-Hall, and Warren- Averbach. They have been reported to give close estimates of volume-averaged size with weight. Thus, this data are approximate since the measurements do not account for the discrepancies in size (Dorofeev et al., 2012). It has been used to determine the type of crystal synthesised or the identity of the metal through the diffraction pattern.

In an attempt to find the crystallinity of the formed gold nanoparticles, X-ray analysis was conducted while measuring the diffraction pattern of *Polyscias Scutellaria* leaf green extract gold nanoparticles made with $NaAuCl4.2H_2O$. It was found that the two theta angles recorded for the diffracting fringes and compared to the one in literature were noticeably matching the reference. Yulizar reported 38.013°, 48.140°, 69.448°, and 77.418° diffraction angles (Yulizar et al., 2017). Those data have been consistent for both gold nanoparticles reduced with reducing agents from plant extracts and those from inorganic chemicals (Lidiawati et al., 2019).

c) Average size and Zeta potential

The average size of the nanoparticles is a measure of the mean value of size between the largest and the smallest one. The determination of zeta potential was a means of determining how stable the particles were in solution. Tantra related the concentration of nanoparticles and size to its zeta potential and observed that as the sample became diluted and small in size, the change in zeta potential was no longer affected by size and concentration. The solution under investigation had all its particles suspended and recorded a negative value of zeta potential between -43 and -56 mV. He called this a stable region (Tantra et al., 2010); therefore when a negative value of zeta potential is observed in a reading of nanoparticle solutions, the belief is that the particles are very stable and suspended uniformly. The more negative this value, the more stable the emulsion in the solution. This is the reflection of how well dispersed and suspended particles are in solution. Rajakumar et al., 2016 measured the zeta potential of his gold nanoparticles and found they had approximately the value of *eclita prostrata* leaf to be -17.4 mV. The literature revealed that the size of particles obtained with sodium borohydride was smaller than 5nm (Deraedt et al., 2014) compared to the one obtained with organic reducing agents, which was between 5 to 20 nm. In addition, the stability of the nanoparticles formed by sodium borohydride showed high stability for nearly a month (Yulizar et al., 2017).

d) High-Resolution Transmission Electron Microscopy

The High-Resolution Transmission Electron Microscopy (HRTEM) is an imaging tool that helps collect images of materials. HRTEM has been very useful in the study of nanoparticles and

many other fields of study such as chemistry, material science, botany, biology, and nanotechnology, etc. Most nanoparticles formed have been analysed using the Transmission Electron Microscope. The instrument has helped visualise nanoparticles made from gold, iron, cobalt, silver, and many others and has also helped establish the specific shape of nanoparticles, the texture thereof, the extent of aggregation, monitoring of nanoparticle synthesis, and extent of completion. The design of the TEM instrument in 1934 provided a better resolution for particles at very low magnification and more information about the phase, crystallography, structure, and composition of the sample.

The technique has been improved by including additional detectors on the instrument to allow other analyses to be performed, such as Convergent Beam Electron Diffraction (CBED), Energy Dispersive X-ray spectroscopy (EDX) for elemental analysis, the High Angle Annular Dark Field (HAADF) mode and the Selected Area Electron Diffraction (SAED). Each one of these analyses has made the TEM a very important technique in the analysis of nanomaterials with the SAED being complementary to XRD (Ruitao et al., 2016). The Selected Area Electron Diffraction function provides diffraction patterns that are necessary to determine the crystallinity of the particles. When crystalline materials are analysed, a diffraction pattern is observed to attest to this fact and when it is not observed, a lack of bright spots in the pattern is also proof the material is amorphous (Ruitao et al., 2016).

The HRTEM has been widely used in the study of gold nanoparticle shape, sizes, and formation layout (distribution). At very low magnification, one can observe the general shape or the overall distribution of particles. Gold nanoparticles have been reported to be mostly spherical and their size varied with the type of reducing agent used. The micrographs allow for a statistical study of particles to be done according to the normal distribution of particles. (Lidiawati et al., 2019).

e) Fourier Transform Infrared (FTIR) analysis

The FTIR technique provides evidence about the functional groups being present or absent in plant extracts toward the synthesis of gold nanoparticles. In an attempt to view what happened to the FTIR peak after the synthesis of gold nanoparticles using banana peels, a shift in wavenumber on the IR spectrum was observed after synthesis (Bankar et al., 2010). It is known that when the right amount of reducing agent and gold salt is used, there is no room for the excess amount of reducing agent, thus not all the peaks should be expected after synthesis. In the synthesis using serial dilution, the formation is very likely to reach a place where stoichiometric proportions are brought together in the synthesis. The change occurring with the absorption can help determine functional groups responsible for the reduction of gold salt.

In general, the contribution of the carbonyl and hydroxide group is important to the synthesis as mentioned in the synthesis using aqueous *elaise guineensis* leaf extract as a reducing agent, the peak intensity was reduced (Ahmad et al., 2016) . In addition, Rajiv reported that IR can be successfully used as a signature of a compound in the fingerprint region (Rajiv et al., 2017). Some peaks are reported to shift right or left after the nanoparticle is formed giving evidence of a change in energy. Reda made this observation with banana peel extracts used in the synthesis to make silver nanoparticles (Reda et al., 2019).

2.6 Application of nanoparticles as Nanomedicine

The use of conventional drugs has sustained life for years. In the early beginning, medicinal plants were used for their healing benefits before moving to conventional ones. Now, however, the record of recurring drug resistance on medication has been reported to be a defining factor to the longevity of the drugs on the marketplace. The increased resistance of drugs causes some products to be taken off the market as they grow weaker with time. To address the situation, scientists increase the dosage of medication to make them more responsive. This increase comes along with the danger of turning the drug toxic toward the patients. In addition to this, the existence of conditions requiring specialised types of drugs such as HIV, tuberculosis, and cancer, calls upon an innovative approach to drug design in the future (De Jong & Borm, 2008).

The innovative approach to the drug design suggested in this work refers to nanoparticles as a potential future cure. These are species with particle sizes ranging between 1-100nm. The nanoparticles used in medicine are referred to as nanomedicine. Nanomedicines are cost-effective and display properties such as better solubility, infusibility, and a fast mechanism of action, as needed in an ideal drug. Some nanoparticles offer the advantage of being optically active so that they can be used both as diagnostic tools and as medication but also above all, they have small sizes, which allow them to penetrate cells that were difficult to penetrate with other drugs (Boxall, 2004). Due to their ability to bind, carry and absorb other organic molecules like proteins, they can be used as drug delivery matrices. Nanoparticles are therefore good for targeted drug delivery to deliver drugs into specific targets like cancer cells (De Jong & Borm, 2008).

Nanomedicines obtained from plants have been reported to improve the bioavailability of the drug while reducing the toxicity of the drug in the bloodstream. Although this is foreign in the case of conventional medicines, the nano-carriers have been reported to bypass the acidic medium as well as the liver’s actions (De Jong & Borm, 2008). The use of plant-based

nanoparticles will have the additional benefit of being biodegradable after use, soothing the toxicity related to the use of drugs found in the environment. In the pharmaceutical industry, dendrites, colloidal nanoparticles, inorganic, and metal nanoparticles, magnetic nanoparticles, etc., have been used (Ansari et al., 2012). However, this work will focus on metal nanoparticles prepared from plant extracts.

The use of the nanoparticles toward biomedical testing would require a plant with biological activity to be selected. Most phytochemicals can cause some changes in biological systems as a result of their presence therein, making them bioactive substances. In addition to this, many known substances display these functions in humans as soon as a small fraction of the substance reaches the blood of a patient. When this occurs, the substance is said to be bioactive.

Therefore, in this work, a plant will be selected to explore if it holds the observed potential to form bioactive nanoparticles, and hence possibly obtain stable biodegradable, bioavailable drugs toward biomedical studies as it has been observed with preceding successful cases. This synthesis will avoid the use of toxic chemicals as much as possible to obtain green products. In addition, to obtain a product with minimal impact on the environment, water will be used as a dispersant and medium instead of chemical solvents that could lead to environmental pollution.

2.6.1 Biological studies

The study of biologically active compounds in plant extracts is key to knowing the specific responses extracts have on the living organism. The finding is necessary for describing the exploration. The type or class of compound used can provide a specific type of biological response. For instance, an antioxidant stops the deterioration of living cells via oxidation. In the same way, the corresponding gold nanoparticles formed by a reducing agent from a class or type of compound produce the corresponding outcome. There is also a direct relationship between the shape and size of nanoparticles with the obtained biological response. A reducing agent with a specific response has its response improved when delivered in the form of a gold nanoparticle. Gold nanoparticles specifically made from plant extracts have been known to undergo the Enhanced Permeability and Retention (EPR). The uptake of nanoparticles below 15nm is a confirmation of their specificity in response (Kovalerchuk & Schwing, 2004).

Since there are many types of biological activities, the choice made on one technique over the other is highly dependent on the activity being assessed. As much as this depends on the

reducing agent, the biological evaluation seeks to determine the ability of specific species to have their biological activities enhanced or reduced. There are many types of bioassays including antimicrobials, antifungal, cytotoxicity, etc., however, in this work, only the cytotoxicity with normal and cancer cells were studied (Aljabali et al., 2018).

The use or exposure to nanoparticles brings some risks associated with their toxicity. Evaluating these risks in human cells is cost-effective, requires a simplified cell design, and is easily reproduced by conducting trials on grown cells in an experiment known as cell culture (Lewinski et al., 2008). Cells are used in place of primary living cells and offer the benefits of being pure, easy to handle, cost-effective, and is of unlimited supply. The use of these cells in vaccines and drug elaboration has helped overcome many barriers related to ethical testing. The use of cells has been reported to require special care because a cell doesn't always reproduce like the natural cell (Noireaux et al., 2019).

Cytotoxicity is a biological response recorded when species are brought in touch with a cell membrane. These responses could be cell death, synthetic inhibition, and binding prevention, enzymatic prevention, etc. The rate of proliferation or variability is reported to be a good indication of a cell's health. Since a special interest was shown in this work in cell destruction, cell death was contemplated here (Picchio et al., 2020). The cell death caused by cytotoxicity would be due to exogenous or endogenous causes. This death can be caused by physical, chemical, or biological effects. Since cytotoxicity is a means of evaluating the toxicity of substances and the safety of substances being analysed, it provides information on the viability of the tested species in a living organism. The technique is sensitive to the environment in which it is conducted. Temperature, pH, concentration, and the environment affect cell culture therefore a proper control of the environment (presence of dyes, pH of wastes, etc.) is to be maintained to ensure reproducibility of results (Lewinski et al., 2008).

The death of a cell can be uncontrolled or controlled. Controlled death of cells is a study that allows one to make important conclusions about the viability of cells or the toxicity or safety of the causing substance (Istifli, 2019). Some cell deaths are related to the size of the gold nanoparticles. Das et al. reported necrosis of cells when 1.4nm gold nanoparticles were used. The gold nanoparticles were less toxic between 2 and 20ppm. Cytotoxicity tests seem to work well with gold nanoparticles because they can report on the safety of particles as a function of size. Cell toxicity has also been reported to be linear with gold nanoparticle concentration. This fact has qualified them as an analyte of the inductively coupled plasma (Das et al., 2011).

When a cell is exposed to the presence of a substance and this causes no damage to it, the substance is considered nontoxic and safe. This substance could be a nanomaterial, in this case, which would then imply that it is safe to use for that specific substance. The notion of selectivity in response is very important when looking at toxicity. A biologically active substance presenting no toxicity is the best-case scenario of the desired drug. In fact, it has no lethal action on the cell but delivers its biological properties.

Many types of tests evaluate cytotoxicity depending on what is being measured. Since the colour indicators provided information of the state of the cell during the experiment or the variable thereof, the classification of the different types of cell viability and cytotoxicity will be related in the classification. They are:

2.6.1.1 Luminometric assay

The luminometric assay is a simple and quick form of cytotoxicity that is used to study a cell's proliferation. The technique is monitored using luminometric microplates. The technique is easy to automate. The ATP assay, which uses adenosine triphosphate (ATP), is one of the luminometric techniques in which the measurement of light intensity is proportional to the amount of ATP formed by the cell. Since the relationship is linear, the technique is used to monitor any proliferation in which ATP is generated to glow in the presence of the magnesium ion. The same principle applies to the real-time viability assay in which the enzyme luciferase is added to the culture to enhance its shininess so that the cells are measured in real-time in the continuous mode (Picchio et al., 2020). The technique offers the benefit of it being the fastest cytotoxicity test, and yet very sensitive. However, the precision of the technique comes from the error in pipetting.

2.6.1.2 Dye exclusion:

The dye exclusion method is a widely known technique reputed for providing the proportion of viable cells. They are identified on the basis that viable cells exclude dye. This technique can also help make a statement on the state of the membrane. Dye exclusion methods make use of eosin, Trypan blue, erythrosine B, Congo red, etc. Dye exclusion techniques offer the advantage of being heat sensitive. The technique is simple and sensitive. It requires a small number of cells. Dye exclusion is not suitable for monolayer cell culture. Trypan Blue dye exclusion assay is one of the known dye exclusion techniques. It is used to measure cell viability. The name of the technique was sourced from the test compound which is a large negatively charged molecule. This technique is applicable for suspensions to evaluate the

ability of a sample to absorb the dye. All viable cells are colourless while the dead ones are coloured blue. The technique is simple, inexpensive, and used to assess the health of cell membranes and yet it has an inherent error associated with the counting tools. The second most widely used dye technique reported was the Erythrosine B dye exclusion assay (Picchio et al., 2020).

2.6.1.3 Colourimetric assays:

A colourimetric assay is a measurement of cell activities employing biological markers. The evidence of cell viability or cytotoxicity for cell lines analysed with colourimetric assays is confined to samples that are suspended and adsorbed easily. The technique is very simple to perform, easy to market, and cost-effective. (3-(4,5-dimethylthiazol-2-yl)-2-5-diphenyl tetrazolium bromide, (MTT) assays is the most common colourimetric assay and the most used cytotoxicity technique providing cell viability by providing information of mitochondrial activities through enzymatic activities. MTT assay provides analysis by turning purple in the presence of an oxidizing agent. It is safe and very reproducible. It has been termed better than dye assays. The other colourimetric assays were MTT assay, WST-1 assay, DH assay, WST-8 assay, NRU assay, XTT assay and MTS assay. All these techniques have a test agent, which by a specific principle, was capable of producing colour which is measured by a spectrometer (Picchio et al., 2020).

2.6.1.4 Fluorometric assays

Fluorometric assays are well-known techniques focusing on the measurement of cell viability and cytotoxicity. It is carried out using any fluorometer or any device that could measure fluorescence. The technique is suitable for cell lines that suspend in solution. Fluorometric assays are more sensitive than the preceding techniques. Alamar Blue assays are fluorometric assays in which a dye resazurin, a non-fluorescent substance is made fluorescent through a redox reaction. It is a non-expensive technique, However, the toxicity and interfering nature of the test compound is not accounted for. CFDA-AM assay is another fluorometric method using a test substance namely 5-carboxyfluorescein diacetate acetoxymethyl ester. This assay is specific for plasma membranes (Picchio et al., 2020).

In short, the choice of any one of the assays or cytotoxicity techniques is very much dependent on the ability of the technique to be reproducible and easy to do and the non-interfering nature of the test agent. The MTT assay in the work of Steckiewicz et al reported that the concentration and shape of gold nanoparticles affected the viability of cells (Steckiewicz et al.,

2019). The real-time polymerase chain reaction (PCR) test has been used along with other techniques to evaluate the biocompatibility of gold nanoparticles (Rajakumar et al., 2016). A biological study of compounds with trypan blue assay extracted from Olea revealed that lutein and its glucoside derivatives showed the highest inhibition activities against cancer cells followed by oleuropein, hydroxytyrosol, and its acetates.

Cell uptake has been a technique in which some gold nanoparticles are taken up in cells to evaluate the host viability after they have induced a physical change. The uptake in question is reported to depend on nanoparticle diameter and the mode of uptake (Steckiewicz et al., 2019).

3. CHAPTER THREE

METHODOLOGY

3.1 Introduction

The methodology section presents the steps taken, materials used, and instruments employed to select the *Olea exasperata* plant leaf and isolate some of its phytochemicals. It further showed how the obtained compounds and *Olea exasperata* extract were identified, used and characterised after the synthesis of green gold nanoparticles from extracts and pure compounds.

3.2 Collection and identification

The aerial part of *Olea exasperata* was collected on the CPUT campus on 18th July 2017 and identified by Dr Davis at the Horticulture department on the updated list of endangered species on the 13th June 2019 and as was declared to be of least concern being ubiquitous in South Africa.

3.3 Materials used

An analytical grade of sodium tetrachloroaurate (III) dihydrate ($NaAuCl_4.2H_2O$) was sourced from Merck (South Africa) and used as a source of gold. A Millipore water purification system Elix 3 UV Water Purification System (120 V/ 60 Hz) Millipore was used to obtain ultrapure water.

Organic solvents used in isolation included methanol (MeOH), ethanol (EtOH), hexane, dichloromethane (DCM), ethyl acetate (EtOAc), formic acid, acetic acid, butanol. They were supplied by Merck (Cape Town, South Africa). The Thin Layer Chromatography (TLC) analysis was conducted on pre-coated aluminium paper with the silica gel 60 PF_{254} to produce a normal phase TLC (Merck, Cape Town, South Africa). Column chromatography was run using both silica gel 60 (0.063 – 0.200 mm) as a stationary phase in the chromatographic column and sephadex LH-20 (Sigma-Aldrich, South Africa). The solvent used for TLC was a mixture of (ethyl acetate, formic acid: acetic acid, and water) in the respective proportions (100: 6.5: 6.5: 12.5). Dimethyl sulfoxide (DMSO) was supplied by Merck, Cape Town.

The spots on the TLC were checked under UV λ 366 and 254 nm. Substances not absorbed under these wavelengths were further made visible by heating gently an immersed plate in vanillin solution prepared by combining: 250 mL ethanol, 15.0 g vanillin powder, 2.5 g sulphuric acid. The plate was dried using hot air to make the compounds visible under normal light

3.4 Extraction and isolation of phytochemicals from *O. exasperata* leaf extract

Fresh plant materials (~ 1.0 kg) were left to dry in the shade for two weeks. The dry plant materials were powdered and extracted with 80% methanol at RT (~25 ^{o}C) for two days. After filtration, the extracts were evaporated under reduced pressure at 55 ^{o}C.

The total extract 113.8 g (10.04%) was then subjected to column chromatography using a solvent system according to Table 3.1. The silica gel column was eluted by order of increasing polarity using a mixture of DCM: MeOH and collecting 250 mL fractions.

Table 3.1 Chromatographic extraction of *O. exasperata* total extract (Main fraction)

N^{O}	DCM	MeOH	H_2O	Total volume
1	100%	-	-	1L
2	98%	2%	-	1L
3	96%	4%	-	1L
4	94%	6%	-	1L
5	92%	8%	-	1L
6	90%	10%	-	1L
7	87,9%	12%	0,1%	1L
8	85,5%	14%	0,5%	1L
9	83,3%	16%	0,7%	1L
10	81,2%	18%	0,8%	1L
11	79%	20%	1,0%	1L
12	73,5%	25%	1,5%	1L
13	68%	30%	2,0%	1L
14	62%	35%	3,0%	1L
15	56%	40%	4,0%	1L
16	49,5%	50%	5,0%	1L
17	0%	100%	0%	1L

The isolation of pure phytochemicals was achieved using either silica gel or Sephadex column chromatography. The latter is a separation technique where a gel is used to isolate the compounds. It has been widely used in the separation of nucleic acids, enzymes,

polysaccharides, and proteins and the former uses the Sephadex gel to separate compounds based on their difference in size (Ó'Fágáin et al., 2017). The technique was used with the water-saturated butanol prepared by mixing 10% of water with butanol. The Sephadex column was used in an isocratic elution mode without changing the concentrations of the solvent nor the mobile phase compositions.

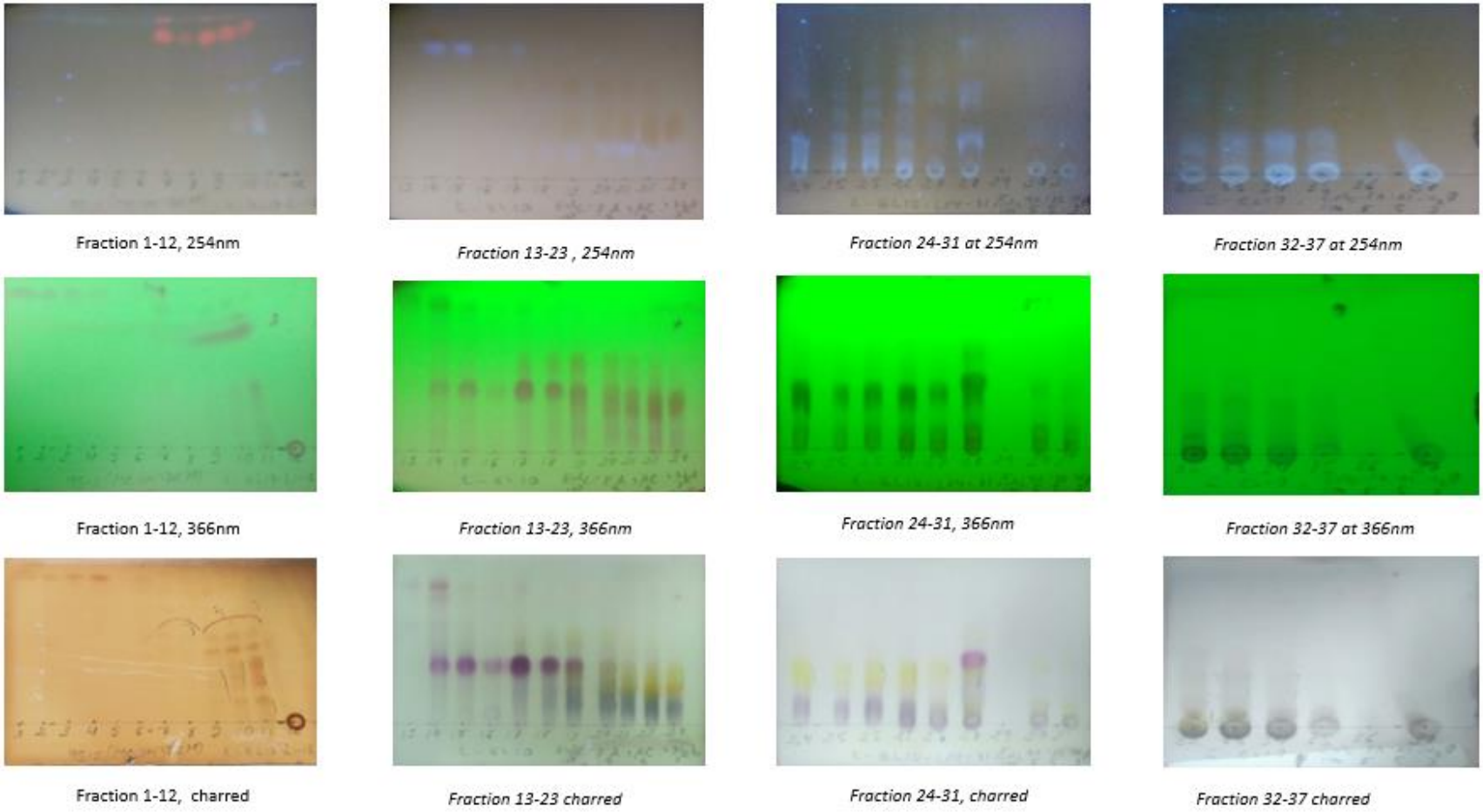

Figure 3.1 Preliminary chromatographic column fraction's TLC fractions under UV (254nm, 366nm, and heated plate with vanillin)

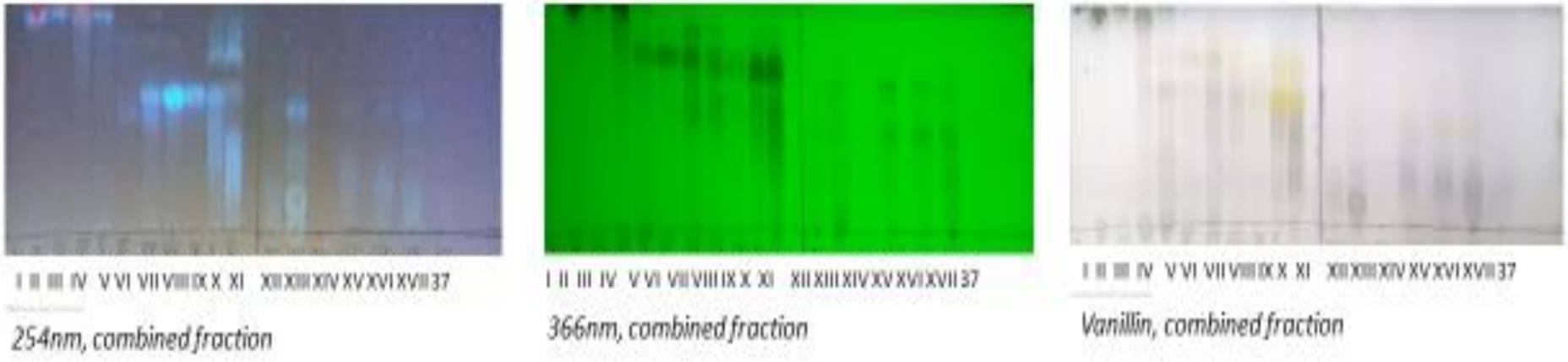

(A) **(B)** **(C)**

Figure 3.2 TLC of combined fraction in Figure 3 1 leading to sub-fractions I to XVIII at 254 nm (A), 366 nm (B), and (C) vanillin charred plate

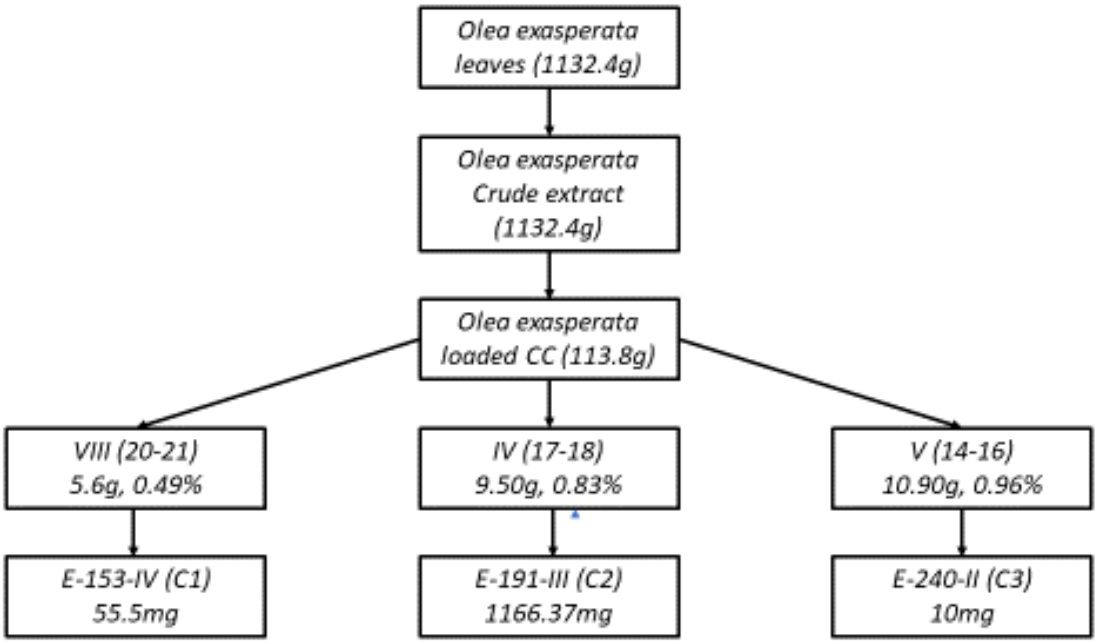

Figure 3.3 Pure phytochemicals isolation pathway and yields

3.4.1 Lyophilisation of total extract

Lyophilisation is defined, in a nutshell, as a technique used to dry dissolved samples in water. It operates through sublimation at extremely low pressure. At this pressure, the boiling point of the solvent is so low that ice turns into vapour without a transition to liquid form. Thus, water is removed from the container leaving its labile solute intact. The choice of this technique has been motivated in the past by the need to make a sample last longer in solid form without alteration, but mostly, it is for the need to separate the solute from its aqueous solvent. In this experiment, it was carried out in two-step processes namely pre-freezing and evaporative freezing. The choice of this technique was related to its ability to preserve the biological properties of the sample before and after freezing for a long time period. It has been widely used in the food industry for its ability to preserve the taste of food for long periods (Khairnar et al., 2012). The technique was thus carried out as follows:

Plant leaves of *O. exasperata* were weighed accurately and allowed to dry. Approximately 50 g of the dried leaves were crushed with a blender and 50 mL of boiling distilled water was added to it to form a 1 mg/mL solution. The solution was homogenised for 30 min with a stirrer at approximately 115 rpm until cooling to room temperature. The solution was filtered using a funnel and cotton before its transfer into a falcon tube. The extract in the falcon tube was then centrifuged for 60 min at 5000 rpm. The centrifuged product was filtered through a 0.45

microliter filter mounted onto a syringe and placed into a clean and sterile 50 mL falcon tube. The 50 mL solution was recovered and filtered before being frozen to zero degrees and then to -80 degrees Celsius in 24 hours. The frozen material was placed into a low-pressure machine for lyophilisation immediately after it was removed from the fridge. The instrument was used at a pressure of -117 mT and a temperature of -54 ℃. Two days later, the dried lyophilised materials were collected as a powder and used in subsequent synthesis to evaluate their nanoparticle forming abilities. The experiment was conducted on 96 well plates to evaluate these properties at different concentrations in a serial dilution manner. The Ultraviolet-Visible was run to evaluate the formation of gold nanoparticles in the presence of serially diluted 1mM $NaAuCl_4.2H_2O$. The reducing agent was diluted by two from one cell to its consecutive one. When the synthesis of the nanoparticles showed that only specific concentrations formed nanoparticles, the determination of an optimal concentration was necessary for the next steps of the synthesis.

3.5 Characterisation of Isolated compounds

Characterisation of isolated compounds was completed using Infrared spectroscopy (Perkin Elmer 100 model in transmission mode) and Nuclear Magnetic Resonance (NMR). NMR spectra were recorded at 20 ^{o}C, using deuterated DMSO-d_6 on a Bruker Advance 400 MHz NMR spectrometer (Germany). Chemical shifts in ppm of ^{1}H (δ_H) and ^{13}C (δ_C) were determined relative to dimethyl sulfoxide (DMSO) as an internal reference.

3.5.1 Isolated phytochemicals

a) Isolation of compound 1(C1)

Main fraction VIII to XII (1048.9 mg) were subjected to three simultaneous Sephadex columns using water-saturated butanol as an isocratic system to yield 55 mg of compound **1**, (as presented on the TLC presented below).

Table 3.2 Fraction collected from the column of C1

Code	Combined fraction code	Solvent sat. Butanol (mL)	Mass recovered (mg)
1-21	I	50	14.2
22-27	II	50	21.4
28-32	III	50	8.1
33-37	IV	50	5.8
38-42	V	50	6.0

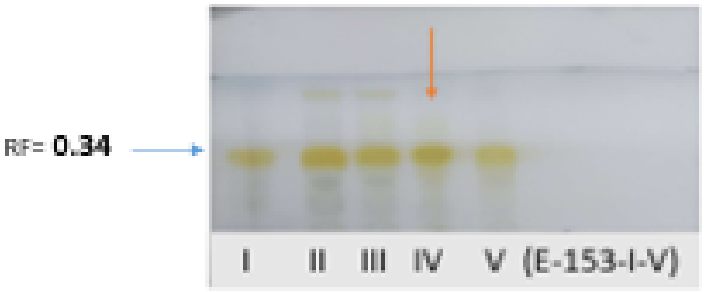

Figure 3.4 TLC featuring a pure C1 in a vanillin charred plate

b) Isolation of compound 2 (C2)

Main fraction VI (6.4248 g) (Figure 3.3) was applied to a silica gel column to yield eleven fractions when ethyl acetate, methanol, and water were used as solvent system to yield 3.1387 g of the fourth fraction. This fraction was then applied under the same condition to obtain 1166.37mg of compound 2.

Table 3.3 Chromatographic column of fractions collected from the column of compound 2

DCM (mL)	EtoAc (mL)	MeOH (mL)	Volume (mL)
20	80	-	200
10	90	-	200
-	100	-	300
-	99	1	200
-	98	2	200
-	97	3	200
-	96	4	200
-	95	5	200
-	94	6	200
-	93	7	200
-	92	8	200
-	91	9	200
-	90	10	200

Table 3.4 Pure fraction collected from the column of compound 2

Code	Combined fraction code	Solvent H2O: But-ol (mL)	Mass recovered (mg)
1-23	I	50	0
24-30	II	50	22.27
31-43	III	50	942.7
44-99	IV	50	189.4
100-104	V	50	12.0

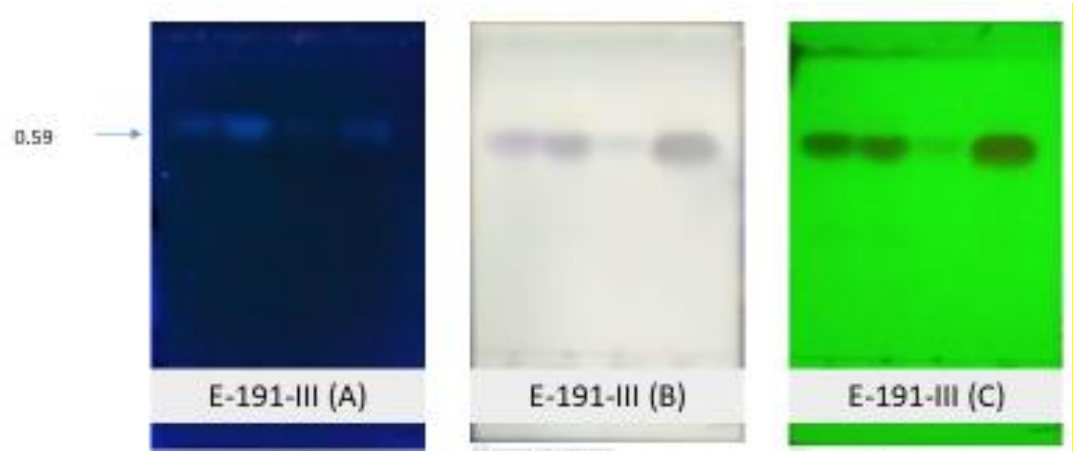

Figure 3.5 TLC of Compound 2 at 254nm (A) vanillin charred plate (B) and 366nm (C)

c) Isolation of compound 3 (C3)

Main fraction V (4.4474 g) (Figure 3.3) was applied to a silica gel column using a gradient elution of ethyl acetate: methanol. The column ran from 100% to 85% of ethyl acetate. After 85%, 0.5% of water was added till it reached 2% of water while maintaining ethyl acetate at 85%. This column produced 11 fractions from which the fraction of interest weighed 33.11 mg of a compound which was taken through a Sephadex column using 10% water-saturated butanol in an isocratic system, whereas 10.3 mg of compound **3** was isolated.

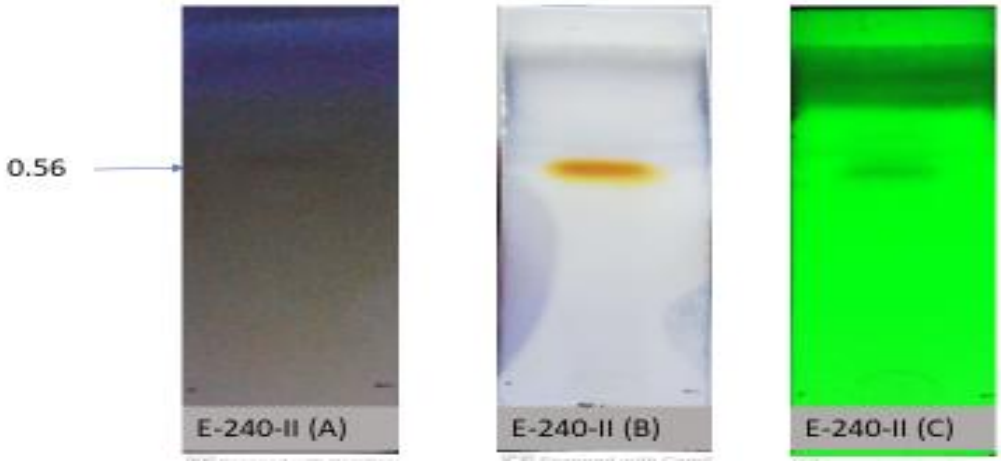

Figure 3.6 Thin layer chromatography structure of compound 3

3.6 Nanoparticle synthesis

3.6.1 Preliminary formation of gold nanoparticles from *O. exasperata* total extract

10.0 mg of *O. exasperata* leaves were crushed in a blender and transferred to 50.0 mL of boiling distilled water for maceration at 100 degrees Celsius. The extract was allowed to be in contact with water for 30 minutes before filtration and collection using a Buchner funnel. The filtrate, a liquid, was then collected under a vacuum. 8335 µL of the obtained freeze-dried material from 1 g/mL filtrate or reducing agent was added to a 10 mL round-bottom flask containing 1667 µL of distilled water and 1mM of $NaAuCl_4.2H_2O$. The reaction was allowed to proceed for beyond an hour at room temperature while monitoring the extent of the formation of gold nanoparticles using the UV-VIS.

The initial solution, which was slightly diluted in the reducing agent, showed some colour change due to nanoparticle formation. The change in colour from green to red was a positive confirmation of gold nanoparticle formation at around 540nm when the UV analysis was run. TEM, XRD, EDS analysis were run to evaluate the outcome of the reaction. The limitation like the total extract led to the lyophilisation thereof.

3.6.2 Determination of optimal concentration through serial dilution of lyophilised *O. exasperata*

16.00 mg of the lyophilised aqueous extract was transferred to a 500 µL Eppendorf (32 mg/mL). 500 µL of water was added to the sample in the Eppendorf and was centrifuged for 3 min at about 10000 rpm until the dissolved extract has been freed from solid impurities. A

sterile 96 well plate was prepared for serial dilution using a 250 µL micropipette. 50 µL of the homogenised extract was placed in the well (A and B of line 1). In line 1, 50 µL of distilled water was added from well B to the last well in this line. Using the micropipette, 50 µL solution of the homogenised solution was added to well B to form 100 µL in well B. This mixture was homogenised and 50 µL was taken from it to the following well where the same process was repeated. This process went on until the end of the line. The last 50 µL taken from the last well was discarded. This allowed a serial dilution of the homogenised extract to be achieved. Finally, 250 µL of gold salt was added throughout line 1 in each well till the end. The plate was then covered with aluminium foil, placed in the oven at 80℃, and was allowed to shake at 40 rpm for an hour. It was then allowed to cool down and analysed with a UV spectrophotometer (Spectro STAR) to determine which well-formed gold nanoparticles were by observing the wavelength against absorption at which they absorb UV light. The completion of this step was expected to lead to a meaningful conclusion about the optimal concentration at which nanoparticles formed. The mass of extract in the wells decreased from 32.0 mg to 16.0 mg, 8.0 mg, 4mg, 2.0 mg, etc. and the gold solution was 1 mM throughout.

3.6.3 Nanoparticle synthesis using pure compounds

Nanoparticle synthesis using isolated compounds was one of the key priorities of this work. It was conducted using the serial dilution technique in a 96 well plate and followed the synthesis route provided in section 3.6.2. In fact, 50 µL of 32.0 mg/mL of reducing agent (in this case, compound*)* were diluted by a fraction of two till the concentration of 0.0625 mg/mL in the presence of 350 µL of $NaAuCl_4.2H_20$ (1mM) to form gold nanoparticles. The formation of the nanoparticles from lyophilised material was characterised using UV, XRD, size and zeta potential measurement evaluation, SAED, histogram, EDX, TEM and IR analysis.

3.7 Characterisation of gold nanoparticles

3.7.1 Ultraviolet-Visible

The UV data were collected using the UV/Vis SPECTRO star. This UV absorption instrument was manufactured by LABTECH. It was designed with an ultra-fast absorbance spectrophotometer interacting with samples either in the cuvette, microplates, and Lvis plate in which the instrument can measure up to 1526 wells, but in the current work, only 96 microplates well were utilised. The design of the instrument included a multi-function shaker that could homogenise the sample in an orbital, and linear motion. A temperature controller function was available in case the incubation of the sample was needed. The instrument was

built to handle low volume samples and was designed to measure the endpoint signal, the kinetic as well as scan. All these modes open the instrument to many biological applications in which it could be used to measure cell growth, DNA and many other known physical chemistry techniques.

The screening process was completed with 96 well-plates in which lyophilised leave extracts were placed in a serial dilution manner in the presence of gold salt to measure the possible UV absorption of the gold nanoparticles and determine the effectiveness of the plants to form gold nanoparticles. The use of the UV instrument was mainly to evaluate the shift in plasmon resonance that occurs in solution when a solution goes from having only colloidal particles to nanoparticles.

The formed nanoparticles were transferred into a 300µL sterile 96 well plate using a 1000µL micropipette. The sample was collected after the formation of gold nanoparticles. Since the UV technique was not destructive to the sample, the sample was recovered after analysis.

3.7.2 X-ray diffraction

The instrument used to evaluate the crystallinity of the sample was the X-ray diffractometer AXS D8 model. The instrument was accessed at Ithemba labs and offered precision of the measured data.

The gold nanoparticle sample was loaded onto a 1 cm^2 glass cut using a diamond blade. The sample was loaded repeatedly until enough amount of gold was placed on the surface of the glass. It was allowed to dry in the oven at 50 degrees after each time fresh gold nanoparticle solution was added.

3.7.3 Size and Zeta potential distribution

The measurement was conducted using the Malvern Zeta sizer instrument. The technique was based on the ability of small particles to intensify light as light interacted with them in their random motion. The Stoke-Einstein relationship is used in the instrument to link light scattered to particle sizes. This technique provided very reproducible results that could be used to monitor the size of particles successfully. A second analysis that was conducted in this work was the electrophoretic light scattering. This is the zeta potential measurement, where the mobility of particles is measured on an electrophoretic scale. Since all particles cannot fit on

that same scale, a conversion was made for comparison's sake. This is the origin of the zeta potential scale often utilised (Malvern 2019).

The sample used for UV was also used for zeta potential analysis by transferring the solvent using a micropipette from the UV cell to the zeta potential sample holder. The sample was introduced into the sample holder by turning the holder upside down before the liquid sample went over the curve. Once it did, the holder was kept straight up and was filled so that no bubble was noticed in the curved sample holder. The size measurement was achieved by transferring the sample into a 1mL cuvette and fitted in the Malvern sample holder.

The size distribution was a measure of the various sizes versus their intensity present. This measurement often provided an average value. In addition to size, the zeta potential was measured. A negative value of zeta potential was a sign that the particles formed were negatively charged and thus repelled each other so that they are partially stable. The more negative this value, the more stable and homogeneously distributed the particles are. Thus the recording of this measurement was good enough to attest formation of stable and well-distributed particles.

The measurement of size and zeta potential were key in the determination of both size and stability of the formed gold nanoparticles. The particles formed were evaluated by the type of graph obtained but mostly by the averaged value reported by the instrument. In fact, the negative charge in the diffuse layer was thick enough to have the particles well repelled against each other to produce a stable solution (Eustis et al., 2006)

3.7.4 High-Resolution Transmission Electron Microscopy

The instrument used in this work to collect micrographs was accessed at the University of the Western Cape (UWC). A TECNAI F20 High-Resolution Transmission Electron Microscope, operated at 200Kv was used. The use of the HRTEM was mandatory for better monitoring of the shape and distribution of the formed gold nanoparticles (Cema, 2019).

The TEM sample was prepared by dropping the liquid sample containing gold nanoparticles onto a carbon-coated Cu-grid. The grid was then allowed to dry for a few minutes under a lamp. After drying, the sample was covered to prevent any contamination.

The data collected from the TEM analysis were processed using the ‘’ImageJ’’ software. This processing tool was used to count and draw a histogram of the gold nanoparticles obtained (Ruitao et al., 2016).

3.7.5 IR spectroscopy

The FT-IR ATR was used to do the infrared analysis. The instrument offered the benefit of running liquid samples. When solid samples are analysed, they are placed on a diamond ring and held unmoved with a clamp. The liquid sample containing gold nanoparticles was placed on the sample holder without clamping. The instrument sample holder was cleaned with methanol in between sample changes.

3.8 Biological studies

The biological studies covered in this work included cytotoxicity (MTT assay) and a stability study of the gold nanoparticles and the Olea extract gold nanoparticles. The MTT assay was restricted to *Olea exasperata* extract, the gold nanoparticles thereof, and the oleuropein-based gold nanoparticles. In fact, the KMST-6 (human normal fibroblast) and HT-29 (human colon cancer) were maintained in DMEM (Lonza, Cape Town, South Africa) supplemented with 1% penicillin-streptomycin (pinstripe) (Lonza, Cape Town, South Africa) and 10% Fetal Bovine Serum (FBS) (Thermo Scientific, Ansfrere, South Africa). The cells were incubated in a 37 °C humidified incubator with 5 % CO_2 saturation.

The cytotoxicity evaluation of the Oleuropein, Olea exasperata extract, and Olea-AuNPs were monitored using MTT assay as previously reported with modifications (Sun et al., 2019). First, 20,000 cells of all the tested cell lines were seeded in 96 well plates for 24 hrs. Then the culture media were replaced with the increasing concentrations of the samples up to 100 µg/mL. The cells were incubated for 24 hrs after which the media were replaced with 100 µL of MTT (5 mg/mL diluted with DMEM 1:10) (Sigma-Aldrich (Cape Town, South Africa) for 3 hrs. To dissolve the formazan, 100 µL of DMSO was added and the UV absorbance of the formed purple solution was measured at 570 nm (POLARstar Omega microtitre plate reader, BMG Labtech, Ortenberg, Germany).

The stability study of oleuropein and the *Olea exasperata* gold nanoparticles was monitored respectively with the POLARstar Omega microtitre plate reader, BMG Labtech, Ortenberg,

Germany). The gold nanoparticle was synthesised by mixing *Olea exasperata* extract and the gold salt $NaAuCl_4.2H_20$ in the ration 1:5 at 80 degrees Celsius.

4. CHAPTER FOUR

RESULTS AND DISCUSSION

4.1 Introduction

The phytochemicals isolated from *Olea exasperata* extracts and their characterisation were presented in this section. Gold nanoparticles were synthesised from the isolated phytochemicals and *Olea exasperata* extracts.

4.2 Isolation and chemical characterisation of *Olea exasperata* phytochemicals

The chemical compounds isolated here were hydroxytyrosol, oleuropein, and hydroxytyrosol glucoside. The use of pure precursors provided a meaningful way to improve the understanding of the synthesis of gold nanoparticles at such a level of purity whereby the effect of the other compounds was removed in this way.

4.2.1 Chemical characterisation of compound 1 (C1)

Compound **1** was isolated as an orange powder and its chemical structure is provided in Figure 4.1.

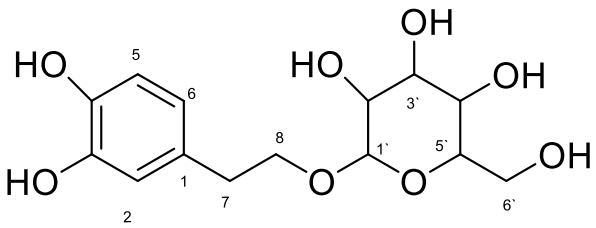

Figure 4.1 Chemical structure of Compound 1

The Infrared spectrum in Figure 4.1 showed a vibration at 3300 cm^{-1} (OH), which was assigned to hydroxide group rocking. The infrared vibration at 2800 cm^{-1} was assigned to an sp^3 hybridised carbon (C-H). The aromatic proton was observed at 1600 cm^{-1}. The vibration at 1050 cm^{-1} was assigned the (C-O) stretch as presented in Figure 4.1

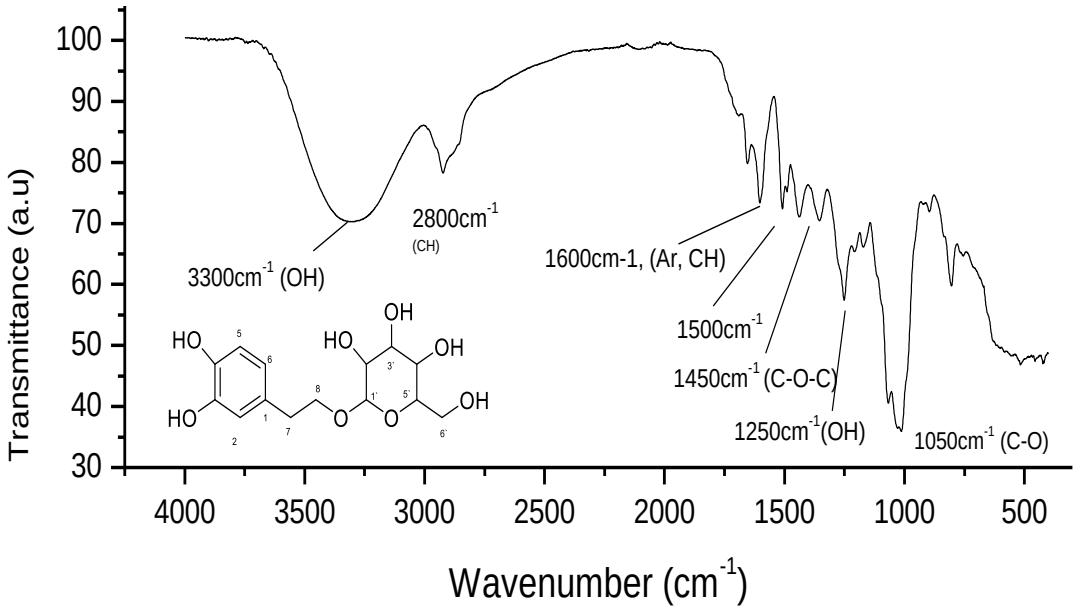

Figure 4.2 Infrared spectrum of Compound 1 confirmed the presence of the functional groups observed in the inserted structure

The proton nuclear magnetic resonance (^{1}H NMR) spectrum of compound 1 (Figure 4.3) showed signals at δ_H 4.2 (*d*, *J*= 7.6Hz), which correspond to the anomeric proton on the sugar.

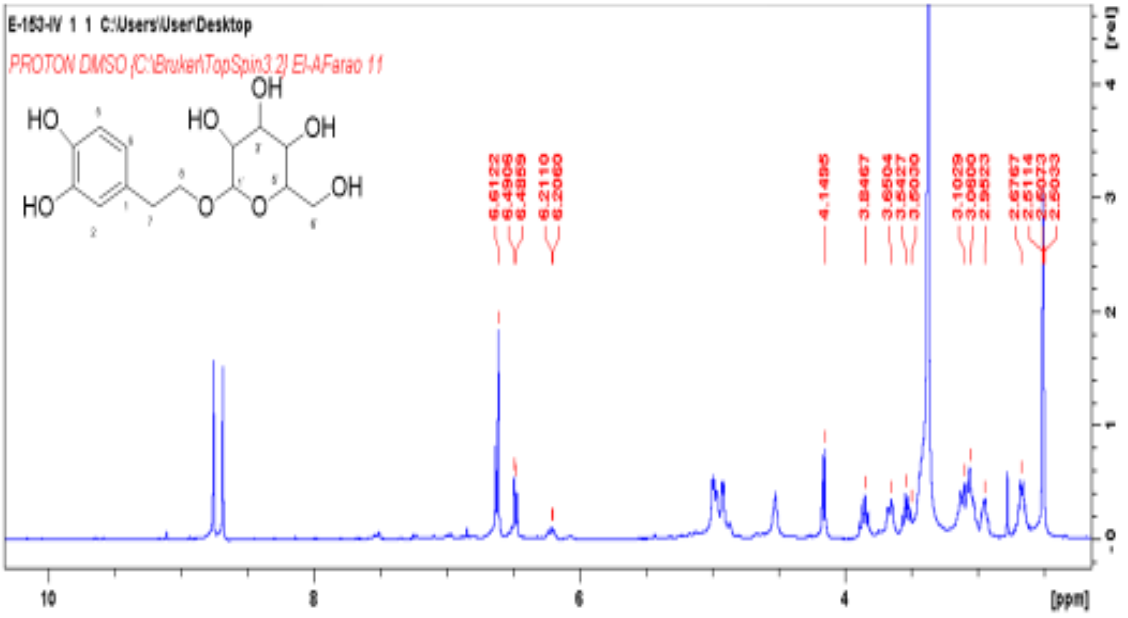

Figure 4.3 ^{1}H-NMR (400 MHz, DMSO) spectrum of Compound 1

In addition, methine groups (CH) were seen on the sugar in the interval δ_H (2.00-3.88). The hydroxytyrosol unit had three aromatic protons, δ_H 4.18 (*t*, *J*= 7.6Hz), 2.82 (t, *J*= 7.6Hz), 4.2 (*d*, J=7.6Hz).

The carbon ^{13}C NMR (Figure 4.4) and DEPT-135 (Figure 4.5) spectra showed 14 carbons, classified as three methylene at δ_H 69.9, 34.9, 60.8 ppm Three quaternary proton carbons were observed on the aromatic ring namely 129.0 ppm, with the two most deshielded by their hydroxyl group being 144.8 ppm and 143.3 ppm. The anomeric carbon was observed at 102.6 ppm and the carbon in the sugars was between 70 ppm and 76.82 ppm. Finally, three carbons δ_H 116.1, 115.2 and 119.3 ppm were aromatics.

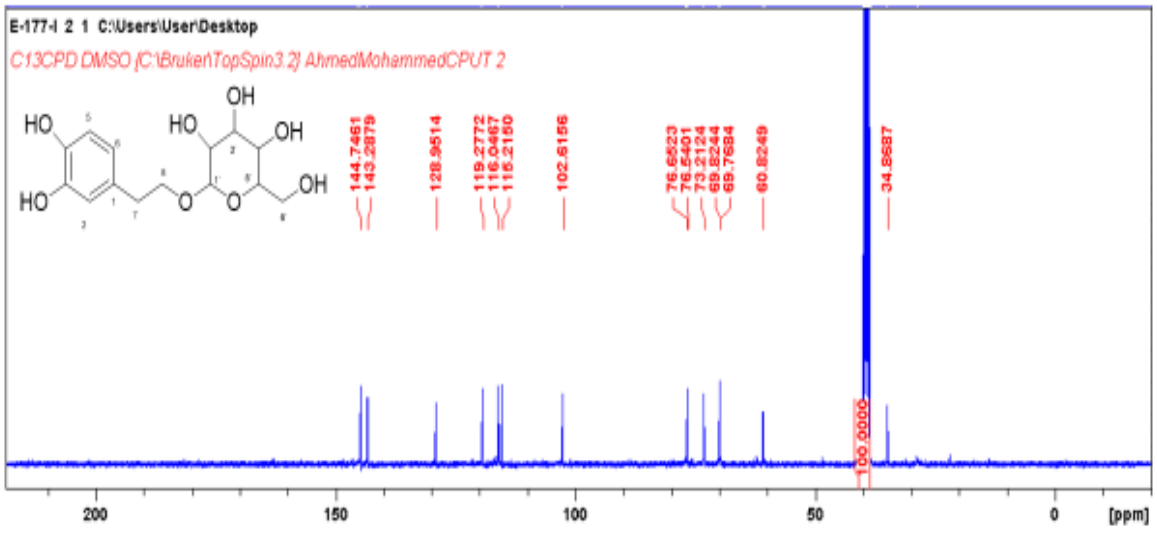

Figure 4.4 ^{13}C-NMR (400 MHz, DMSO) spectrum of Compound 1

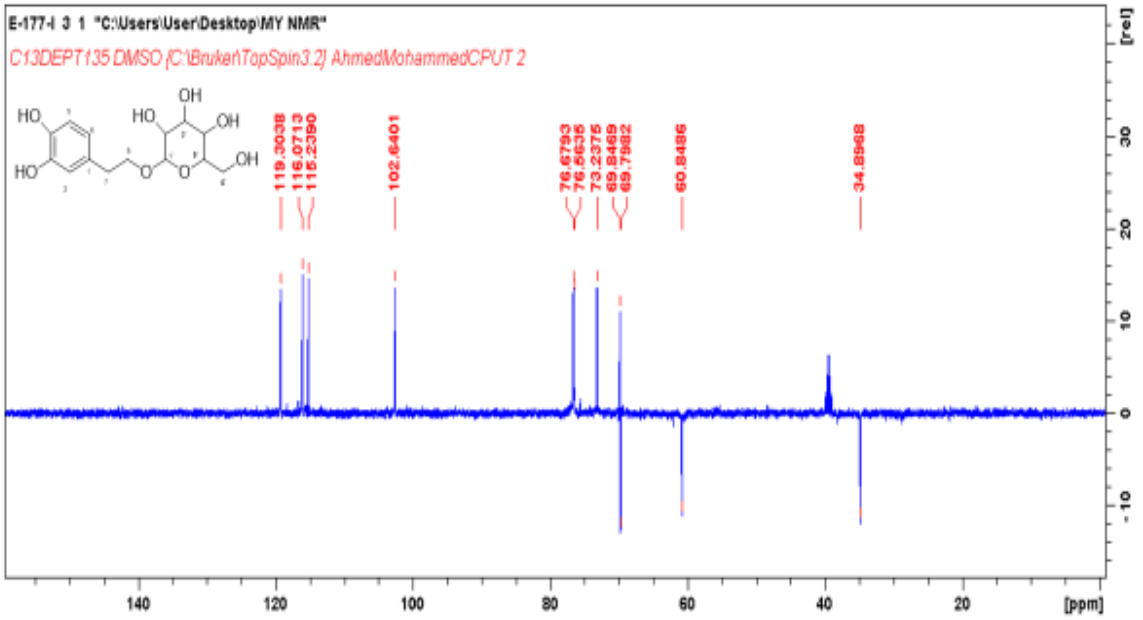

Figure 4.5 DEPT135-NMR (400 MHz, DMSO) spectrum of Compound 1

Figure 4.1 is a detailed summary table for all the chemical shifts of the NMR analysis. It revealed that the observed structure was similar to the hydroxytyrosol 4'-β-D glucoside (Romero et al., 2002), its chemical shift was more close to hydroxytyrosol 1'-β-D glucoside (Líter et al., 2019).

Table 4.1 ^{1}H and ^{13}C NMR spectroscopic data assignments (400 MHz) for C1 (δ in ppm, m, J in Hz) in DMSO

Nº	Experimental (DMSO-d_6)		Reported data (DMSO-d_6)	
	^{13}C NMR (ppm)	^{1}H NMR (ppm, *J*, Hz)	^{13}C NMR (ppm)	^{1}H NMR (ppm, *J*, Hz) **
1	129.0	-	129.2	
2	119.3	6.60 (*d*, .1.7)	119.5	6.73 (*d*, 1.8)
3	144.8	-	145.0	
4	143.3	-	143.5	
5	116.1	6.61 (*dd*, 8.0, 1.7)	116.3	6.62 (*dd*, 8.0 1.8)
6	115.2	6.67 (*d*, 8.6)	115.5	6.75 (*d*, 8.0)
7	69.9	4.18 (*t*, 7.6)	70.0	4.19 (*t*, 8.0)
8	34.9	2.82 (*t*, 7.6)	35.1	2.78 (*t*, 8.0)
1`	102.6	4.2 (*d*, 7.6)	102.9	4.53, (*d*, 7.9)
2`	76.7	(2.00-3.88) *	76.8	(2.00-3.88) *
3`	76.6		76.9	
4`	73.2		73.4	
5'	69.8		70.1	
6`	60.8		61.1	

*Overlapping signals; **(Goulas et al., 2009)

After careful analysis of all the spectra, it was found that the compound isolated was consistent with the structure of hydroxytyrosol 1'-β-D glucoside.

4.2.2 Chemical characterisation of Compound 2 (C2)

Compound **2** was isolated as a white powder with a chemical structure presented in Figure 4.6.

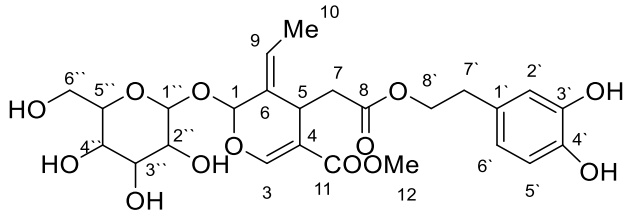

Figure 4.6 Chemical structure of oleuropein

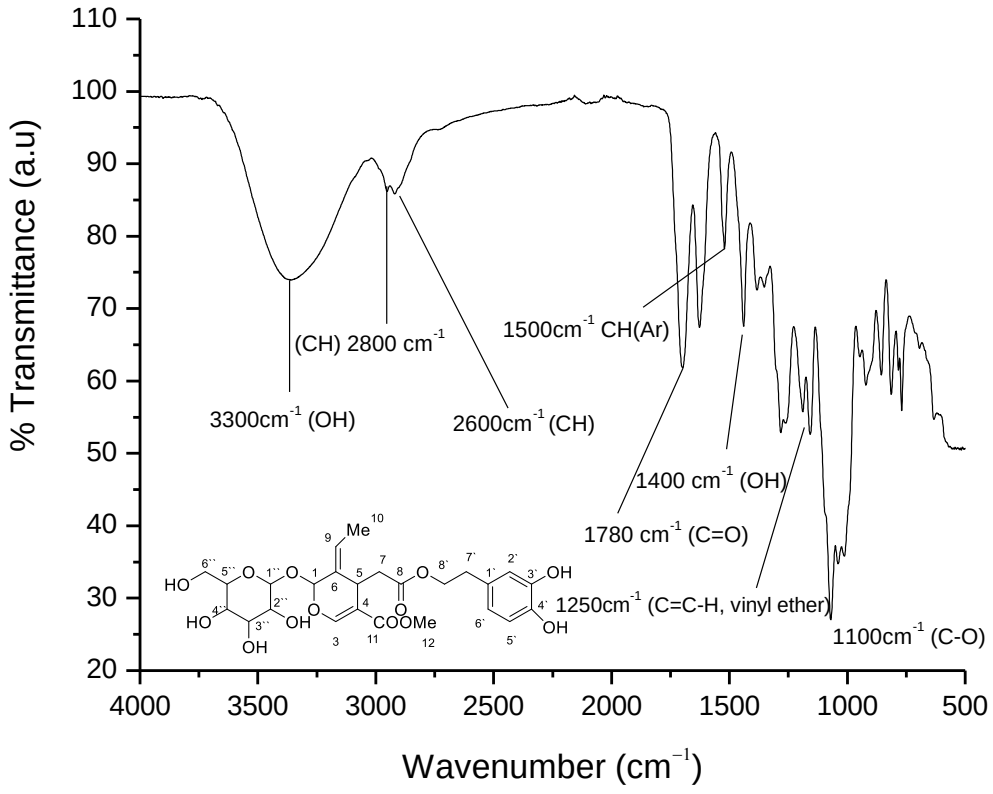

Figure 4.7 Infrared spectrum of Compound 2 confirmed the presence of all the functional groups of the inserted structure

The IR spectrum in Figure 4.7 showed the following functional group stretches and vibrations: the hydroxyl group was ascribed to the band at 3300 cm^{-1} (OH), the CH sp^2 was assigned the stretch at 2800 cm^{-1} (CH), the sp^3 CH was assigned the rocking at 2600 cm^{-1} (CH). The aromatic protons rocked at 1500 cm^{-1} (C-C=C-, Ar), the carbonyl on the ester was ascribed the stretch at 1780 cm^{-1} (C=O), and finally, the (C-O) stretch was assigned to 1100 cm^{-1}, the stretch on the COO^- was seen around 1400 cm^{-1} and the stretch at 1250 cm^{-1} was that vinyl ether stretch (Rajakumar et al., 2016). This analysis provided evidence of the existence of chemical functions in Figure 4.6 (Rajakumar et al., 2016).

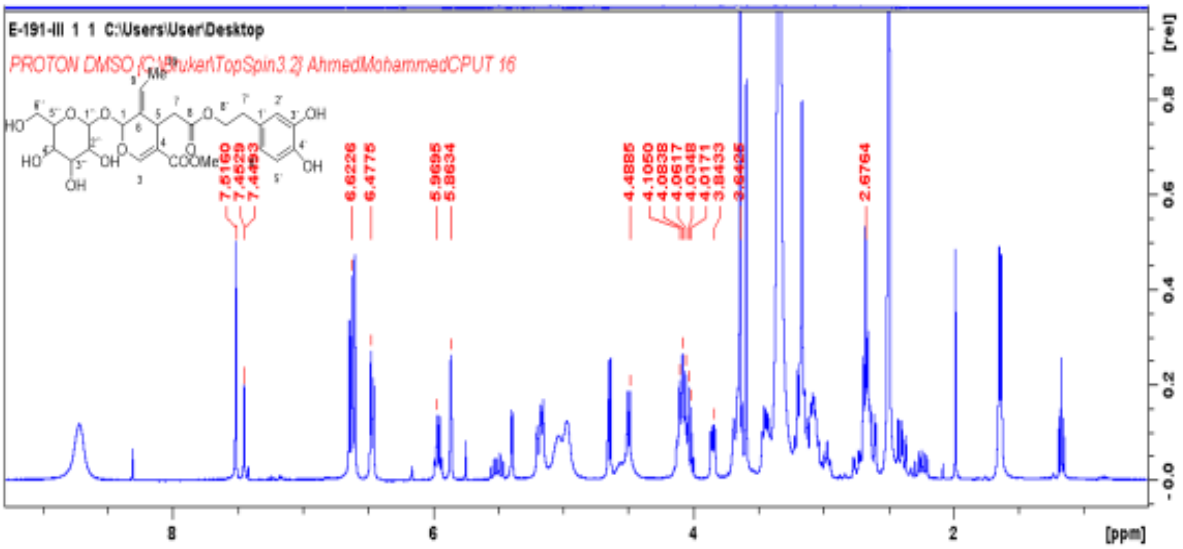

Figure 4.8 H-NMR (400 MHz, DMSO) spectrum of C2

The ^{1}H NMR (Figure 4.8) showed sugar peaks in the ranges between (*m*, 3.88 – 2.00 ppm) attesting to the presence of a sugar unit in the structure. In addition, an anomeric proton at 4.49 ppm (d, J= 7.9 Hz) was observed. Three aromatic CH were identified around 6.45 ppm (*d*, J= 8Hz), 6.62ppm (*s*, J_1= 1.7Hz) and 6.5 ppm (*dd*, J_2 = 1.9Hz). A singlet at 3.7 ppm belonged to the sp^3 hybridised CH next to the COO$^-$ group and the last singlet at 7.52 ppm was highly de-shielded being in conjugation with the carbonyl.

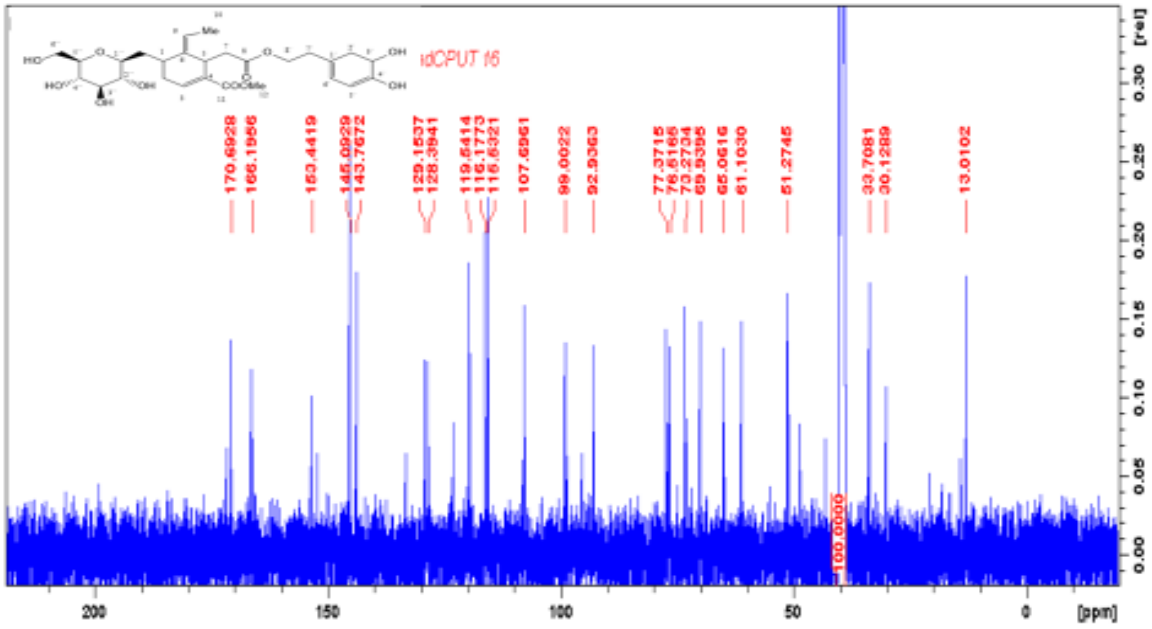

Figure 4.9 13C-NMR (400 MHz, DMSO) spectrum of C2

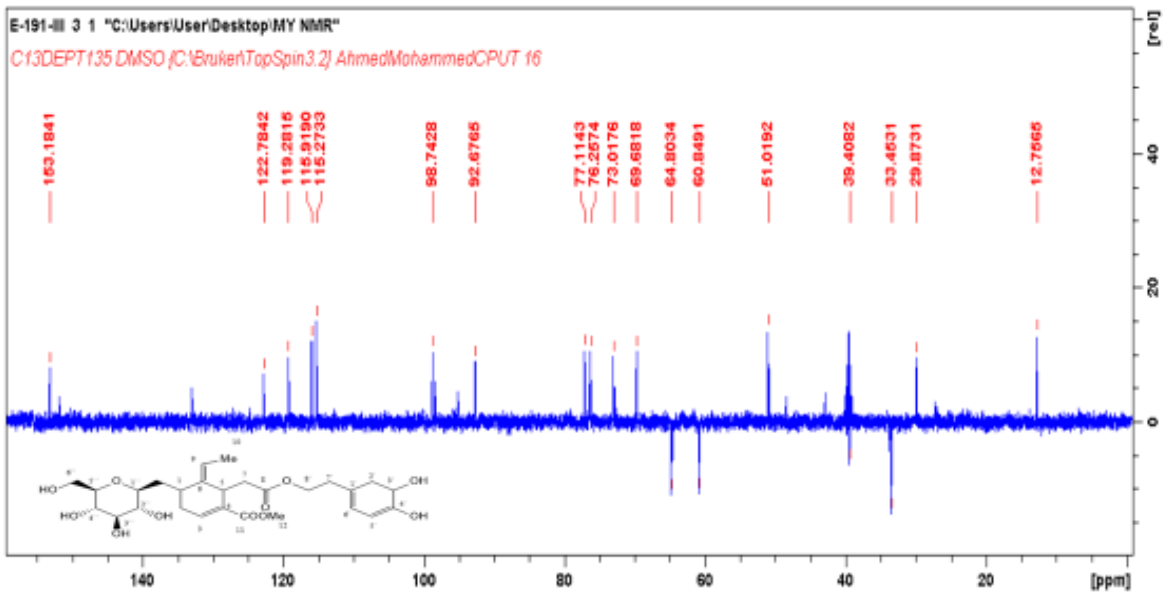

Figure 4.10 DEPT135-NMR (400 MHz, DMSO) spectrum of C2

The chemical shift of the ^{13}C NMR was present on the sugar ranging from 69.93 to 78.1 ppm. ^{13}C NMR (Figure 4.9) and its DEPT 135 (Figure 4.10) confirmed the presence of carbon on the aromatic ring at 145.09 ppm, 143.77 ppm, and 129.15 ppm. The two-position 8` and 7` were 64.1 ppm and 33.7 ppm (Goulas et al., 2009). Carbons at positions 4, 7, and 10 had no protons and could only be identified with ^{13}C-NMR at 122.78 ppm, 129.15 ppm, and 170.69 ppm with the last one being the carbonyl carbon (Kontogianni et al., 2013).

Table 4.2 ^{1}H and ^{13}C NMR spectroscopic data assignments (400 MHz) for compound 2 (δ in ppm, m, J in Hz) in DMSO

	Experimental ^{1}H NMR (ppm, *J*, Hz) (DMSO-d_6)		Reported data ^{1}H NMR (ppm, *J*, Hz) (DMSO-d_6)	
	(^{13}C NMR)	^{1}H NMR(ppm, *J*, Hz)	(^{13}C NMR)**	(^{1}H NMR (ppm, *J*, Hz)
1	107.7	5.60 (s)	100.7	5.76 (s)
3	153.4	7.50 (s)	154.9	7.45 (s)
4	107.7		109.4	
5	30.1		31.5	
6	129.2		130.3	
7	39.4	2.60 (*d*, 4.0), 2.40 (*d,* 4.0)	39.98	2.66 (*d*, 4); 2.37 (*d*,4)
8	170.7		172.0	
9	122.8	5.90 (*q,*7)	124.6	5.98 (q)
10	13.0	1.30(*d*)	13.01	1.59
11	170.6		168.5	
12	51.3	3.72 (*s*)	53.0	3.8 (*s*)
1`	128.39		130.3	
2`	119.5	6.62 (*d*, 1.7)	121.0	6.74, (*d*, 2)
3`	115.5	6.54 (*dd*, 8.0, 1.9)	116.8	6.58 (*dd*, 2, 8)
4`	143.8		144.7	
5`	145.1		146.0	
6`	116.2	6.45 (*d*, 8)	116.2	6.74 (*d*, 2)
7`	33,72	.2 (*m*)	35.5	2.71 (*m*)
8`	65.1	4.00 (*m*), 3.95 (*m*)	68.6	4.18 (*m*, 4.04 (*m*)
1``	99.0	4.49 (*d*, 7.9)	100.7	4.18 (*dd*, 2, 2); 4.04 (*m*)
2``	76.5	(3.88–2.00)*	77.7	(3.88–2.00)*
3``	69.9		71.2	
4``	77.4		78.1	
5``	73.1		74.9	
6``	61.1		62.5	

* Overlapping signals (sugars) **(Tsukamoto et al., 1984), (Goulas et al., 2009)

A summary of structure elucidation with NMR is provided in Table 4.2. It led to conclude that the obtained structure was consistent with oleuropein as reported in the literature (Tsukamoto et al., 1984).

4.2.3 Chemical characterisation of compound 3 (C3)

Compound 3 was isolated as a yellow powder of chemical structure presented in Figure 4.11.

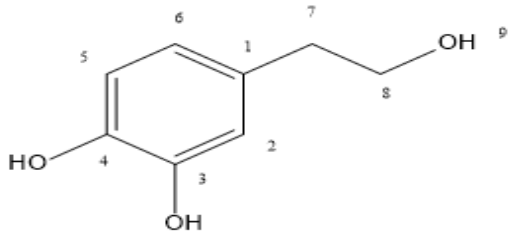

Figure 4.11 Chemical structure of compound 3 (C3)

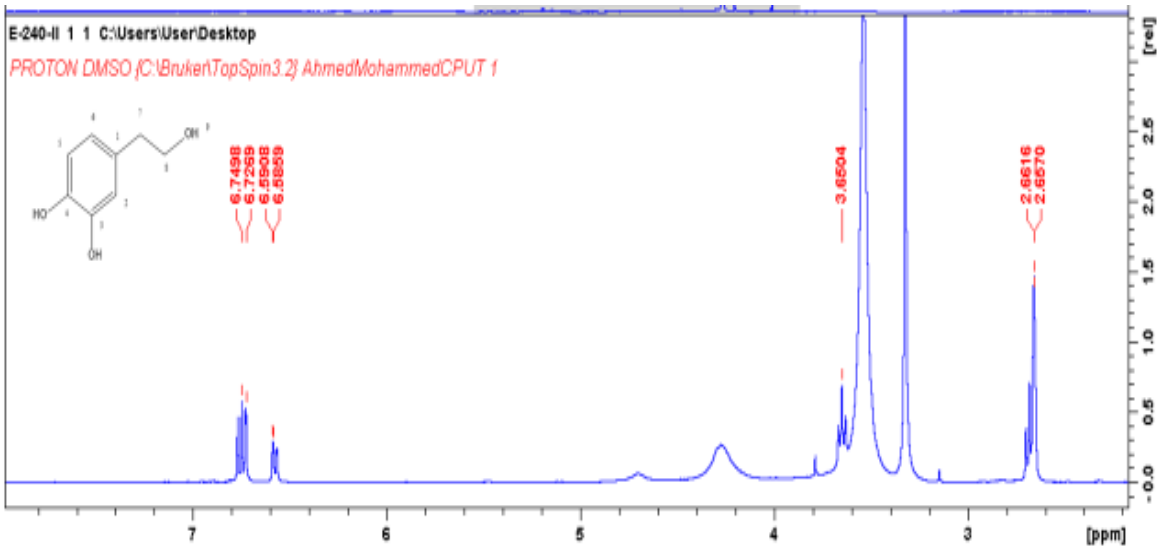

Figure 4.12 1H-NMR (400 MHz, DMSO) spectrum of compound 3

The ^{1}HNMR (Figure 4.12) of hydroxytyrosol had two triplet at $\delta_{H(ppm)}$ 2.65 (*t, J* = 7.0Hz) and 3.65 (*t, J*=7.6Hz) non-aromatic and on the aromatic ring, the following chemical shifts were observed δ_H 6.59 (*dd*, J_1= 7.9Hz & J_2= 1.9Hz), 6.75 (*d*, J_1= 7.9 & J_2= 1.8 Hz), 6.72 (*d, J*= 8.1 Hz).

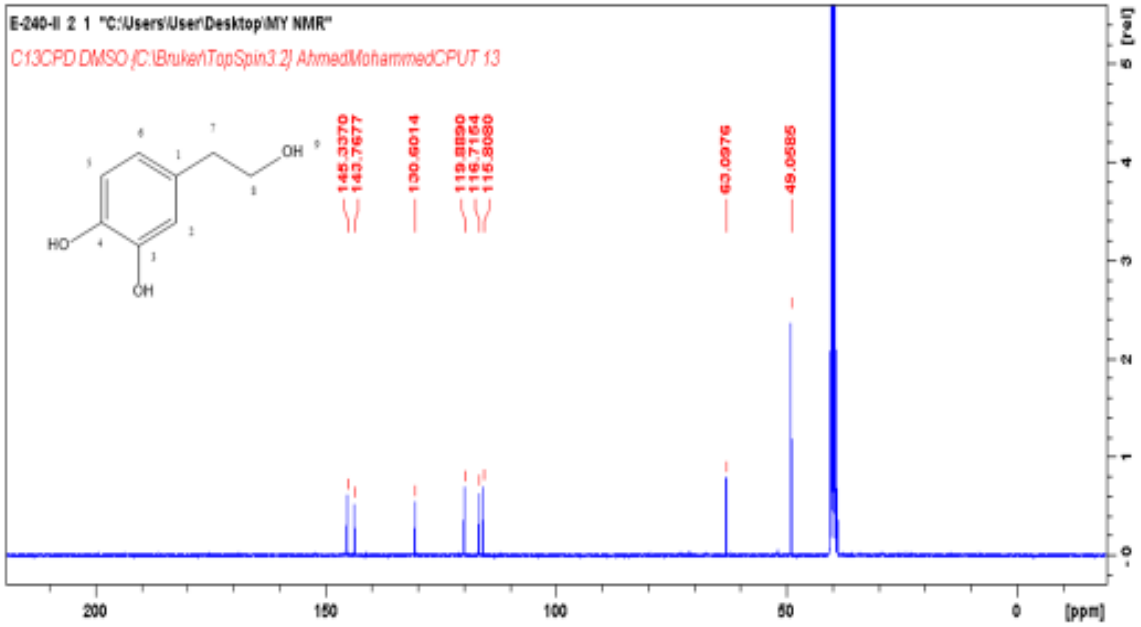

Figure 4.13 ^{13}C-NMR (400 MHz, DMSO) spectrum of compound 3

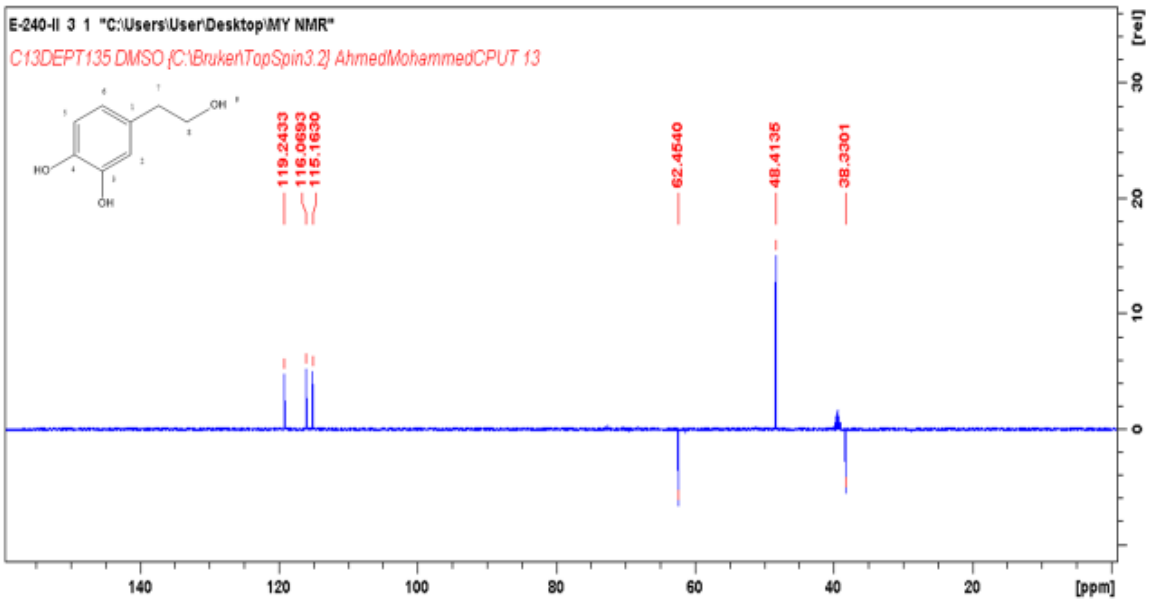

Figure 4.14 DEPT-135-NMR (400 MHz, DMSO) spectrum of C3

The ^{13}C NMR confirmed the presence of aromatic carbon from 115.9 ppm and upfield. The CH_2 peaks were observed at 38.3 and 63.1 ppm. The hydroxyl peak was expected to be deshielded by the induction effect from the oxygen and it was observed at 48 ppm.

Table 4.3 ^{1}H and ^{13}C NMR spectroscopic data assignments (400 MHz) for compound 4 (δ in ppm, m, J in Hz) in DMSO

	Experimental data (DMSO-d_6)*		Reported data (ACN-d_3)*	
	^{13}C NMR (ppm, *J*, Hz)	^{1}H NMR (ppm, *J*, Hz)^{13}C	^{13}C NMR (ppm, *J*, Hz)	^{1}H NMR (ppm, *J*, Hz)
1	130,60		131.5	
2	115,81	6.7 (*d*, 1.8)	116.4	6.72 (d, 1.8)
3	143,77		145.6	
4	145,34		144.5	
5	116,72	6.7 (*dd*, 7.9, 1.8)	115.9	6.75 (*d,* 8.1)
6	119,89	6.6 (*dd*, 8.0; 1.7)	122.1	6.60 (*dd,* 8.1 & 1.8)
7	38,33	3.7 (*t*, 7.2)	39.2	3.66 (*t*)
8	63,10	2.7 (*t*, 7.29)	61.1	2.67 (*t*)

*(Goulas et al., 2009)

Table 4.3 of Compound 3 proved that the structure was consistent with the structure of hydroxytyrosol (Savarese et al., 2007). The chemical shift observed led to confirm the structure of Hydroxytyrosol (Goulas et al., 2009).

Hydroxytyrosol glucoside and oleuropein were taken for the synthesis of gold nanoparticles but hydroxytyrosol wasn't used to make gold nanoparticles due to its poor yield.

4.3 Synthesis of gold nanoparticles

4.3.1 Nanoparticle synthesis using *O. exasperata* total extract

The evaluation of *O. exasperata* total extract as a reducing agent in the formation of gold nanoparticles was an attempt to evaluate gold nanoparticle formation with plant extracts. The synthesis of gold nanoparticles using the total extract was achieved by using a blend of aqueous leave extracts. The colour changed from gold yellow to red, which confirmed successful gold nanoparticle formation. (Yulizar et al., 2017). The colour change was justified by the reduction of the gold salt from Au^{3+} to Au^{0} (Ozaki et al., 2020).

The need to find ideal conditions for nanoparticle synthesis was also necessary for the screening using 1mM $NaAuCl_4.2H_20$ (Sridhar & Ramakrishna, 2015). Therefore, a freeze-

drying technique was used to obtain a homogeneous reducing agent. This technique preserves the biological and chemical properties of the reducing agents, allowing the production of materials that are free from decay for an extended period of time without altering the initial nature of the material (Khairnar et al., 2012). The lyophilised sample (20,00 g) was passed through a 0.45 µm syringe filter to yield 2.3216 g (11.6%) of lyophilised material.

4.3.1.1 Reducing ability of *O. exasperata* extract

a) Optical properties

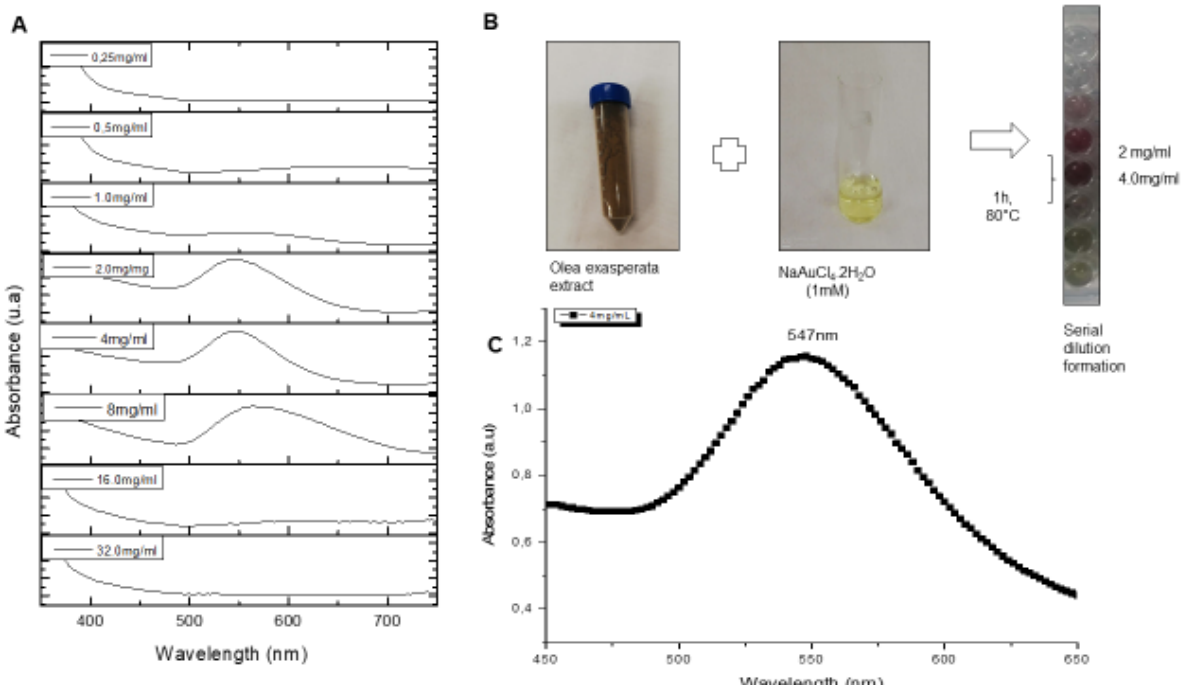

Figure 4.15 The UV absorption band of gold nanoparticles from serially diluted *O. exasperata* (A) showed they were concentration-dependent (B) and the absorption at 4mg/mL reflected a good peak symmetry (C) suggesting the existence of spherical gold nanoparticles

The formation of gold nanoparticles is shown in Figure 4.15. The first two cells (Figure 4.15), from the bottom up) with concentrations 32 and 16 mg/mL had no formation of gold nanoparticles. The formation only occurred at 8 mg/mL, 4 mg/ mL, and 2 mg/mL of the total extract concentration. This confirmed that gold nanoparticles were concentration-dependent (Tantra et al., 2010). There were therefore specific concentrations at which the synthesis of gold nanoparticles was successful.

Monacu argued in 2009 that the broadening of peaks provided information on the extent of aggregation of gold nanoparticles. For a highly aggregated solution, the peaks are reported to lose their symmetry and were broad resulting in the gold solution turning purple rather than

red. This observation was encountered at a concentration of 8 mg/mL in Figure 4.15 A. There was thus a formation at 8 mg/mL but with larger particles (Mocanu et al., 2009). The formation at 4 mg/mL was optimum and presented a UV band that was symmetrical about the wavelength of maximum absorption. In addition to this observation, the synthesis in the same figure showed that there was a shift in wavelength as the concentration changed. While Enas and Khalil also observed this back in 2012 (Khalil & Ismail, 2012), a similar study conducted recently confirmed that there was a blue shift as the concentration decreased to low values. This result alluded that particles formed at lower concentrations were the smallest and were stable; in this case at 4 mg/mL and 2 mg/mL in Figure 4.15 A (Jimenez-ruiz et al., 2021).

According to the work completed by Eustis in 2006, UV measurements have been a great help as far as predicting the shape of nanoparticles is concerned. When the wavelength of maximum absorption was around 540 nm (for gold), Eustis predicted the particles were spherical. When an additional wavelength is observed at a lower frequency on the same spectrum, the particles are more likely to be rod-shaped depending on their frequency. In 2020, the study was confirmed in a study in which cysteine gold nanoparticles were functionalised and studied. It turned out that when the particles were symmetrical or spherical, only one surface plasmon was observed. This was not true for particles with a complete lack of symmetry. Sakellari reported the appearance of a second peak at higher wavelengths to that of the formed gold nanoparticles, therefore confirming the existence of a longitudinal and transversal absorption (Sakellari et al., 2020). In the present case, the observation of a single absorption band was proof that gold nanoparticles had a spherical shape with absorption at 547nm (400 – 600 nm) when 4 mg/mL of reducing agent was used (Figure 4.15 C).

b) Crystallinity

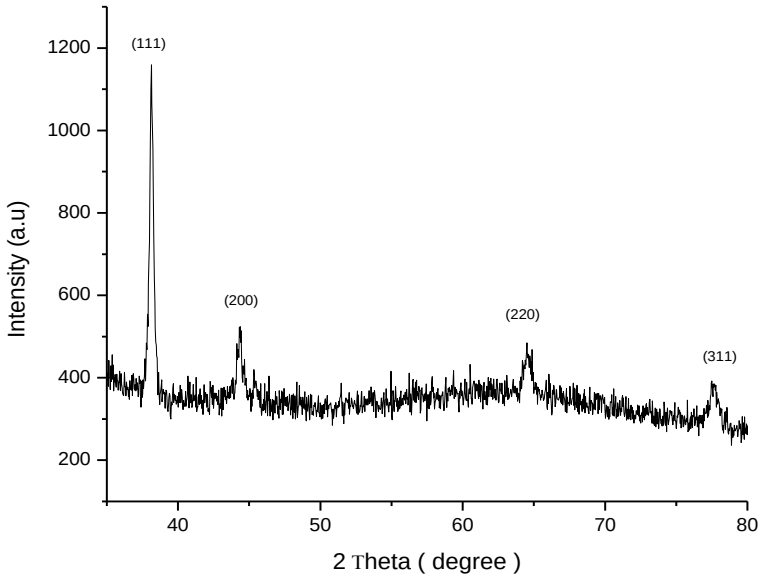

Figure 4.16 XRD pattern of Olea exasperata extract gold nanoparticles

X-ray diffraction analysis of gold nanoparticles of *Olea* extract was carried out to perform elemental analysis and confirm the crystallinity of the metal. The resulting diffraction provided inherent properties used to characterise the specific metal. The presence of gold nanoparticles has been confirmed by measuring the diffraction pattern at 2θ degree angles as recorded in the standard provided for gold by the joint committee on Powder Diffraction Standards (file 04-0784) in 1991 (Marlene C. et al., 1991). The peaks observed in Figure 4.16 at 2 theta angles 38.2°, 44.4°, 64.5°, and 77.5° were in agreement with the standard provided, and corresponded to the (111), (200), (220), and (311) planes respectively, of a face-centred cubic (FCC) crystal of gold. The peak at 44° (200) could also be linked to the presence of NaCl according to the experiment of Hoo in 2017. In fact, he reported that NaCl is one of the side products of such synthesis and was present in solution and reported that NaCl did not interfere with the gold nanoparticle formation (Hoo et al., 2017), (Doan et al., 2020). The (111) plane at 38.0° was very intense because it was in that plane that the nanoparticles were more in favour of growing for the metal being studied (Dabbousi et al., 1997). This observation was evidence that the observed and formed gold nanoparticles were crystalline.

c) Size and zeta potential measurement

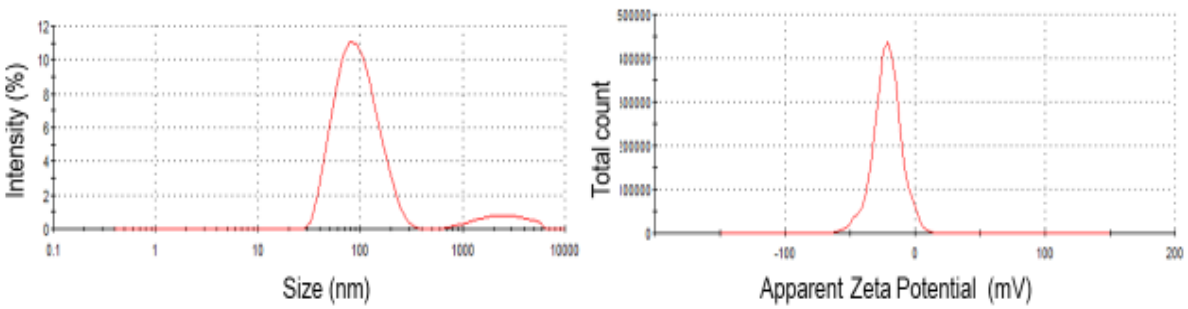

Figure 4.17 The size distribution graph of gold nanoparticles prepared from Olea exasperata showing a size distribution below 100nm with a mean value around 73.9nm its corresponding zeta potential distribution graphed had a value was -21.6 mV.

The zeta potential reading provides a measure of the extent of stability of the nanoparticles in solution. In fact, the mobility of particles toward the electrode of the opposite charge is expressed into zeta potential. It is a measure of the speed at which an ion would travel to an electrode of an opposite charge but it is also a measure of the stability of particles in solution. In fact, particles of the same charge repel each other causing a layer around the electrode whose thickness and stability are the measured properties after repulsion. The more negative the charge of particles, the greater the repulsion and thus the greater the stability (Castaneda-gill, 2018). The zeta potential and size distribution in Figure 4.17 A and B were measured for *Olea exasperata* gold nanoparticles at 4 mg/mL. The obtained value of zeta potential was -21.6 mV. This value of the zeta potential was negative enough to imply a stable solution of gold nanoparticles. The size measurement of the same solution in Figure 4.17 B was recorded to be 74 nm with a bi-modal mode ranging from 30 nm to above 100 nm. The size distribution band was more shifted toward sizes above 100 nm.

Table 4.4 Summary of the screening of lyophilised *O. exasperata*

Plant name	Code	Concentration (mg/mL)	Zeta potential (mV)	Dilution ratio	Particle size (nm)	Wavelength (nm)
***O. exasperata* (lyophilised)**	3D	1	-21,6	1/16	74	547

A summary of the size and zeta potential distribution experiment is given in Table 4.4 in which the size, the zeta potential, and the wavelength of absorption are presented. These values were all within the range of 540-560 nm for gold nanoparticles. In fact, the formation of gold nanoparticles was confirmed only by a colour shift from yellow to red in some specific wells. In previous work completed by Wang, sizes below 100 nm were found in their synthesis of nanoparticles from plant extracts. It was found that lignin gold nanoparticles had an average

diameter value between 5 and 30 nm. This suggested that the sizes of nanoparticles are dependent on the type of reducing agent used (Wang et al., 2020).

d) Morphological examination and particle size measurement

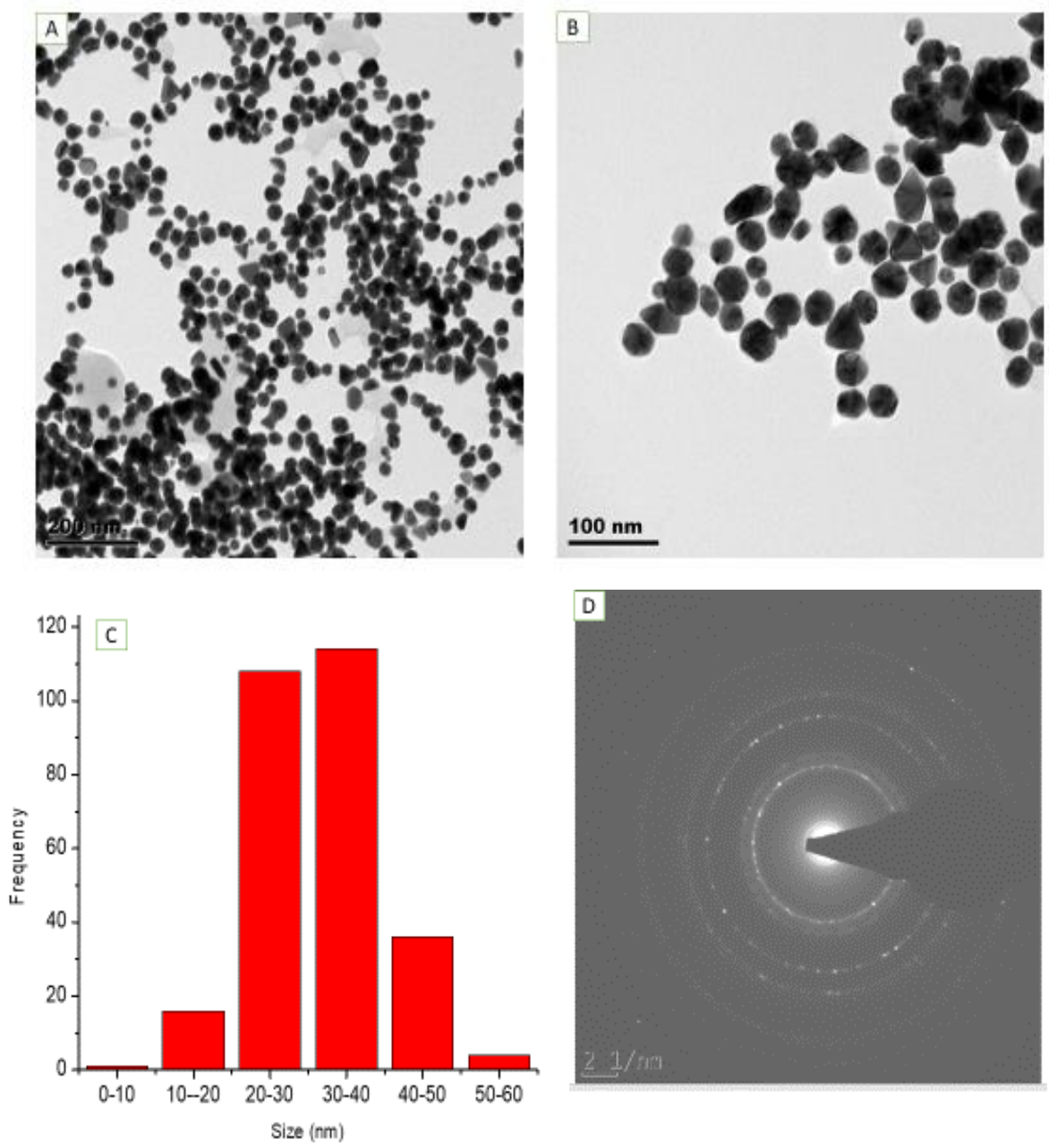

Figure 4.18 TEM micrograph of *O. exasperata* GNPs (A) and its magnified image showing defined shapes (B) with corresponding histogram pattern (C) showing spherical and crystalline rings (D), with sizes within 20-40 nm bracket.

The gold nanoparticles formed were visualised using an HRTEM. The TEM micrograph of gold nanoparticles synthesised from *Olea exasperata* in Figure 4.18 A showed that gold nanoparticles were successfully synthesised and formed round-shaped gold nanoparticles with

sizes ranging between 10 and 60 nm according to the histogram in D. It further showed that there were many particles per unit area. The successful synthesis of gold nanoparticles confirmed the reducing ability of *Olea exasperata* total extract. Previous studies using *Olea* reported by Antony found the size of the gold nanoparticles between 20 and 25 nm (Antony et al., 2016). The difference in size with the reported technique could be due to the nature of the reducing agent or its matrix. In fact, this work used filtered lyophilised materials in the synthesis to do away with any useless interference in the extract. This experiment provided a wider range of formation of gold nanoparticles compared to the other two techniques suggesting lyophilisation is essential in the process because it improved the nature of the reducing agent.

SAED analysis has been known as a complementary technique to XRD, providing crystallographic information. The SAED pattern of Figure 4.18 D of the gold nanoparticles presents bright spots in a circular pattern attesting to the polycrystalline nature of the sample.

e) Energy dispersive x-ray analysis

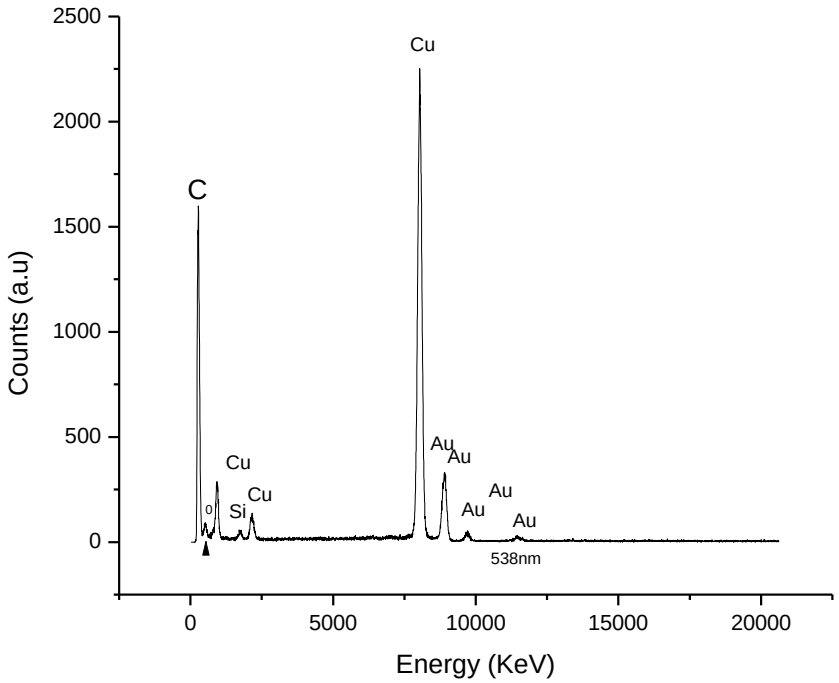

Figure 4.19 Energy-dispersive X-ray spectrum of Olea exasperata gold nanoparticles

Energy-dispersive X-ray spectroscopy (EDX) was used to obtain elemental composition data to confirm the identity of the particle shown in the TEM micrograph. The EDX spectrum (Figure 4.19) confirmed the presence of gold, carbon and copper. The copper was due to the TEM grid. The analysis confirmed that the particle observed in the TEM micrograph was indeed gold nanoparticles. Rajakumar reported similar results back in 2016 in the synthesis of gold

nanoparticles from *eclipta prostrata leaves* (Rajakumar et al., 2016). The observed Si peak is the spectral artefact due to excess energy reaching the detector and recorded as a Kα signal at 1.65Kev (Tanaka et al., 2016).

f) Infrared analysis of *Olea exasperata* extract gold nanoparticles

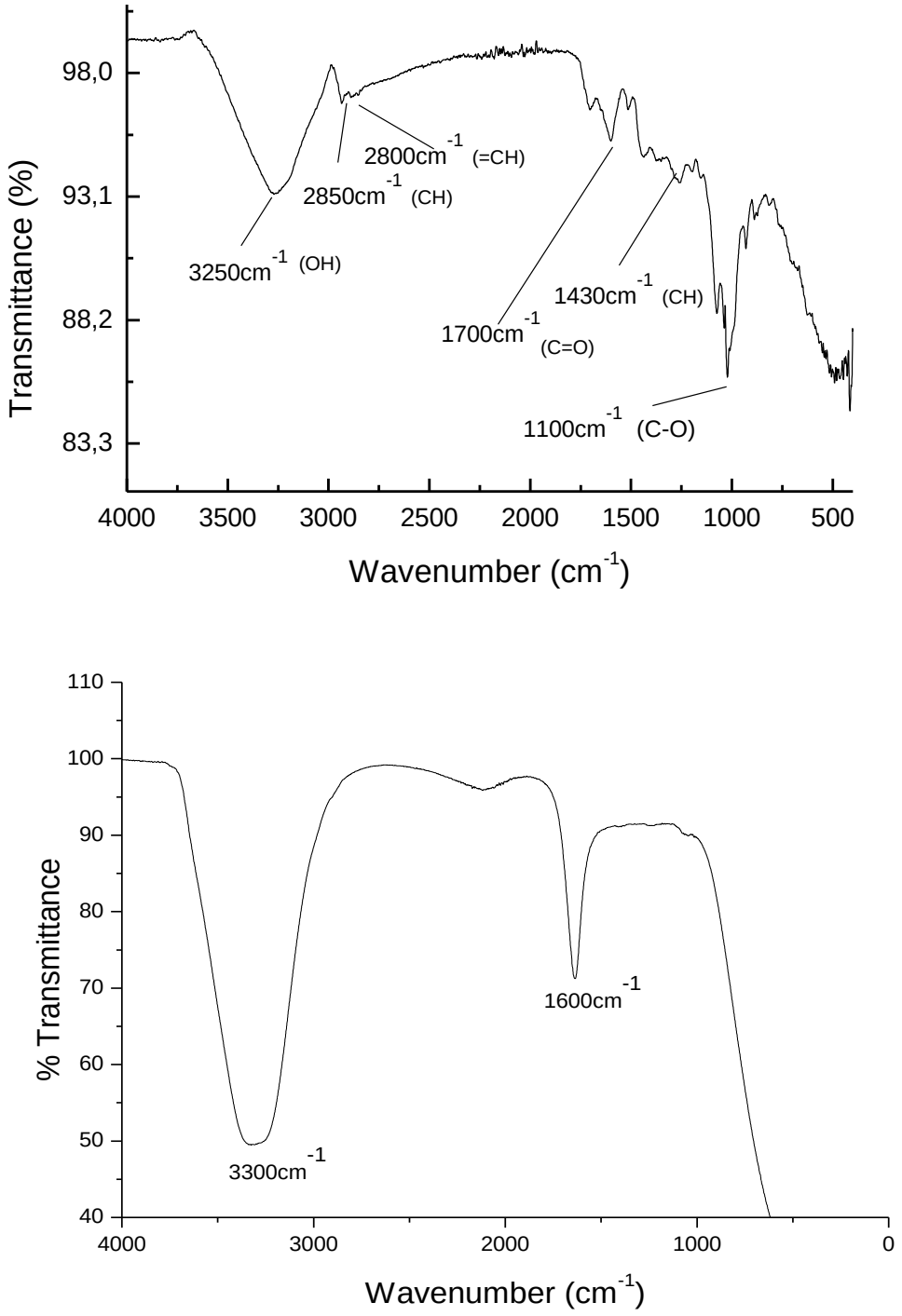

Figure 4.20 Infrared spectra of *O. exasperata* leave extract (A) and gold nanoparticles (B) showed an increase in transmitted intensity as the gold nanoparticle formed

The infrared analysis of *O. exasperata* leaves extract in Figure 4.20 A confirmed the presence of the hydroxyl group at 3300 cm^{-1}, and the sp^3 C-H bond at 2850 cm^{-1}, sp^2 C-H bond at 2800 cm^{-1} The carbonyl group was identified at 1700 cm^{-1} and the C-O bond was confirmed at 1100 cm^{-1}. The aromatic proton C=C-H was confirmed at 1430 cm^{-1}.

The formation of gold nanoparticles produced a spectrum reported in Figure 4.20 B with only alcohol and a carbonyl peak at 3300 cm^{-1} and 1750 cm^{-1} respectively. In addition, a shift to low wavenumbers was observed for both the alcohol and the carbonyl. The intensity of the transmission band grew smaller in energy to express that the functional groups of the substance are now strained by the formation of the gold nanoparticles. Yulizar experimented in 2017 in which he observed a similar drop in intensity of transmission and underwent a shift (Yulizar et al., 2017). This IR cannot be conclusive to the nature or the type of reducing agent, but in this case, the shift in percentage transmittance intensity which occurred were observed in Yulizar's work and were ascribed to the formation of gold nanoparticles and the capping of the formed gold nanoparticles.

4.3.2 Nanoparticle synthesis using pure compounds

The preceding sections evaluated the synthesis of gold nanoparticles using the *Olea exasperata* total extract as the reducing agent. In this section, isolated pure compounds were used as reducing agents in the synthesis of gold nanoparticles to evaluate their ability to form gold nanoparticles. Due to the low yield of the hydroxytyrosol pure product obtained, it wasn't part of the following study.

4.3.2.1 Reducing ability of hydroxytyrosol glucoside

Compound 1, also identified as hydroxytyrosol glucoside (Figure 4.1) was isolated and characterised according to the procedure presented in section 4.2.1. It was identified as a hydroxytyrosol unit coupled with a sugar unit. Compound 1 successfully reduced the yellow solution of gold salt to produce a red solution of gold nanoparticles.

a) Optical properties

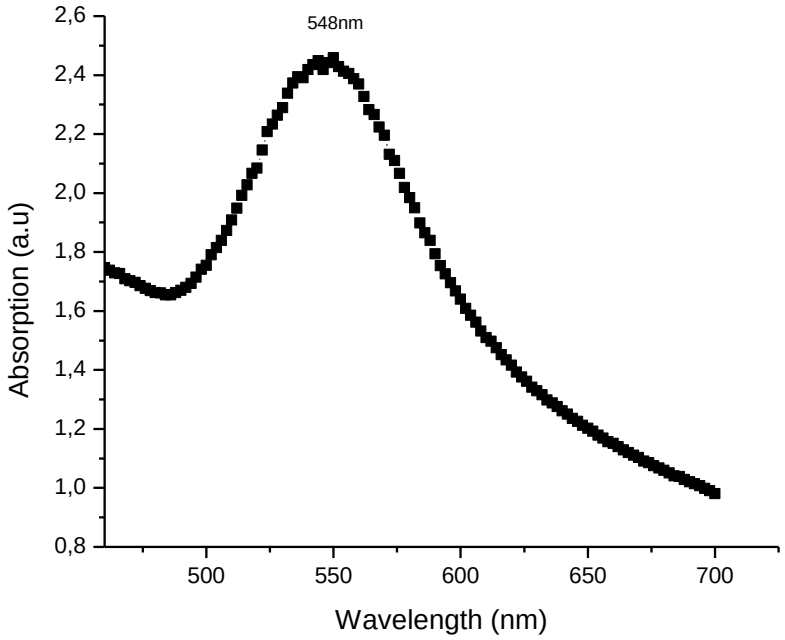

Figure 4.21 UV-Vis spectrum of gold nanoparticles from hydroxytyrosol glucoside showing a symmetrical absorption peak at 548nm

The surface plasmon resonance of gold nanoparticles synthesised using hydroxytyrosol glucoside as a reducing agent formed gold nanoparticles at the respective concentrations of 4mg/mL (λ_{max} = 544 nm) and 2mg/mL (λ_{max} = 548 nm). The concentration at 2 mg/mL (548 nm) was used in this study. This solution had a much intense absorption leading to conclude, according to Beer Lambert's law, that it contained more gold nanoparticles. In fact, it is known that the higher the concentration of an analyte, the more the absorbance of the substance being analysed (Casasanta & Garra, 2018). Absorptions have been described in Eustis's work as a means to predict the shape of the formed gold nanoparticles, in fact, for spherical nanoparticles, it would have only a single band of absorption as the radius is constant throughout. For a bi-dimensional object like an ellipse, an additional band should be expected since it would undergo both the transversal and longitudinal absorption (Eustis et al., 2006). In Figure 4.21 only a transversal absorption symmetrical about the wavelength of maximum absorption at 548 nm was observed.

b) Crystallinity

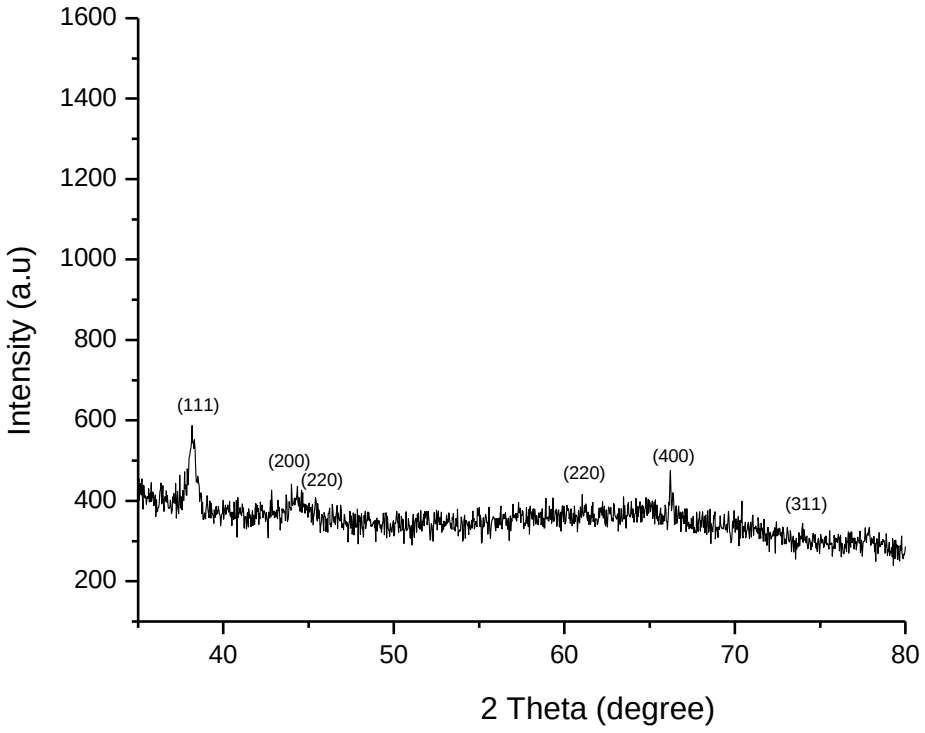

Figure 4.22 XRD pattern of gold nanoparticles formed using hydroxytyrosol glucoside

Several peaks were observed in the XRD spectrum Figure 4.22 of the gold synthesised using hydroxytyrosol glucoside at 38°, 44°, 64°, and 77°. The peak at 38° was matching the (111) diffraction plane. The peak at 44° matched the (200) plane. The one at 64°and 75° were respectively matching the (220) and (311) planes. The peak at 38° was observed to be the most intense one. This peak was matching the configuration of the face-centred crystal (Rajakumar et al., 2016). The peak at 44° (200) and the one at 66° (400) relate to the presence of NaCl as a bi-product reported similarly in Hoo experiments. NaCl salt is a side product in this relation (Hoo et al., 2017). The obtained gold nanoparticles were crystalline as per the record in the standard provided for gold structure by the joint committee on Powder Diffraction Standards (file nos 04-0784) in 1991 (Marlene C. et al., 1991).

c) Size and zeta potential measurement

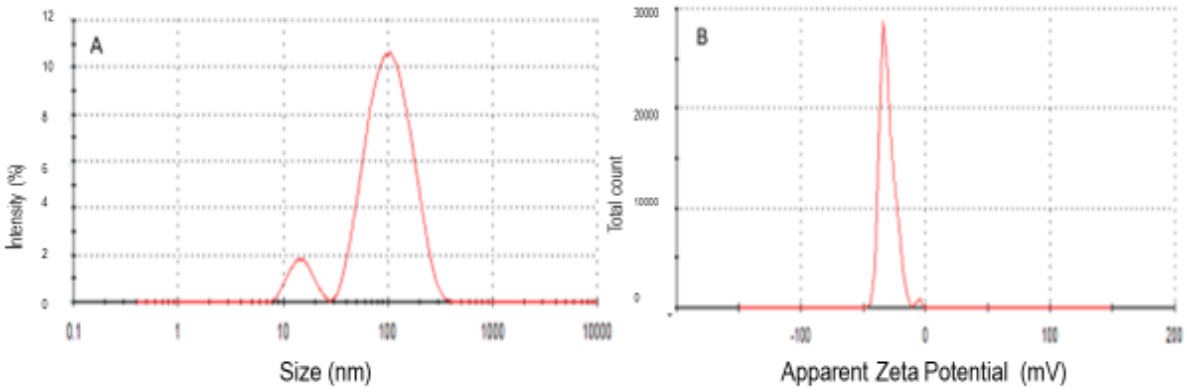

Figure 4.23 Size (A) and zeta potential (B) of gold nanoparticle from hydroxytyrosol glucoside

The size distribution by the intensity in Figure 4.23 A showed that it was a bimodal graph (Elbagory et al., 2019) with one set of particles occurring from 10nm to 30 nm and another from 30 to above 100nm where they average at about 73nm. The size of the gold nanoparticles from the extract, as reported in section 4.3.1.1 C, was similar to the bimodal size toward larger particles as a result of a complex matrix of the extract. The use of a purer material provided particles occurring at a lower size which suggested that using a purer material or compound as a reducing agent was essential for forming small gold nanoparticles from *O. exasperata extract*.

The zeta potential in Figure 4.23 B confirmed the obtained gold nanoparticles had a negative surface charge (-30.3 mV) which implied that the particles are stable. This value also indicated that the reducing agent was made up of negatively charged reducing sites (Rajakumar et al., 2016) giving rise to a high level of stability of the formed gold nanoparticles (Wang et al., 2020).

a) Morphological examination and particle size measurement

Figure 4.24 shows the TEM micrograph (A) of the gold nanoparticles synthesised using hydroxytyrosol glucoside as the reducing agent. The gold nanoparticles were fairly uniformly spread. The particles appeared to be within the same size range and were spherical in appearance as predicted from the optical properties. The micrograph in Figure 4.24 B is a higher magnification image of the area circled in Figure 4.24 A. It showed a monodispersed layer of gold nanoparticles. The micrograph revealed that the formed gold nanoparticles had

specific shapes with the majority being circular. The histogram in Figure 4.24 C predicted no particles above 100 nm; In fact, the Gauss distribution-shaped histogram had its particles between 40 and 50 nm with the highest around 64 nm and a mean value around 45 nm. The distribution intensity revealed a small fraction of gold nanoparticles occurred above 100nm. This distribution was consistent with TEM data reported in Figure 4.24. In fact, the Gauss distribution observed from the size distribution confirmed the particles were dispersed. The SAED pattern in Figure 4.24 D showed bright diffraction rings attesting to the crystalline nature of the gold nanoparticles. According to Hoo, those angles matched the planes (111), (200), (220), and (311). The most intense ring was the innermost ring (111) suggesting the direction in which most plans were oriented (Hoo et al., 2017).

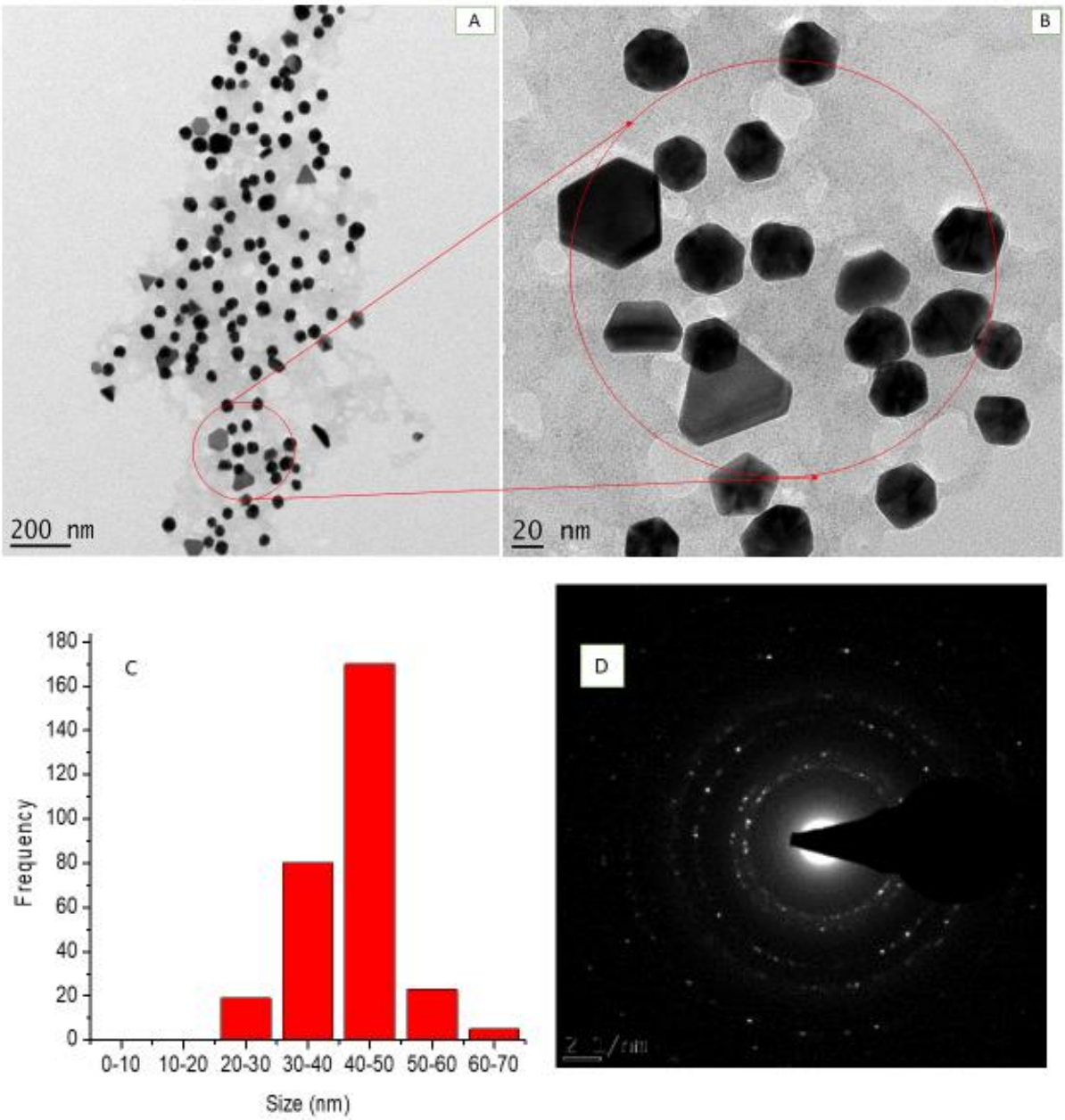

Figure 4.24 TEM micrograph of hydroxytyrosol glucoside gold nanoparticles showed spherical crystalline particles on micrograph A. The micrograph B was an insert of some selected area in A. The histogram in C and SAED in D were corresponding to the micrograph in A. The histogram of the same gold nanoparticles revealed particles with sizes 40 and 50nm were abundant

e) Energy dispersive X-ray analysis

Energy-dispersive X-ray spectroscopy provided qualitative analysis on the hydroxytyrosol glucoside-based gold nanoparticles and confirmed the presence of gold nanoparticles in the sample prepared from hydroxytyrosol glucoside (Rajakumar et al., 2016).

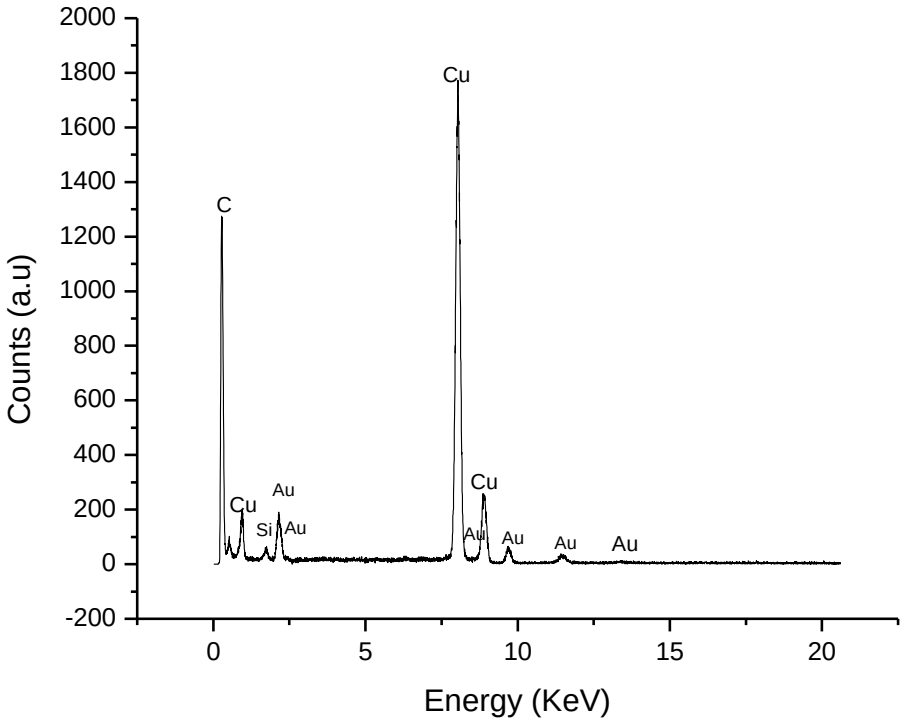

Figure 4.25 EDS spectrum of hydroxytyrosol glucoside gold nanoparticles showing the presence of gold nanoparticles

The spectrum in Figure 4.25 revealed the presence of gold, copper, silicon, and carbon. The observed copper was from the TEM grid used. The carbon peak was from the grid used as well as the sample. An additional Si peak was also observed, which is a known spectral artefact; in fact, the detector emits a Kα Si peak known as an escape peak at 1.65 Kev resulting from the excessive intensity of the incoming x-rays to the detector (Tanaka et al., 2016).

a) Infrared analysis of hydroxytyrosol glucoside gold nanoparticles

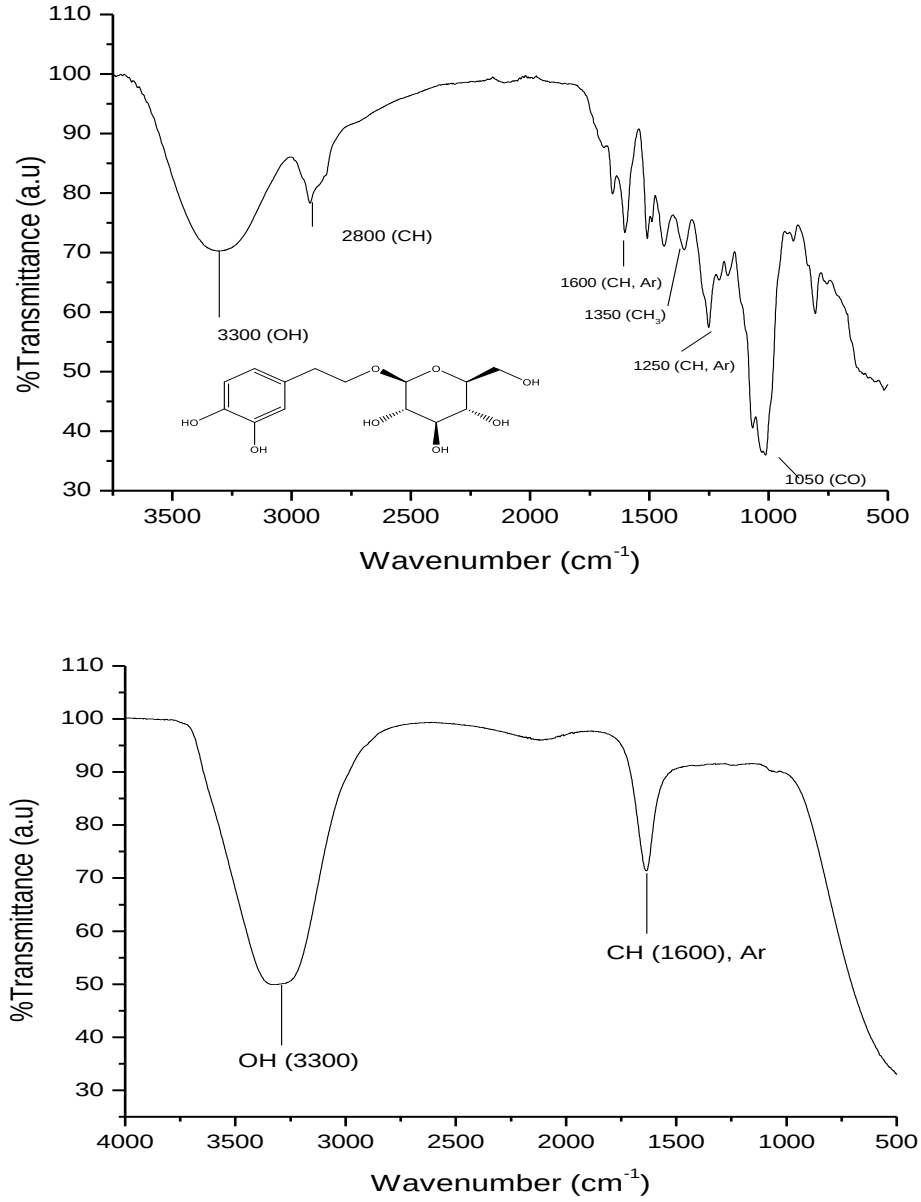

Figure 4.26 Infrared spectra of hydroxytyrosol glucoside compound (A) and its gold nanoparticles (B)

The infrared spectra in Figure 4.26 were that of hydroxytyrosol glucoside compound (A) along with its associated gold nanoparticles (B). A mere observation of Figure 4.26 A showed that the number of functional groups in the hydroxytyrosol gold nanoparticles was less than they were in the compound IR shown in Figure 4.26 A. The hydroxytyrosol functional groups observed were 3300 cm^{-1} (OH), 1600 cm^{-1} (C=C-H, aromatic), 2800 cm^{-1} (CH), and 1050 cm^{-1} (C-O). After synthesis, there was only the OH peak at 3300 cm^{-1} and the (C=C-H, aromatic) at 1600 cm^{-1}. In addition to this, there was a shift in functional groups so that the OH group shifted

to higher-value from 3300 cm^{-1} to 3350 cm^{-1} and became less intense. The aromatic (C=C-H) peak remained at 1600 cm^{-1}. The change in intensity when nanoparticles were formed confirmed their formation. In Wang's experiment, the intensity of some functional groups decreased after synthesis while some of them did not (Wang et al., 2020).

4.3.2.2 Reducing ability of oleuropein

Compound 2 has also been known as oleuropein (Figure 4.6). It was isolated as specified in section 4.2.2. It has been reported to be one of the most abundant components in *Olea* (Omar, 2010), in fact, it was also collected here in good yield. The synthesis of gold nanoparticles using oleuropein produced a solution that caused a 1mM yellow gold solution to turn red.

a) Optical properties

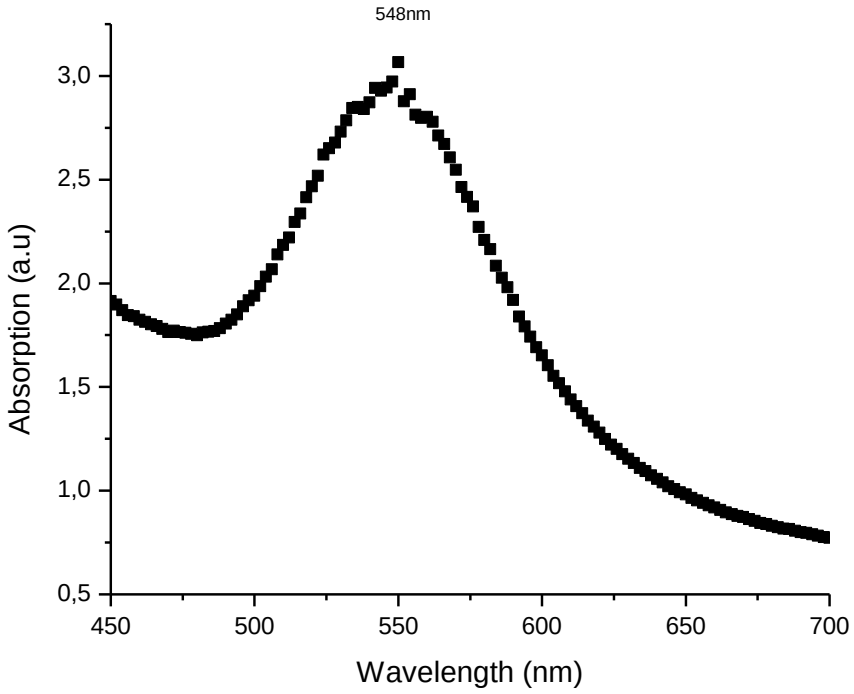

Figure 4.27 UV absorption spectrum of Oleuropein gold nanoparticles

Gold nanoparticles have a characteristic absorption that falls in the UV region. This makes them easy to monitor using UV spectroscopy over an acceptable range of absorption. The formation of gold nanoparticles using Oleuropein as a reducing agent occurred at two consecutive concentrations namely 4gm/mL (λ_{max} = 540 nm) and 2mg/mL (λ_{max} = 548 nm) of this reducing agent. The formation of gold nanoparticles revealed it had a characteristic gold absorption at 548 nm with a peak ranging between 470 to 625 nm in the above spectrum.

Casasanta made a similar observation of gold nanoparticle absorption (Casasanta & Garra, 2018). It was also proven that the absorption value of Oleuropein-based gold nanoparticles was pH-dependent in a study by Khalil. He monitored the change in absorption by changing the pH between 9.6 and 2.3. It was noted that in a basic solution, the absorption was near 540nm, but as the pH was dropped to 2.3, the absorption underwent a redshift coupled with a loss of curve symmetry (Khalil et al., 2012). This study suggested that in a basic medium the formed gold nanoparticles were small and stable in solution.

b) Crystallinity

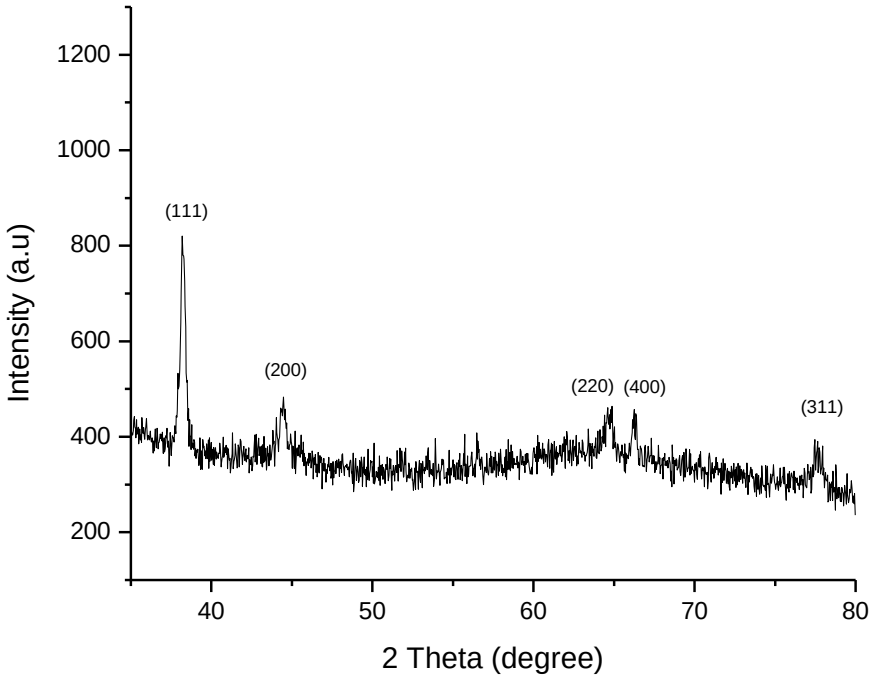

Figure 4.28 XRD pattern of gold nanoparticles synthesised using oleuropein

The XRD pattern of oleuropein gold nanoparticles in Figure 4.28 revealed peaks at 2 theta diffraction angles 38°, 44°, 64°, and 77°. The values were respectively equivalent to the planes (111), (200), (220), and (311) of the face-centred cubic lattice of gold. The collected pattern, therefore, confirmed the sample to be crystalline. Rajakumar made a similar observation in the work he published in 2016 (Rajakumar et al., 2016). The most intense peak observed at 38° has been reported in Rajakumar's work and it corresponds to the plane (111) known as the preferential plane for particle growth. (Rajakumar et al., 2016). There was a peak at 44° (200) and the one at 66° (400) confirmed the presence of NaCl (Hoo et al., 2017). The gold nanoparticles were crystalline as per the record in the files of the joint committee on Powder Diffraction Standards (file nos 04-0784) in 1991 (Marlene C. et al., 1991).

c) Size and Zeta potential

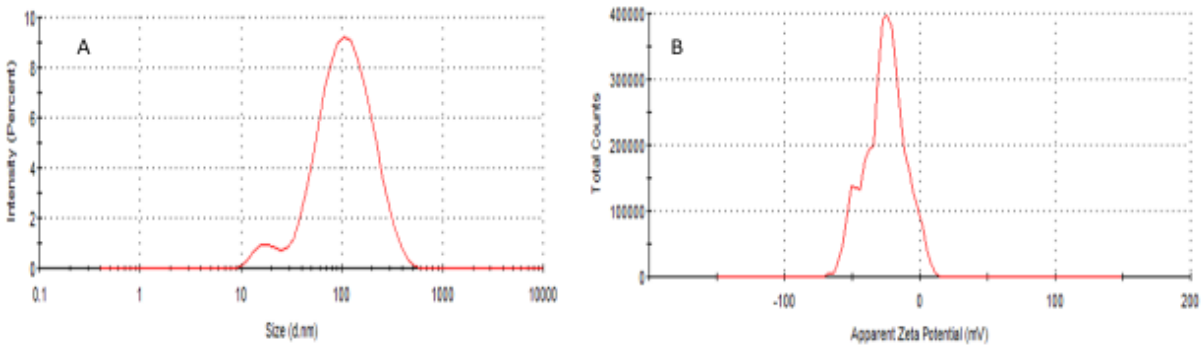

Figure 4.29 Oleuropein gold nanoparticle size distribution by intensity graph (A) and Zeta potential measurement (B)

Oleuropein gold nanoparticle size distribution by intensity Figure 4.29 A showed that oleuropein gold nanoparticles had a bimodal graph with a small size of particles around 12nm and a much larger one averaging around 71 nm. The observation of these types of modes was also observed in Elbagory's work. Many works reported the size of oleuropein gold nanoparticles to occur below 100nm (Elbagory et al., 2019).

The zeta potential distribution by the intensity of the oleuropein gold nanoparticles was measured to evaluate the stability of the formed gold nanoparticles. The zeta potential measurement in Figure 4.29 B showed that oleuropein gold nanoparticles had a negative zeta potential with an average value of -25.9 mV. To explain the stability of gold nanoparticles, Badeggi discussed the interaction occurring in the lieu of interaction between the reducing agent and the metal being reduced. He argued that the polyphilicity resulting from the polyphenolic compound was responsible for the negative charge due to the presence of lone pairs of electrons and electronegative atoms providing a site for the reduction of gold nanoparticles (Badeggi et al., 2020). This was the reason the gold nanoparticles formed had a negative charge. The zeta potential value observed for hydroxytyrosol gold nanoparticles in section 4.3.2.1 C was -30.3 mV, which was more negative or more stable than the particles formed by the oleuropein reducing agent. This zeta potential value showed oleuropein needed a capping agent or a stabiliser.

d) Morphological examination and particle size measurement

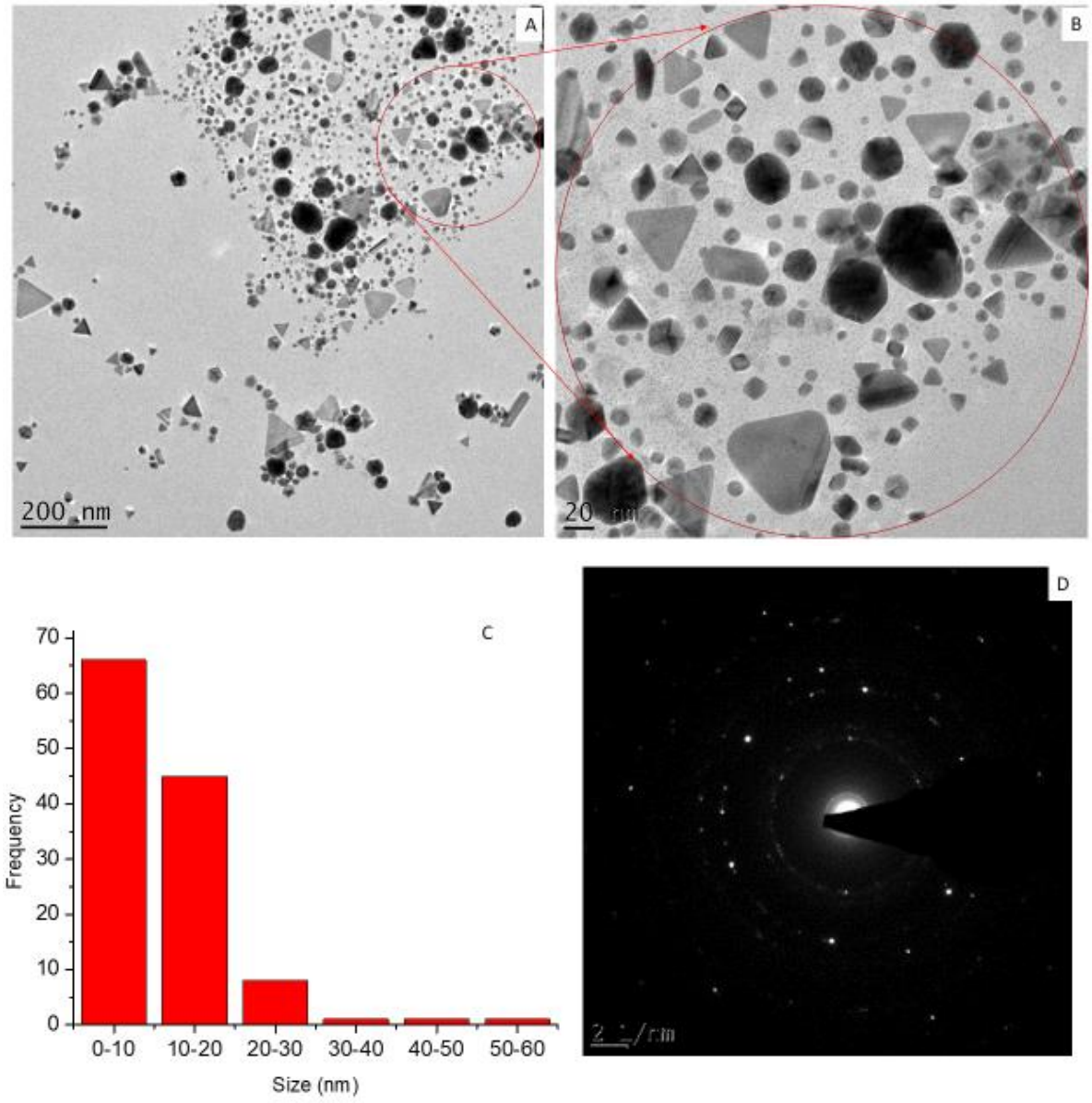

Figure 4.30 TEM micrograph of oleuropein gold nanoparticles (A) and its magnified image (B), presenting broad size distribution of particles. The histogram (B) and SAED pattern (C) corresponding to the micrograph showed particles were crystalline. The TEM image in D was an insert of A showing abundant spherical particles below 10nm.

The TEM micrograph in Figure 4.30 A of the gold nanoparticles synthesised from oleuropein showed particles with two sets of sizes (large and small) implying a broad size distribution. The histogram in C confirmed that the smallest particles were below 10 nm with an average of 3 nm and the largest around 80nm with an average of 67 nm, as observed in the higher magnification image (Figure 4.30 B) of the circled area in A. The particles below 20nm were higher in number as was confirmed in the TEM micrograph (Figure 4.30 A, B). As seen in the

insert in B, the particles appeared agglomerated as a result of a lack of capping agent. This was observed in the size distribution graph covering a broad size range (Figure 4.30 C) suggesting a lack of stabilising properties in the reducing agent. The formation of particles with such a broad size distribution showed that the synthesis didn't yield very stable gold nanoparticles. The SAED pattern in Figure 4.30 D revealed there were bright diffracted spots forming a ring pattern confirming the crystallinity of the formed gold nanoparticles as observed by Yulizar in his work. (Yulizar et al., 2017), (Ankamwar, 2010).

e) Energy dispersive x-ray spectroscopy

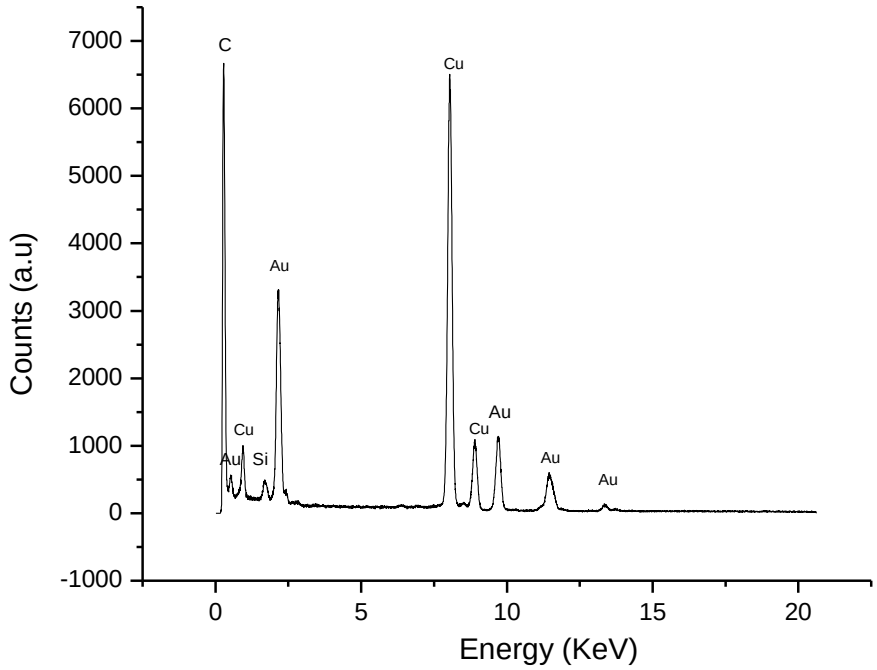

Figure 4.31 EDS spectrum of oleuropein gold nanoparticles provided evidence of the presence of gold

EDX was used to confirm the presence of gold in the sample of oleuropein-based gold nanoparticles as presented in Figure 4.31. The elements present were identified and gold, copper, silicon, and carbon. Similar results were obtained as presented in section 4.3.2.1 and confirmed the presence of gold in the sample. This technique was useful in providing qualitative information on the composition of gold nanoparticles. Bankar reached a similar conclusion while evaluating gold nanoparticles made with banana peel extracts (Bankar et al., 2010). The copper is part of the TEM grid. The Si peak was ascribed to the spectral artefact emitted by the detector. It is also known as the escape peak recorded at 1.65 KeV and often due to excessive intensity reaching the detector (Tanaka et al., 2016)

f) Infrared analysis of oleuropein gold nanoparticles

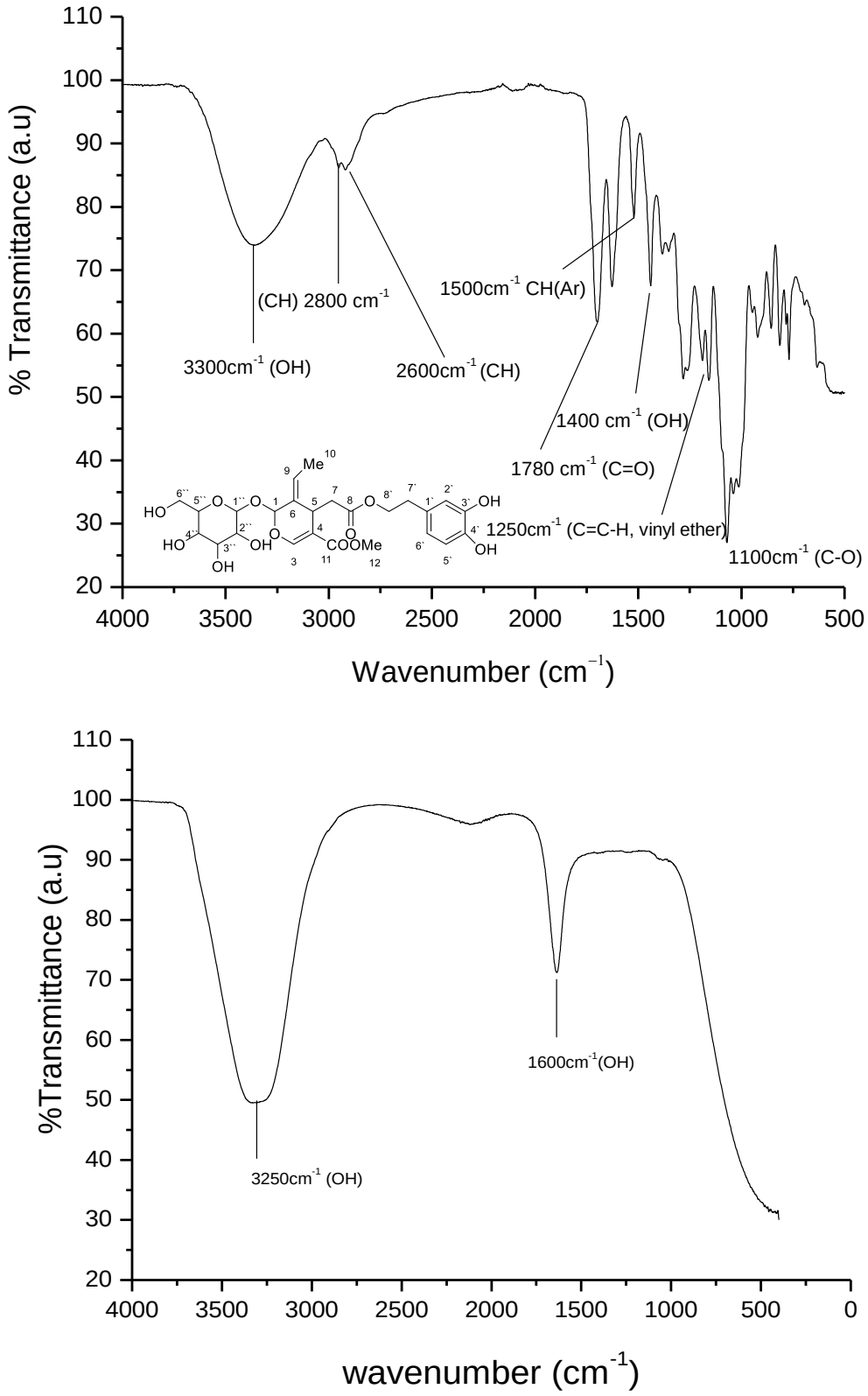

Figure 4.32 Oleuropein compound infrared (A) and oleuropein gold nanoparticle infrared (B) showing the shifted intensity to the right and increased intensity. The absence of some peaks that are involved in gold nanoparticle formation after forming the gold nanoparticle

The Infrared spectrum of the Oleuropein is given in Figure 4.32 A and that of its gold nanoparticle in Figure 4.32 B. A reduction of chemical functional groups was observed as the gold nanoparticle formed. It went from 3250 cm^{-1} (OH), 2800 cm^{-1} (CH, Sp^2), 1250cm^{-1} (Vinyl ether) 2600 cm^{-1} (CH, Sp^2), 1400 cm^{-1} (=C-C=C-, Ar), 1780 cm^{-1} (C=O), 1100 cm^{-1} (C-O) to only 3250 cm^{-1} (OH). The remaining bonds were shifted so that the OH group went from a large stretch at 3300 cm^{-1} to a short one at 3250 cm^{-1}, and the carbonyl group went from 1780 cm^{-1} to a shorter stretch at 1600 cm^{-1}. The C-O stretch was at 1100 cm^{-1} and the COO^- stretch was at 1400 cm^{-1} (Rajakumar et al., 2016). The formation of gold nanoparticles occurred with a change in energy which testifies to the existence of a new substance formed. In addition, the change observed in the shift and the % transmission of the stretch was an indication of the change that accompanied the formation of gold nanoparticles as observed in Yulizar experiment (Yulizar et al., 2017).

5. CHAPTER FIVE

BIOLOGICAL STUDIES

5.1 Introduction

In this chapter, the stability test of both oleuropein and *O. exasperata* extract gold nanoparticles were carried out. The cytotoxicity test of the same nanoparticles was also completed on multiple cell lines and finally, the drug delivery mechanism was assessed using the uptake experiment.

5.2 Stability test

The biological studies were conducted on lyophilised extracts, oleuropein and the nanoparticles thereof. The stability of the synthesised gold nanoparticles, in the presence of the media, was monitored using UV-vis absorption spectroscopy (Wang et al., 2014). An absorption peak that remained constant with time would be indicative of the stability of the gold nanoparticles in the media (Ishii et al., 2004). Due to the instability of the oleuropein gold nanoparticles (Jimenez-ruiz et al., 2021), its stability was achieved by removing a fifth of the volume of the formed gold nanoparticles and replacing it with an equal volume of 1% of Poly Ethylene Glycol dissolved in water, and *O. exasperata* extract monitored in a freshly prepared MTT reagent medium for a period of 24 hrs.

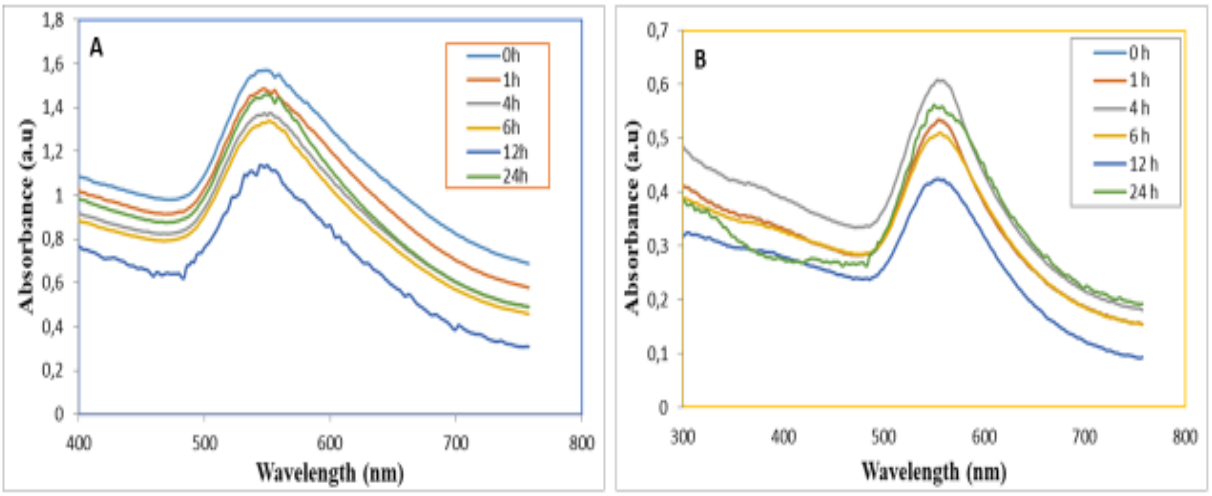

Figure 5.1 Stability tests of *O. exasperata* extract gold nanoparticles (A) and PEG stabilised oleuropein based gold nanoparticles (B) showing their stability over a 24hr period

The UV-VIS absorption spectra (Figure 5.1 A) showed that *Olea exasperata* extract gold nanoparticles had an absorption peak at 548 nm and that the wavelength of maximum absorption remained constant at 548nm. However, the peak reached its maximum value of growth rate at 12 h before decreasing in the last 12 hrs to some equilibrium position. This was not different from the observation made in Wang's work where the drop in peak intensity was due to particle sedimentation as a result of their growth (Wang et al., 2014).

The stability test of oleuropein in the media was observed at the maximum wavelength of absorption of 556 nm revealing a similar trend to what was observed in Wang's work. In fact, oleuropein gold nanoparticles underwent a redshift in the MTT reagent (1mg/ml) because the reagent had an absorption of its own causing the peak of the gold nanoparticles to shift. The wavelength of maximum absorption remained 556 nm as observed in Figure 5.1 (B). The absorption started small, grew and faded within 12 h by 50 % of its maximum absorbance value. Wang made a similar observation in his experiment (Wang et al., 2014). The stability of the particles within 24 hours is a necessity to drug delivery which requires that it is stable during the process of the delivery.

5.3 MTT Cytotoxicity assay and safety of gold nanoparticles

Drug safety is a very important feature in drug design. To evaluate the safety of the olea extracts and the nanoparticles thereof, an MTT viability assay, introduced in section 2.6.1.3, was conducted with a modification from its original version (Sun et al., 2019). The exposure of Oleuropein, O. extract, oleuropein gold nanoparticles and the extract gold nanoparticles did not inhibit the proliferation of the following cell lines: KMST-6, HaCaT, MCF-7, HT-29, B16 and Mel-1 (Ozaki, 1994) up to a concentration of 100 µg/mL. Since the outcome of the viability test state the viability of a cell, and it was so in the presence of the *Olea exasperata* extracts and its gold nanoparticles, it is thus safe to confirm that gold nanoparticles made with olea extracts are safe to use in human and animal biological systems.

5.4 Gold nanoparticle uptake

Drug delivery is an important part of any clinical trial. It is the evaluation of the bioavailability of the drug or the determination of the number of lead molecules reaching the targeted organs or cells.

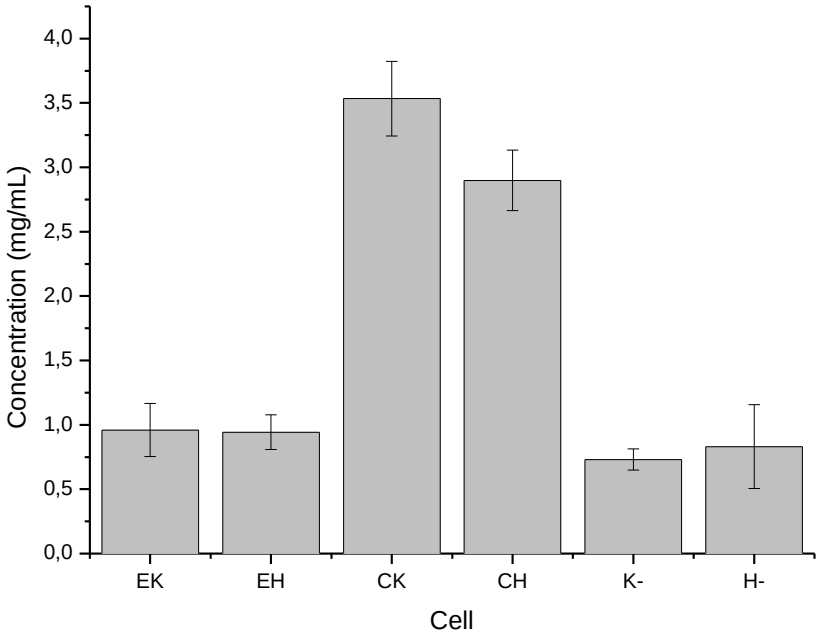

Figure 5.2 Error bars of cells KMST-6 treated with *O. exasperata* GNPs (EK), HT-29 cells treated with *O. exasperata* GNPs (EH), KMST-6 cells treated with OL GNPs (CK), HT-29 cells treated with OL GNPs (CH), KMST-6 cells with no GNPs (K-), HT-29 cells with no GNPs (H-)

Gold nanoparticle uptake was achieved for both gold nanoparticles formed from *O. exasperata* extracts and oleuropein. The error bars in Figure 5.2 informed that gold nanoparticle uptake in KMST-6 cells treated with oleuropein (CK) was prominent over the uptake of the same cells (EK) treated with *O. exasperata*. The uptake of gold nanoparticles in oleuropein was more likely to happen in comparison to the uptake in the extract. The error bar revealed that the oleuropein treated sample (CK) was less precise or had its data more spread-out for the triplicate measurement used. It is thus observed that the use of a pure compound was beneficial to have a much better uptake for delivery of the drug in living cells (Cumming et al., 2007) as observed in HT-29 cells absorption. The negative control K- and H- were used as references.

Figure 5.2 shows that the uptake levels of both gold nanoparticles were more in the HT-29 cells compared to the KMST-6 cell (0.94 ± 0.13 mg/mL and 0.73 ± 0.08 mg/mL respectively). This shows that both nanoparticles have an affinity towards cancerous cells in comparison to normal cells. The uptake of both nanoparticles in KMST-6 was similar to the negative controls. These data highlight the potential of using these nanoparticles as drug delivery systems in the treatment of cancer.

6. CHAPTER SIX

GENERAL CONCLUSIONS AND RECOMMENDATIONS

The present work successfully achieved the isolation and elucidation from *Olea exasperata* of the following phytochemicals: hydroxytyrosol glucoside (compound 1), oleuropein (compound 2), and hydroxytyrosol (compound 3). The compounds were characterised using nuclear magnetic resonance and infrared spectroscopy. The obtained data were crossed checked against reported structures in literature to confirm the existence thereof.

Olea exasperata leaf extract was successfully used in the synthesis of gold nanoparticles as the reducing agent of gold ions found in the 1mM of sodium tetra aurate (III) dehydrate ($NaAuCl_4.2H_20$). The optical properties of the red solution of Olea gold nanoparticles were confirmed with UV light absorbing at a wavelength of 547 nm. The observed gold nanoparticles were crystalline according to both the X-Ray diffraction pattern and the SAED pattern analysis. The size of the gold nanoparticles from the Olea extract was confirmed to be around 73nm on average and the Zeta potential was -21.6 mV.

After the synthesis of gold nanoparticles from the total extract, hydroxytyrosol glucoside was used in the synthesis of gold nanoparticles in the presence of 1 mM of sodium tetraaurate (III) dehydrate ($NaAuCl_4.2H_20$). The optical properties were also monitored and the red solution absorbed UV light at 548nm. They were confirmed to be crystalline and had an average size of 73 nm with the Zeta potential at about -30.3 mV.

The gold nanoparticles made from oleuropein were also made from 1mM of sodium tetra aurate (III) dehydrate ($NaAuCl_4.2H_20$). The optical properties revealed that the gold solution also absorbed UV light at 548nm and formed crystalline gold nanoparticles. The average size of the gold nanoparticles formed using oleuropein as a reducing agent was 71nm in diameter and the Zeta potential was -25.9 mV.

The cytotoxicity studies conducted proved that the O. exasperata extract and its nanoparticles were safe to introduce in biological systems. This implies that these materials are safe for use in humans and animals without any side effects associated with them. The stability of Olea extract and oleuropein gold nanoparticles was confirmed over 24 hours. The gold nanoparticles uptake revealed that GNPs showed an affinity for cancerous cells compared to normal cells. In addition, oleuropein gold nanoparticles have better bioavailability compared to

O. exasperata extract gold nanoparticles. Isolating pure compounds to make gold nanoparticles was thus essential to having better drug delivery.

It is recommended here that more compounds be isolated from various plants for the same purpose of assessing their nanoparticle forming potential for their biological evaluation. This will help develop a library of plants that are suitable to supply nanoparticles with improved efficacy as a potential cure. In addition to this suggestion, rare plant species should be cultivated and disseminated to help with their species.

The reducing ability of the total extract is a sum of all the contributing phytochemicals in the extract. While this can be a good thing, it was considered a hindrance to the understanding of the process beyond the reduction of gold nanoparticles. In fact, while stability is measured as a physical property, it is maintained by two factors: the reducing agent and the capping agent. In this case, one substance was used but did not always display both physical and chemical properties. Isolating pure compounds from their matrix in the total extract has helped establish that the reducing ability of plants could be localised in specific individual compounds. However, the process remains a cost-effective process given the yield of pure compounds versus the amount of starting materials.

Reference

Ahmad, T., Irfan, M. & Bhattacharjee, S. 2016. Parametric Study on Gold Nanoparticle Synthesis Using Aqueous Elaise Guineensis (Oil palm) Leaf Extract: Effect of Precursor Concentration. *Procedia Engineering*, 148: 1396–1401.

Alarcón-Flores, M.I., Romero-González, R., Vidal, J.L.M. & Frenich, A.G. 2015. Systematic study of the content of phytochemicals in fresh and fresh-cut vegetables. *Antioxidants*, 4(2): 345–358.

Ali, S.I., Gopalakrishnan, B. & Venkatesalu, V. 2017. Pharmacognosy, Phytochemistry and Pharmacological Properties of Achillea millefolium L.: A Review. *Phytotherapy Research*, 31(8): 1140–1161.

Aljabali, A.A.A., Akkam, Y., Al Zoubi, M.S., Al-Batayneh, K.M., Al-Trad, B., Alrob, O.A., Alkilany, A.M., Benamara, M. & Evans, D.J. 2018. Synthesis of gold nanoparticles using leaf extract of Ziziphus and their antimicrobial activity. *Nanomaterials*, 8(3): 1–15.

Ankamwar, B. 2010. Biosynthesis of Gold Nanoparticles (Green-Gold) Using Leaf Extract of Terminalia Catappa. , 7(4): 1334–1339.

Ansari, S.H., Islam, F. & Sameem, M. 2012. Influence of nanotechnology on herbal drugs: A Review. *Journal of Advanced Pharmaceutical Technology and Research*, 3(3): 142–146.

Antony, E., Gunasekaran, S., Sathiavelu, M. & Arunachalam, S. 2016. A REVIEW ON THE USE OF PLANT EXTRACTS FOR GOLD AND SILVER NANOPARTICLE SYNTHESIS AND THEIR POTENTIAL ACTIVITIES AGAINST FOOD PATHOGENS. , 9(4).

Apu, A.S., Liza, M.S., Jamaluddin, A.T.M., Howlader, M.A., Saha, R.K., Rizwan, F. & Nasrin, N. 2012. Phytochemical screening and in vitro bioactivities of the extracts of aerial part of Boerhavia diffusa Linn. *Asian Pacific Journal of Tropical Biomedicine*, 2(9): 673–678.

Badeggi, U.M., Ismail, E., Adeloye, A.O., Botha, S. & Hussein, A.A. 2020. Green Synthesis of Gold Nanoparticles Capped with Procyanidins from Leucosidea sericea as Potential Antidiabetic and Antioxidant Agents.

Bankar, A., Joshi, B., Ravi Kumar, A. & Zinjarde, S. 2010. Banana peel extract mediated synthesis of gold nanoparticles. *Colloids and Surfaces B: Biointerfaces*, 80(1): 45–50.

Biao, L., Tan, S., Meng, Q., Gao, J., Zhang, X., Liu, Z. & Fu, Y. 2018. Green synthesis, characterization, and application of proanthocyanidins-functionalized gold nanoparticles. *Nanomaterials*, 8(1).

Boxall, A.B.A. 2004. The environmental side effects of medication: how are human and veterinary medicines in soils and water bodies affecting human and environmental health? *EMBO Reports*, 5(12): 1110–1116.

Boyer, J. & Liu, R.H. 2004. Apple phytochemicals and their health benefits. *Nutrition Journal*, 3: 1–45.

Casasanta, G. & Garra, R. 2018. Towards a Generalized Beer-Lambert Law. : 1–7.

Castaneda-gill, J. 2018. ZETASIZER PRO AND ZETASIZER ULTRA LIGHT SCATTERING ANALYSIS numerous analytical combinations .“. : 5.

Choi, C.G., Kim, S.H., Kim, J.S., Chi, J.G., Song, E.S. & Han, M.C. 1993. Adenoma malignum of uterine cervix in peutz-jeghers syndrome: Ct and us features. *Journal of Computer Assisted Tomography*, 17(5): 819–821.

Cumming, G., Fidler, F. & Vaux, D.L. 2007. Error bars in experimental biology. *Journal of Cell Biology*, 177(1): 7–11.

Dabbousi, B.O., Rodriguez-Viejo, J., Mikulec, F. V., Heine, J.R., Mattoussi, H., Ober, R., Jensen, K.F. & Bawendi, M.G. 1997. (CdSe)ZnS core-shell quantum dots: Synthesis and characterization of a size series of highly luminescent nanocrystallites. *Journal of Physical Chemistry B*, 101(46): 9463–9475.

Das, M., Shim, K.H., An, S.S.A. & Yi, D.K. 2011. Review on gold nanoparticles and their applications. *Toxicology and Environmental Health Sciences*, 3(4): 193–205.

Dave, N. & Joshi, T. 2017. A Concise Review on Surfactants and Its Significance. *International Journal of Applied Chemistry*, 13(3): 663–672.

Deraedt, C., Salmon, L., Gatard, S., Ciganda, R., Hernandez, R., Mayor, M. & Astruc, D. 2014. Sodium borohydride stabilizes very active gold nanoparticle catalysts. *Chemical Communications*, 50(91): 14194–14196.

Doan, V.D., Huynh, B.A., Nguyen, T.D., Cao, X.T., Nguyen, V.C., Nguyen, T.L.H., Nguyen, H.T. & Le, V.T. 2020. Biosynthesis of Silver and Gold Nanoparticles Using Aqueous Extract of Codonopsis pilosula Roots for Antibacterial and Catalytic Applications. *Journal of Nanomaterials*, 2020.

Dorofeev, G.A., Streletskii, A.N., Povstugar, I. V., Protasov, A. V. & Elsukov, E.P. 2012. Determination of nanoparticle sizes by X-ray diffraction. *Colloid Journal*, 74(6): 675–685.

Elbagory, A.M., Hussein, A.A. & Meyer, M. 2019. The in vitro immunomodulatory effects of gold nanoparticles synthesized from hypoxis hemerocallidea aqueous extract and hypoxoside on macrophage and natural killer cells. *International Journal of Nanomedicine*, 14: 9007–9018.

Eustis, S., El-Sayed, M.A. & Kasha, M. 2006. Why gold nanoparticles are more precious than pretty gold : Noble metal surface plasmon resonance and its enhancement of the radiative and nonradiative properties of nanocrystals of different shapes. : 209–217.

Fong, T.S., Johan, M.R. & Ahmad, R.B. 2012. Synthesis and Characterization of Gold-Titanium-Mesoporous Silica Nanomaterials. , 7: 4716–4726.

Freitas, L.F. De, Henrique, G. & Varca, C. 2018. An Overview of the Synthesis of Gold Nanoparticles Using Radiation Technologies.

Fuller, M. 2018. The Effect of Salt and Polyelectrolyte Concentration on Colloidal Stability.

Galib, Barve, M., Mashru, M., Jagtap, C., Patgiri, B.J. & Prajapati, P.K. 2011. Therapeutic potentials of metals in ancient India: A review through Charaka Samhita. *Journal of Ayurveda and Integrative Medicine*, 2(2): 55–63.

Goulas, V., Exarchou, V., Troganis, A.N., Psomiadou, E., Fotsis, T., Briasoulis, E. & Gerothanassis, I.P. 2009. Phytochemicals in olive-leaf extracts and their antiproliferative activity against cancer and endothelial cells. *Molecular Nutrition and Food Research*, 53(5): 600–608.

Haroon Anwar, S. 2018. A Brief Review on Nanoparticles: Types of Platforms, Biological Synthesis and Applications. *Research & Reviews Journal of Material Sciences*, 06(02).

Hoo, X.F., Razak, K.A., Ridhuan, N.S., Nor, N.M. & Zakaria, N.D. 2017. Synthesis of tunable size gold nanoparticles using seeding growth method and its application in glucose sensor. *AIP Conference Proceedings*, 1877(September).

Ishii, T., Otsuka, H., Kataoka, K. & Nagasaki, Y. 2004. Preparation of functionally PEGylated gold nanoparticles with narrow distribution through auto reduction of auric cation by α-Biotinyl-PEG-block-[poly(2-(N,N-dimethylamino)ethyl methacrylate)]. *Langmuir*, 20(3): 561–564.

Istifli, E.S. 2019. *Cytotoxicity*.

Jimenez-ruiz, A., Prado-gotor, R., Fern, G. & Gonz, A. 2021. Encased Gold Nanoparticle Synthesis as a Probe for Oleuropein Self-Assembled Structure Formation.

De Jong, W.H. & Borm, P.J.A. 2008. Drug delivery and nanoparticles: Applications and hazards. *International Journal of Nanomedicine*, 3(2): 133–149.

Kalyani, S., Sangeetha, J. & Philip, J. 2016. Effect of Precipitating Agent and Solvent Polarity on the Size and Magnetic Properties of Magnetite Nanoparticles Prepared by Microwave-Assisted Synthesis. , 16(9): 9591–9602.

Khairnar, S., Kini, R., Pharmaceuticals, G., Harwalkar, M., Pharma, A. & Salunkhe, K. 2012. A Review on Freeze Drying Process of Pharmaceuticals. , (April).

Khalil, M. & Ismail, E.H. 2012. Biosynthesis of Au nanoparticles using olive leaf extract. , (October).

Khalil, M.M.H., Ismail, E.H. & El-Magdoub, F. 2012. Biosynthesis of Au nanoparticles using olive leaf extract. *Arabian Journal of Chemistry*, 5(4): 431–437.

Kim, H. seok, Seo, Y.S., Kim, K., Han, J.W., Park, Y. & Cho, S. 2016. Concentration Effect of Reducing Agents on Green Synthesis of Gold Nanoparticles: Size, Morphology, and Growth Mechanism. *Nanoscale Research Letters*, 11(1).

Kovalerchuk, B. & Schwing, J. 2004. NANOPARTICLES AND THEIR APPLICATIONS IN CELL AND MOLECULAR BIOLOGY. *Library*, 6(1): 576.

Kraynov, A. & Müller, T.E. 2011. Concepts for the Stabilization of Metal Nanoparticles in Ionic Liquids. , 1.

Küster, A. & Adler, N. 2014. One contribution of 18 to a Theme Issue 'Assessing risks and impacts of pharmaceuticals in the environment on wildlife and ecosystems. Pharmaceuticals in the environment: scientific evidence of risks and its regulation. *Philosophical Transactions of The Royal Society B*, 369(20130587).

Lewinski, N., Colvin, V. & Drezek, R. 2008. Cytotoxicity of nanoparticles. *Small*, 4(1): 26–49.

Lidiawati, D., Wahid Wahab, A. & Karim, A. 2019. Synthesis And Characterization Of Gold Nanoparticles Using Beluntas Leaf Extract Plucheaindica. *Jurnal Akta Kimia Indonesia (Indonesia Chimica Acta)*, 12(1): 13.

Líter, M., Cell, M., Antonio, J., Líter, M., Tundidor, I., Domínguez, M.N., Toro, B.F. De, Santana, A.G., Eugenio, L.I. De, Prieto, A., Asensio, J.L., Cañada, F.J., Sánchez, C. & Martínez, M.J. 2019. Transglycosylation products generated by Talaromyces amestolkia e GH3 β - glucosidases : effect of hydroxytyrosol , vanillin and its glucosides on breast cancer cells. *Microbial Cell Factories*: 1–12.

Makarov, V. V, Love, A.J., Sinitsyna, O. V, Makarova, S.S. & Yaminsky, I. V. 2014. " Green " Nanotechnologies : Synthesis of Metal Nanoparticles Using Plants. , 6(20): 35–44.

Marlene C. Morris, Howard F. McMurdie, E.H.E. & Boris Paretzkin, Harry S. Parker, Winnie Wong-Ng, A. 1991. *Standards, Joint Committee on Powder Diffraction*.

Merck, G.W. 1950. Medicine is for the patient, not for profits.

Mocanu, A., Cernica, I., Tomoaia, G., Bobos, L.D., Horovitz, O. & Tomoaia-Cotisel, M. 2009. Self-assembly characteristics of gold nanoparticles in the presence of cysteine. *Colloids and Surfaces A: Physicochemical and Engineering Aspects*, 338(1–3): 93–101.

Mustafa, I.F. & Hussein, M.Z. 2020. Synthesis and technology of nanoemulsion-based pesticide formulation. *Nanomaterials*, 10(8): 1–26.

Nadeem, M., Abbasi, B.H., Younas, M. & Khan, T. 2017. Green Chemistry Letters and Reviews A review of the green syntheses and anti-microbial applications of gold nanoparticles. , 8253.

Noireaux, J., Grall, R., Hullo, M., Chevillard, S., Oster, C., Brun, E., Sicard-Roselli, C., Loeschner, K. & Fisicaro, P. 2019. Gold nanoparticle uptake in tumour tumours: Quantification and size distribution by sp-ICPMS. *Separations*, 6(1): 1–13.

Ó'Fágáin, C., Cummins, P.M. & O'Connor, B. 2017. Gel-filtration chromatography. *Methods in Molecular Biology*, 1485: 15–25.

Omar, S.H. 2010. Oleuropein in olive and its pharmacological effects. *Scientia Pharmaceutica*, 78(2): 133–154.

Ozaki, M., Yoshida, S., Oura, M., Tsuruoka, T. & Usui, K. 2020. Effect of tryptophan residues on gold mineralization by a gold reducing peptide. *RSC Advances*, 10(66): 40461–40466.

Ozaki, S. 1994. Cell Lines and Hybridomas. *Cellular Immunology*: 65–93.

Pathway, R., Cheraghali, R., Moradi, S. & Sepehrian, H. 2014. Research and Reviews :

Journal of Pharmaceutics and Nanotechnology. , 2(2): 17–20.

Petrovska, B.B. 2012. Historical review of medicinal plants' usage. *Pharmacognosy Reviews*, 6(11): 1–5.

Picchio, V., Cammisotto, V., Pagano, F., Carnevale, R. & Chimenti, I. 2020. In Vitro Cytotoxicity and Cell Viability Assays: Principles, Advantages, and Disadvantages. *intechopen*, (Cell Interaction-Regulation of Immune Responses, Disease Development and Management Strategies): 1–15.

Rafique, M., Sadaf, I., Rafique, M.S. & Tahir, M.B. 2017. A review on green synthesis of silver nanoparticles and their applications. *Artificial Cells, Nanomedicine and Biotechnology*, 45(7): 1272–1291.

Rai, B.S.S.V.R. 2015. Biosynthesis of highly monodispersed, spherical gold nanoparticles of size 4 – 10 nm from spent cultures of Klebsiella pneumoniae. *3 Biotech*: 671–676.

Rajakumar, G., Gomathi, T., Rahuman, A.A., Thiruvengadam, M., Mydhili, G., Kim, S.H., Lee, T.J. & Chung, I.M. 2016. Biosynthesis and biomedical applications of gold nanoparticles using eclipta prostrata leaf extract. *Applied Sciences (Switzerland)*, 6(8).

Rajiv, P., Deepa, A., Vanathi, P. & Vidhya, D. 2017. SCREENING FOR PHYTOCHEMICALS AND FTIR ANALYSIS OF MYRISTICA DACTYLOIDS FRUIT EXTRACTS. , 9(1): 1–4.

Ramakrishna, A. & Ravishankar, G.A. 2011. Influence of abiotic stress signals on secondary metabolites in plants. *Plant Signaling and Behavior*, 6(11): 1720–1731.

Rasethe, M.T., Semenya, S.S. & Maroyi, A. 2019. Medicinal Plants Traded in Informal Herbal Medicine Markets of the Limpopo Province, South Africa. *Evidence-based Complementary and Alternative Medicine*, 2019.

Reda, M., Ashames, A., Edis, Z., Bloukh, S., Bhandare, R. & Sara, H.A. 2019. Green synthesis of potent antimicrobial silver nanoparticles using different plant extracts and their mixtures. *Processes*, 7(8).

Romero, C., Brenes, M., García, P. & Garrido, A. 2002. Hydroxytyrosol 4-β-D-glucoside, an important phenolic compound in olive fruits and derived products. *Journal of Agricultural and Food Chemistry*, 50(13): 3835–3839.

Ruitao, Q., Atoms, A., Li, R., Li, Z., Dong, Z. & Khor, K.A. 2016. A Review of Transmission Electron Microscopy of Quasicrystals-How are atoms Arranged? : 1–16.

Sakellari, G.I., Hondow, N. & Gardiner, P.H.E. 2020. Factors Influencing the Surface Functionalization of Citrate Stabilized Gold Nanoparticles with Cysteamine, 3-Mercaptopropionic Acid or l-Selenocystine for Sensor Applications. *Chemosensors*, 8(3): 80.

Salager, J.-L. 2002. SURFACTANTS Types and Uses. , 2.

Sasidharan, S., Tradit, A.J., Altern, C., Chen, Y., Saravanan, D., Sundram, K.M., Latha, L.Y., Bedong-semeling, J. & Nasi, B.A. 2007. Proper Actions. *Lecture Notes in Mathematics*,

1902: 121–130.

Savarese, M., Marco, E. De & Sacchi, R. 2007. Food Chemistry Characterization of phenolic extracts from olives (Olea europaea cv . Pisciottana) by electrospray ionization mass spectrometry. , 105: 761–770.

Sentkowska, A. & Pyrzyńska, K. 2019. Investigation of antioxidant activity of selenium compounds and their mixtures with tea polyphenols. *Molecular Biology Reports*, 46(3): 3019–3024. http://dx.doi.org/10.1007/s11033-019-04738-2.

Da Silva, T.C., Da Silva, J.M. & Ramos, M.A. 2018. What factors guide the selection of medicinal plants in a local pharmacopoeia? A case study in a rural community from a historically transformed Atlantic forest landscape. *Evidence-based Complementary and Alternative Medicine*, 2018.

Sridhar, R. & Ramakrishna, S. 2015. Electro-sprayed nanoparticles for drug delivery and pharmaceutical applications. , (September 2013): 1–12.

Steckiewicz, K.P., Barcinska, E., Malankowska, A., Zauszkiewicz–Pawlak, A., Nowaczyk, G., Zaleska-Medynska, A. & Inkielewicz-Stepniak, I. 2019. Impact of gold nanoparticles shape on their cytotoxicity against human osteoblast and osteosarcoma in in vitro model. Evaluation of the safety of use and anti-cancer potential. *Journal of Materials Science: Materials in Medicine*, 30(2): 1–15..

Sun, B., Hu, N., Han, L., Pi, Y., Gao, Y. & Chen, K. 2019. Anticancer activity of green synthesised gold nanoparticles from *Marsdenia tenacissima* inhibits A549 cell proliferation through the apoptotic pathway. *Artificial Cells, Nanomedicine, and Biotechnology*, 47(1): 4012–4019.

Supriadi, B., Astuti, W. & Firdiansyah, A. 2017. Green Product And Its Impact on Customer Satisfaction. *IOSR Journal of Business and Management (IOSR-JBM)*, 19(8): 1 9.

Tanaka, R., Kawai, J. & Alawadhi, H. 2016. Artificial peaks in energy dispersive X-ray spectra : sum peaks, escape peaks, and diffraction peaks : Artificial peaks in energy dispersive X-ray spectra. , (January).

Tantra, R., Schulze, P. & Quincey, P. 2010. Effect of nanoparticle concentration on zeta-potential measurement results and reproducibility. *Particuology*, 8(3): 279–285.

Tao, C. 2018. Antimicrobial activity and toxicity of gold nanoparticles: research progress, challenges and prospects. *Letters in Applied Microbiology*, 67(6): 537–543.

Taylor, A.F., Rylott, E.L., Anderson, C.W.N. & Bruce, N.C. 2014. Investigating the toxicity, uptake, nanoparticle formation and genetic response of plants to gold. *PLoS ONE*, 9(4).

Teramae, F., Makino, T., Lim, Y., Sengoku, S. & Kodama, K. 2020. International strategy for sustainable growth in multinational pharmaceutical companies. *Sustainability (Switzerland)*, 12(3): 1–14.

Toma, A. & Crişan, O. 2018. Green Pharmacy – A Narrative Review. *Medicine and Pharmacy*

Reports, 91(4): 391–398.

Tripoli, E., Giammanco, M., Tabacchi, G., Di Majo, D., Giammanco, S. & La Guardia, M. 2005. The phenolic compounds of olive oil: structure, biological activity and beneficial effects on human health. *Nutrition Research Reviews*, 18(1): 98–112.

Tsukamoto, H., Hisada, S., Nishibe, S. & Roux, D.G. 1984. Phenolic glucosides from Olea europaea subs. africana. *Phytochemistry*, 23(12): 2839–2841.

Wang, A., Ng, H.P., Xu, Y., Li, Y., Zheng, Y., Yu, J., Han, F., Peng, F. & Fu, L. 2014. Gold nanoparticles: Synthesis, stability test, and application for the rice growth. *Journal of Nanomaterials*, 2014.

Wang, B., Yang, G., Chen, J. & Fang, G. 2020. Green Synthesis and Characterization of Gold Nanoparticles Using Lignin Nanoparticles. : 1–12.

Weiss, E.B. 2011. The Evolution of International Environmental Law. , 27.

Yulizar, Y., Utari, T., Ariyanta, H.A. & Maulina, D. 2017. Green Method for Synthesis of Gold Nanoparticles Using Polyscias Scutellaria Leaf Extract under UV Light and Their Catalytic Activity to Reduce Methylene Blue. , 2017.

Zewde, B., Ambaye, A., Iii, J.S. & Raghavan, D. 2016. A Review of Stabilized Silver Nanoparticles – Synthesis, Biological Properties, Characterization, and Potential Areas of Applications. , 4.

Zhang, Q.W., Lin, L.G. & Ye, W.C. 2018. Techniques for extraction and isolation of natural products : a comprehensive review. *Chinese Medicine*: 1–26.